

**Identification and characterization of aldehyde
dehydrogenases (ALDHs) and their suitability as
drug targets against the liver fluke *Fasciola hepatica***

Inaugural-Dissertation

zur Erlangung des Doktorgrades der Naturwissenschaften

(Dr. rer. nat.)

im Fachbereich Biologie und Chemie der

Justus-Liebig-Universität Gießen

vorgelegt von

Hicham Houhou

aus Barja, Libanon

Juni 2022

The present work was carried out at the Institute of Parasitology (Faculty 10), Justus Liebig University Gießen between March 2018 and June 2022 under the supervision of Prof. Dr. Nikola-Michael Prpic-Schäper and Prof. Dr. Christoph G. Grevelding.

First supervisor: **Prof. Dr. Nikola-Michael Prpic-Schäper**

Institute of zoology and developmental biology, Justus Liebig University Gießen, Heinrich-Buff-Ring 38, 35392 Gießen, Germany.

Second supervisor: **Prof. Dr. Christoph G. Grevelding**

Institute of Parasitology, BFS, Justus Liebig University Gießen, Schubertstraße 81, 35392 Gießen, Germany.

LIST OF ABBREVIATIONS

Abbreviations	Full name
ABAM	Antibiotic-Antimycotic
ALDHs	Aldehyde dehydrogenases
AP	Alkaline phosphatase
APS	Ammonium persulphate
ATP	Adenosine triphosphate
BLAST	Basic Local Alignment Search Tool
BSA	Bovine serum albumin
cDNA	complementary DNA
CLSM	Confocal laser scanning microscope
CO ₂	Carbon dioxide
CTP	Cytosine triphosphate
DDC	Diethyldithiocarbamate
DEPC	Diethylpyrocarbonate
DIG	digoxigenin
DMSO	Dimethyl sulfoxide
DNA	deoxyribonucleic acid
DSF	Disulfiram
dsRNA	Double-stranded RNA
DTT	Dithiothreitol
EDTA	Ethylenediaminetetraacetic acid
EdU	5-ethynyl-2'-deoxyuridine

ELISA	Enzyme-linked immunosorbent assays
EtOH	Ethanol
gDNA	Genomic DNA
GTP	Guanine triphosphate
HCl	Hydrogen chloride
HRP	Horseradish peroxidase
HSCs	Hematopoietic stem cells
IPTG	Isopropyl β -D-1-thiogalactopyranoside
KCl	Potassium chloride
KH ₂ PO ₄	Monopotassium phosphate
LiCl	Lithium chloride
MeDTC-SO	S-methyl-N,N-diethylthiocarbamate sulfoxide
MeOH	Methanol
MgCl ₂	Magnesium chloride
mRNA	Messenger ribonucleic acid
Na ₂ HPO ₄	Disodium phosphate
Na ₃ C ₆ H ₅ O ₇	Trisodium citrate
NaCl	Sodium chloride
NaClO	Sodium hypochlorite
NaHCO ₃	Sodium bicarbonate
NEJ	Newly excysted juvenile
NTD	Neglected tropical diseases
PBS	Phosphate-buffered saline
PCR	Polymerase chain reaction

PFA	Paraformaldehyde
qRT-PCR	Quantitative real-time polymerase chain reaction
RNA	Ribonucleic acid
RNAi	RNA interference
ROS	Reactive oxygen species
RT	Room temperature
SDS	Sodium Dodecyl Sulfate
SDS-PAGE	Sodium dodecyl sulfate–polyacrylamide gel electrophoresis
SMART	Simple Modular Architecture Research Tool
SSC	saline-sodium citrate
SSDH	Succinic semialdehyde dehydrogenase
ssRNA	Single stranded RNA
TAE	Tris-acetate-EDTA
TBS	Tris-Buffered Saline
TCBZ	Triclabendazole
TCBZ	Triclabendazole
TEMED	tetramethylethylenediamine
Tris	tris(hydroxymethyl)aminomethane
TTP	Thymine triphosphate
UTP	Uracile triphosphate
WHO	World-Health Organization
X-Gal	5-bromo-4-chloro-3-indolyl- β -D-galactopyranoside

LIST OF FIGURES

Figure 1. The life cycle of the liver fluke <i>Fasciola hepatica</i> (picture source: www.cdc.gov).....	4
Figure 2. Different developmental stages of <i>F. hepatica</i>	5
Figure 3. Quantity and quality of total RNA isolated from exemplary liver fluke samples..	26
Figure 4. Cloning strategy to complete the full-length cDNA sequence of <i>Fhaldh1</i>	30
Figure 5. Motility analysis of NEJs. Screenshot showing parameters settings for the analysis of NEJs motility using wrMTrck plugin in Image J software.	43
Figure 6. Different life stages of <i>F. hepatica</i>	48
Figure 7. Ranking of eight candidate reference genes in the three different intra-mammalian life stages of <i>F. hepatica</i>	51
Figure 8. Ranking of eight candidate reference genes during <i>in vitro</i> culture of <i>F. hepatica</i>	53
Figure 9. Average ranking of expression stability of eight candidate reference genes in <i>F. hepatica</i> .54	
Figure 10. Relative expression levels of stably and least stably expressed reference gene candidates in <i>F. hepatica</i> ..	55
Figure 11. Relative expression levels of kinases in three different intra-mammalian life stages of <i>F. hepatica</i>	58
Figure 12. Relative expression levels of kinases during <i>in vitro</i> culture of juvenile <i>F. hepatica</i>	59
Figure 13. Phylogram of a phylogenetic tree analysis of FhALDH1 and FhALDH2.....	61
Figure 14. Multiple sequence alignment. Clustal omega was used to generate a multiple sequence alignment for FhALDH1 among several ALDH protein sequences.	62
Figure 15. Expression of two <i>Fhaldh</i> orthologues of <i>F. hepatica</i> . (A) qRT-PCR analyses show the transcript levels of <i>Fhaldh1</i> and <i>Fhaldh2</i> throughout the life cycle	63
Figure 16. Protein expression of both ALDHs orthologues. Western blot analyses of lysates of <i>E. coli</i> LOBSTR using an α -His antibody.....	65
Figure 17. FhALDH1 protein expression, purification, and enzymatic activity	66
Figure 18. Effect of disulfiram (DSF) on intra-mammalian stages of <i>F. hepatica</i>	67
Figure 19. Effect of disulfiram derivatives on the motility of 12-week-old flukes.....	69
Figure 20. Effect of compound 028 on intra-mammalian stages of <i>F. hepatica</i>	70
Figure 21. Expression of oxidative stress-related genes by DSF and 028 in adult <i>F. hepatica</i>	72
Figure 22. Transcript profiles of <i>Fhaldh1</i> and <i>Fhaldh2</i> and effects of compound 028 on stem-cell renewal in 4 weeks-grown juveniles	73
Figure 23. Effect of <i>Fhaldhs</i> knock-down on cell proliferation in 4 weeks <i>in vitro</i> -grown juveniles. 74	

LIST OF TABLES

Table 1. List of proteins used for phylogenetic tree construction of ALDH including the names of the species, the Gene IDs, the accession numbers, and the web sources.....	25
Table 2. Overview of candidate reference genes for the study of gene expression in <i>F. hepatica</i>	47
Table 3. Overview of genes of interest for the study of gene expression in <i>F. hepatica</i>	57

LIST OF CONTENTS

1. INTRODUCTION	1
1.1. Platyhelminthes (flatworms)	1
1.2. Trematodes.....	1
1.3. Epidemiology and transmission of <i>Fasciola hepatica</i>	2
1.4. Symptoms and diagnostic	3
1.5. Life cycle and pathogenic stages	4
1.6. Current therapeutic options against fasciolosis.....	6
1.7. Aldehydes as cellular toxicants.....	7
1.8. Aldehyde dehydrogenases in health and disease	8
1.8.1. Aldehyde dehydrogenases (ALDHs) and cell proliferation.....	9
1.8.2. ALDHs and drug resistance	10
1.9. Disulfiram (DSF)	11
1.10. Objectives of the study	11
2. MATERIALS AND METHODS	13
2.1. Materials	13
2.1.1. List of liquid chemicals.....	13
2.1.2 List of solid chemicals	14
2.1.3 Buffers and solutions	15
2.1.4 Media and supplements.....	16
2.1.5 List of qRT-PCR primers and size of the PCR product	17
2.1.6 List of primers and the purpose of their usage	18
2.1.7 Bacterial strains used for cloning.....	19
2.1.8 Enzymes	19
2.1.9 Kits and antibodies.....	20
2.1.10 Molecular weight standards	20
2.1.11 Online databases and Software	21
2.2 Methods	22
2.2.1. Ethics statement	22
2.2.2. Biological samples	22
2.2.3. <i>In silico</i> analyses	23
2.2.4. Total RNA isolation	26
2.2.5. Reverse transcription.....	27
2.2.6 Primer design for qRT-PCR.....	27
2.2.7. Polymerase chain reaction	28

2.2.8.	Cloning.....	32
2.2.9.	Evaluation of expression stabilities of reference genes	34
2.2.10.	<i>In situ</i> hybridization	34
2.2.11.	Expression and purification of FhALDH in <i>E. coli</i>	37
2.2.12.	Protein analyses.....	39
2.2.13.	RNA interference in <i>in vitro</i> -grown juveniles	40
2.2.14.	<i>In vitro</i> compound testing	42
2.2.15.	Analysis of cell proliferation.....	44
2.2.16.	Statistical analysis.....	45
3.	RESULTS.....	46
3.1.	Identification of housekeeping genes for real-time qPCR analyses in <i>F. hepatica</i>.....	46
3.1.1.	Choice of candidate reference genes.....	46
3.1.2.	RNA quality of parasite samples and performance of qRT-PCR primers	48
3.1.3.	Identification of the most stable reference genes	49
3.1.4.	Using the identified reference genes to study the expression of selected target genes in different fluke stages.....	55
3.2.	Identification of aldehyde dehydrogenases (ALDHs) in <i>F. hepatica</i> and evaluation of their suitability as drug targets.....	60
3.2.1.	Identification of ALDH1 and ALDH2 orthologues in <i>Fasciola hepatica</i>	60
3.2.2.	Expression pattern of <i>Fhaldh1</i> and <i>Fhaldh2</i> during life stages of the liver fluke	62
3.2.3.	Expression of the FhALDHs orthologues.....	64
3.2.4.	Treatment of the intra-mammalian liver fluke stages with disulfiram.....	66
3.2.5.	Treatment of adult flukes with chemically synthesized derivatives of disulfiram.....	68
3.2.6.	Treatment of NEJs and immature flukes with compound 028.....	69
3.2.7.	Effects of DSF and 028 on oxidative stress-related genes	71
3.2.8.	Compound 028 possibly affects stem cell self-renewal	72
3.2.9.	Knock-down (KD) of both <i>Fhaldh</i> orthologues and testing effects on cell proliferation	74
4.	DISCUSSION.....	76
4.1.	Identification of housekeeping genes for real-time qPCR analyses in <i>F. hepatica</i>.....	76
4.1.1.	A stably expressed reference genes for more reliable qRT-PCR analyses	76
4.1.2.	Two different sets of reference genes for two different experimental settings	77
4.1.3.	Kinases as important drug target analyses	78
4.1.4.	A solid basis for future gene expression analyses in <i>F. hepatica</i>	80
4.1.5.	Are kinases the end of the story or just the beginning?	80
4.2.	Identification of aldehyde dehydrogenases (ALDHs) in <i>F. hepatica</i> and evaluation of their suitability as drug targets.....	82

4.2.1.	Why are aldehyde dehydrogenases (ALDHs) interesting molecules to study in the context of fighting NTDs?	82
4.2.2.	Presence of ALDHs in <i>F. hepatica</i> and the conserved nature of their key domains.....	82
4.2.3.	Analyzing the expression profiles of <i>Fhaldhs</i>	83
4.2.4.	Is FhALDH1 capable of oxidizing aldehydes?	84
4.2.5.	Effect of the ALDH-inhibitor DSF on <i>F. hepatica</i>	85
4.2.6.	Chemical derivatization for a more potent inhibitor	86
4.2.7.	Why might DSF be less potent against liver flukes compared to O28?.....	86
4.2.8.	Co-therapy efficacy of DSF together with other drugs	88
4.2.9.	Stem cells as an important drug target	88
4.2.10.	Hurdles in genetic validation of ALDH as a target.....	89
4.3.	Conclusion	91
5.	SUMMARY/ZUSAMMENFASSUNG	92
5.1.	Summary	92
5.2.	Zusammenfassung.....	93
6.	REFERENCES	95
7.	SUPPLEMENTARY FIGURES	112
	ACKNOWLEDGMENTS	117
	CONTRIBUTIONS	118
	Publications.....	118
	Conferences.....	118
	DECLARATION	120

1. INTRODUCTION

To coexist together in a well-defined and balanced ecosystem, living organisms have established over time the art of “living together” or symbiosis. The first description of a symbiotic relationship refers to the intimate relationship that takes place between a fungus and blue-green algae. The invention of the word symbiosis was made by Albert Bernhard Frank in 1877, who defined this phenomenon as “where two species live on or in one another” (Roossinck, 2005). Symbiotic relationships can be cooperative or antagonistic. In the first case, this relationship is known as mutualistic symbiosis, in other words, the two interactive species provide each other with crucial functions, from which both benefit as one entity. In the second case, which is also called parasitic symbiosis, here one of the species takes advantage of the second one (receives benefits) without contributing to the mutual relationship (Roossinck, 2005). In this case, the fitness of the parasitized species is threatened. The present work focuses on a parasite called *Fasciola hepatica* or common liver fluke, which belongs to the Platyhelminthes or flatworms, and which represents a threat to the health of both, humans, and animals.

1.1. Platyhelminthes (flatworms)

Platyhelminthes (from Greek, *platys*=flat; *helminthos*=worm) or flatworms are worms that lack a coelom and possess a blind gut, which means that food enters and exits via the same orifice, in other words, they lack the anus. Moreover, flatworms lack a specialized respiratory or circulatory system. They have bilateral symmetry and, as their name indicates, are dorsoventrally flattened, which guarantees the diffusion of oxygen and nutrients, and thus their survival (Collins, 2017). Neodermata, a monophyletic superclass of Platyhelminthes, encompasses parasitic flatworms including Trematoda, Monogenea, and Cestoda (Olson and Tkach, 2005). In this thesis, the focus will be on *Fasciola hepatica*, a species within the class of trematodes.

1.2. Trematodes

Trematodes are divided into 2 different subgroups, Aspidogastrea and Digenea. The archaic Aspidogastrea are characterized by the absence of asexual reproduction, and they rather display more direct development. Digenea, on the contrary, has a more complex life cycle involving

both sexual and asexual reproduction, each one of these takes place in different hosts, which makes their life cycles more complicated (Adell et al., 2015). Trematodes are usually hermaphrodites. Some digenean trematodes, which belong to the genus *Schistosoma*, are the exception. These worms are dioecious, which means they have separated male and female individuals (Laurence Després and Sandrine Maurice, 1995). Paramount examples of hermaphroditic trematodes are liver flukes of the genus *Fasciola*. They are named “liver” flukes because the liver is their final destination within their definitive hosts, where they reproduce and feed. Liver flukes can survive inside their host for many years. For instance, the estimated life span in sheep is around 11 years, and the estimated life span in humans is between 9 and 13.5 years (Santiago Mas-Coma, M. Adela Valero, M. Dolores Bargues, 2015).

1.3. Epidemiology and transmission of *Fasciola hepatica*

The two major species within the genus *Fasciola* are *Fasciola hepatica* and *Fasciola gigantica*, which differ by their geographical distribution. *F. hepatica* is more found in temperate zones, while *F. gigantica* is more abundant in tropical regions (Cwiklinski et al., 2016). Hybridization was observed in some shared regions such as subtropical zones where both species co-exist (Agatsuma et al., 2000). Fasciolosis is considered one of the so-called neglected tropical diseases (NTD). NTD, as defined by the World Health Organization (WHO), is a group of 20 conditions that are mainly prevalent in tropical areas, where they mostly affect impoverished communities and cause diseases with devastating health, social and economic consequences on more than one billion people. Fasciolosis is a zoonotic disease, which are diseases that are naturally transmitted from vertebrate animals to humans and vice versa, and which is caused by all types of pathogens, such as bacteria, fungi, viruses, and parasites (Wang and Crameri, 2014). The WHO has estimated that at least 2.4 million people are infected in more than 75 countries worldwide, and several million are at risk (WHO, 2020). The infection is not exclusive to humans but also animals are highly infected, which is the origin of economical loss that has been estimated to be 3 billion dollars per year (Cwiklinski et al., 2016). Humans and animals both follow the same route of infection, which starts with the ingestion of encysted infective larvae, so-called metacercariae, via contaminated water or by eating vegetation near infested bodies of freshwater, like watercress (Lalor et al., 2021). The life cycle of *F. hepatica* is a “play” that takes place between several actors. The latter should take a part in the same ecosystem to guarantee a maintained and closed cycle. Therefore, factors that influence the presence of the intermediate or definitive hosts, such as environmental and geographical

factors, will influence the maintenance of the life cycle and infection. Lymnaeid snails favor low temperatures (Mas-Coma & M.D. Bargues, 1997). Likewise, metacercariae survive for long periods under low temperatures but in contrast, they suffer from desiccation and high temperature (over 25 °C) (Mas-Coma & M.D. Bargues, 1997). Haydon et al. highlighted the role of the definitive vertebrate hosts in the transmission of fasciolosis. These hosts act like reservoirs for the infection, and in case of a high parasitic infection of these hosts, the shedding of eggs will be high, thus the transmission of the disease is high (Haydon et al., 2002). The main hosts are cattle and sheep, but it has been shown that other domestic animals such as horses and donkeys can also act as reservoirs for this parasite. The eggs shed by those animals are viable, which makes them a source of transmission of the disease (Mas-Coma & M.D. Bargues, 1997). Humans contribute as well to the spread of the disease. For example, in some hyperendemic zones, where outdoor defecation is practiced, the output of eggs in the stool is considerably high (Santiago Mas-Coma, M. Adela Valero, M. Dolores Bargues, 2015).

1.4. Symptoms and diagnostic

Fascioliasis can be characterized by either acute or chronic phases. The acute phase takes place when immature flukes migrate through the liver parenchyma, which happens approximately two weeks after infection. This phase is characterized by fever, abdominal pain, and high eosinophil counts (Dietrich et al., 2015; Mas-Coma & M.D. Bargues, 1997). The chronic phase or the obstructive phase takes place when the adult flukes reach the bile duct (last destination) which happens approximately 8-12 weeks after infection. This phase is characterized by dilatation of duct and gallbladder walls and fibrosis of the liver (Mas-Coma & M.D. Bargues, 1997; Santiago Mas-Coma, M. Adela Valero, M. Dolores Bargues, 2015). The diagnosis of *F. hepatica* infection is made by the detection of parasite eggs in the feces. Despite the efficiency of this method, a major limitation is that only the late stage (adults) can be detected since only adults are capable of egg production (Beesley et al., 2018). In the past years, several serological and immunological methods have been optimized to confer more accurate and earlier detection of the infection. These methods rely on antibody detection by indirect enzyme-linked immunosorbent assays (ELISA) (Alvarez Rojas et al., 2014). All the stages of *F. hepatica* secrete the endopeptidase cathepsin L, a proteinase that is secreted by epithelial cells and that facilitates the penetration of the parasite in the host tissues (Dalton et al., 2003). The ELISA technique is used to detect the presence of antibodies secreted by the host targeting this endopeptidase (Beesley et al., 2018). Although this technique is highly sensitive, it has a

downside. Antibodies secreted by the host to target the parasite have a long half-life and can therefore be detected, for instance in the milk, even after successful treatment (Beesley et al., 2018).

1.5. Life cycle and pathogenic stages

A deeper understanding of the life cycle of *Fasciola hepatica* is key to completing our understanding of this parasite. Its life cycle is indirect and complex with an alternation between a sexual phase (that takes place in the definitive host) and an asexual phase (that takes place in the intermediate host) (Cribb et al., 2003) (Figure 1).

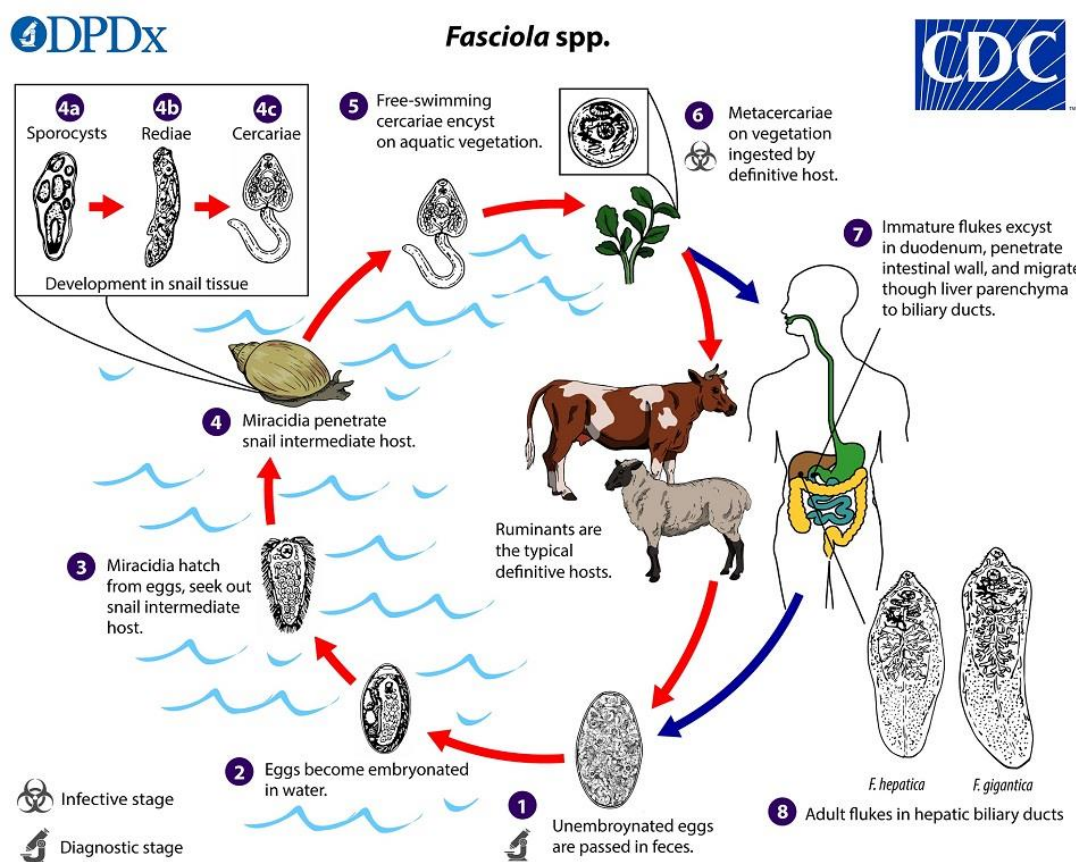


Figure 1. The life cycle of the liver fluke *Fasciola hepatica* (picture source: www.cdc.gov).

After the uptake of metacercariae, these dormant larvae undergo excystment in a two-phase process, activation first/emergence second, which takes place within the duodenum (Dixon, 1966). The first phase is triggered by carbon dioxide, reducing conditions, and a temperature of 39°C. Whereas the second phase depends on bile (Dixon, 1966). Once excysted, the newly excysted juveniles (NEJs), using cathepsin proteases as well as peristaltic-like movements and cycles of attachment/detachment via the ventral and anterior suckers, cross the barrier of the

intestine to migrate to the liver (Dalton et al., 2003; Sukhdeo and Mettrick, 1986). Within a week, NEJs reach the liver parenchyma by crossing Glisson's capsule (Lalor et al., 2021). The migration through the liver parenchyma boosts NEJs' growth by providing important nutrient sources (cells and blood) (Bennett, 1977). Hemorrhagic migratory tracts can be easily observed in the liver and are caused by the digestion of the tissue and the mechanical actions of the suckers (Lalor et al., 2021). To reach their final destination, i.e., bile duct, NEJs need 3 to 4 months. In the bile duct, the adults reach sexual maturity (**Figure 2**).

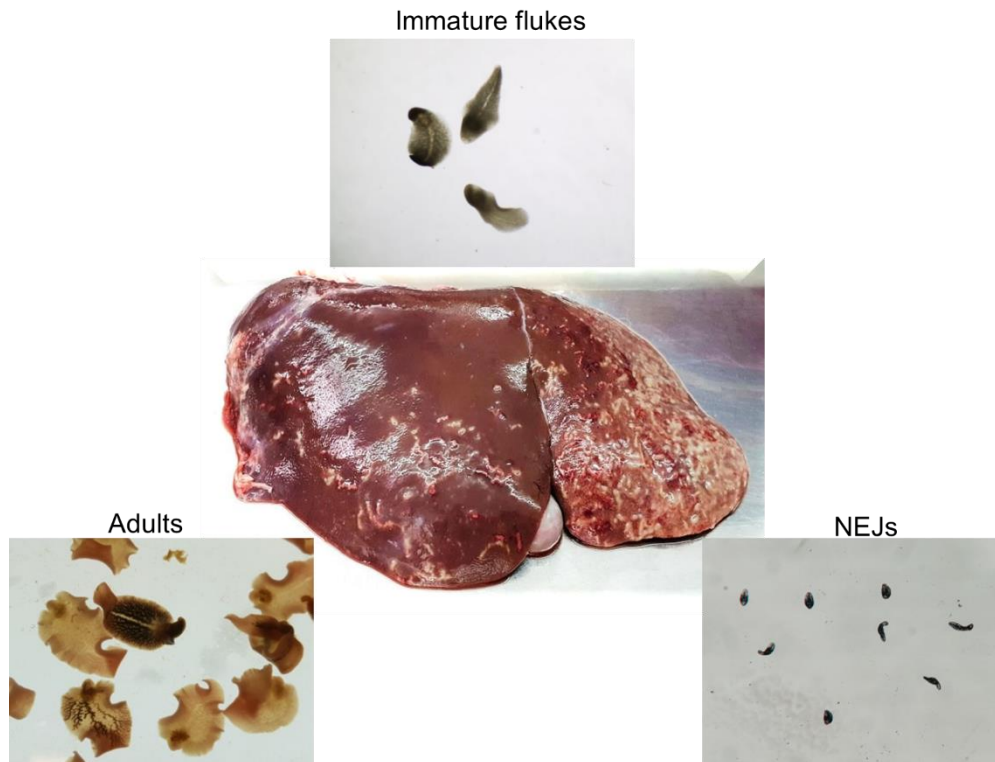


Figure 2. Different developmental stages of *F. hepatica*. An acutely infected sheep liver is shown with migration tracts and the different life stages. Before entrance into the liver, parasites are called newly excysted juveniles (NEJs), which grow into immature flukes feeding on parenchyma cells until they reach the bile duct to become sexually mature adults, which are capable of reproduction and shedding eggs (NEJs 200 μm ; Immature flukes 0.3-0.7 cm; Adult flukes up to 3 cm).

F. hepatica is a hermaphrodite. Although self-fertilization can also occur, cross-fertilization is the most common way of reproduction, (Cwiklinski et al., 2015, 2016). The adult flukes can remain in the bile duct for years, where they feed on hemorrhagic ulcers in the hyperplastic mucosa (Sukhdeo et al., 1988). Sexually mature adults can shed on average about 25,000 unembryonated eggs per fluke per day (Happich and Boray, 1969). Eggs are released in the intestine and finally to the surrounding environment through feces. These eggs are opaque in

color and oval in shape, measuring 130-150 μm by 63-90 μm (Mas-Coma & M.D. Bargues, 1997). Several factors influence egg development and hatching including pH, moisture to prevent the egg from desiccation, to be feces-free, and temperature which should range between 10°C and 30°C. With a temperature above 30°C, the development of the eggs slows, and at 37°C, the egg dies (Rowcliffe and Ollerenshaw, 1960). When conditions become favorable, the egg will embryonate and finally hatch. The miracidium, which represents the first and ciliated non-feeding larva, hatches through the operculum of the eggshell to reach the moist environment searching for a host snail (Rowan, 1956). The lifespan of the miracidium is between 8 and 24h and depends on its stock of glycogen and lipid granules, which is considered its energy source (Anderson et al., 1982). Therefore, the miracidium must find the host snail as soon as it hatches, and those, who fail, die within the next 24 h (Mas-Coma & M.D. Bargues, 1997). The intermediate host snail belongs to the genus *Lymnaea* (*Lymnaea truncatula*). The snail is entered by the miracidium via enzymatically driven perforation of the integument (Dawes, 1959). Within the snail, asexual multiplication takes place, which allows an expansion of a specific clone in a way that one single miracidium gives rise to almost 700 free-swimming cercariae (Lalor et al., 2021). The sporocyst is the second stage in the snail and develops from the miracidium through migration via the snail to become a ball packed with germ cells (Moazeni and Ahmadi, 2016). Next, a more damaging and active stage, the redia, is generated, which will give rise to the final stage found in the snail, the cercaria. This larval stage consists of a body with an oral and a ventral sucker, and a tail that allows swimming in water to find the final host (Lalor et al., 2021). After the development of cercariae is completed in the snail (4-6 weeks post-infection), they leave the snail under appropriate temperature and light conditions. With the help of their ventral suckers, cercariae attach to the vegetation of the surrounding moist (Lalor et al., 2021). Finally, cercariae form a protective double-layered cyst, the metacercariae, the dormant larval form.

1.6. Current therapeutic options against fasciolosis

Since the 1980s, triclabendazole (TCBZ) is the drug of choice to treat fasciolosis (Hodgkinson et al., 2013). And this is due to its broad range of action, which includes both juvenile and adult flukes (Novobilský and Höglund, 2015). This characteristic is unique to TCBZ and distinguishes this drug from others such as closantel or clorsulon, which both exert effects only against adult flukes but not against the younger stages (Fairweather, 2011).

Drug resistance is a heritable characteristic, this means that the frequency of the resistant genes will increase among the population of parasites subjected to a specific drug (Sangster, 1999). The first report that highlights resistance to TCBZ was on a Victorian sheep farm (Overend and Bowen, 1995). Cases of TCBZ resistance have emerged in several countries on different continents (Cabada et al., 2016; Ortiz et al., 2013). Concerning humans, the first case of TCBZ resistance was reported in the Netherlands for a 71-year-old man (sheep farmer), who remained positive for fecal eggs despite a long and combined treatment with TCBZ (Winkelhagen et al., 2012). TCBZ belongs to the family of benzimidazoles, which interfere with microtubule formation by binding to tubulin (Oxberry et al., 2000). Therefore, it is believed that TCBZ action resides in its capacity of blocking microtubule formation. Consequently, it is initially thought that the underlying mechanism of TCBZ resistance is through mutations in the β -tubulin gene, a mechanism that has been already shown in nematodes, for instance, *Haemonchus contortus* that was resistant to benzimidazole treatment, which was not the case in *F. hepatica* (Robinson et al., 2002). On the contrary, it has been well known that the alteration in the multidrug resistance efflux-pump activity is the origin of the resistance of some cancer cells to chemotherapy (Modok et al., 2006). In the related trematode *S. mansoni*, an association between an increased expression of the multidrug resistance (MDR) transporters and a reduced sensitivity to praziquantel (PZQ) has been shown (Kasinathan et al., 2010; Pinto-Almeida et al., 2015). Moreover, it has been suggested that the mechanism by which parasites resist anti-helminthics treatments often resides in the drug uptake and its metabolism. Similar findings in the liver fluke go in the same direction. For instance, it has been suggested that the alteration of the drug influx/efflux, as well as the enhancement of the metabolic capacity identified in TCBZ-resistant strains of *F. hepatica*, could explain the occurrence of resistance (Alvarez et al., 2005).

Altogether, because of the limited number of drugs with cross-stage activity and the already widespread resistance to TCBZ, finding an alternative drug is of great importance.

1.7. Aldehydes as cellular toxicants

Organisms are constantly under challenges from both the surrounding environment and from endogenous origins. One of the most important challenges is the presence of aldehydes. Therefore, challenging cells with aldehydes might be a strategy to affect the vitality of parasites. Thus, the toxic function of aldehydes might be employed as a therapeutic option. Aldehydes are organic compounds usually referred to R-CHO, where R can be any functional

moiety/carbon-containing substituent (O'Brien et al., 2005). Whether they are aliphatic or aromatic, aldehydes are considered a serious threat to the cells, and thus to the entire organism. Aldehydes are everywhere, not just in the environment such as in food materials, soil, water, air, cigarettes smoke, and combustion of fuels, but aldehydes have also endogenous origins, which are very diverse. They are the product of different processes such as lipid-peroxidation, metabolism of amino acids, carbohydrates, lipids, and vitamins (Feron et al., 1991; O'Brien et al., 2005). Why are aldehydes so dangerous? Aldehydes are highly reactive organic species, which are electron deficient (electrophiles). This feature of aldehydes allows them to easily react with electron-rich molecules (nucleophiles) by forming adducts. The latter is considered the primary source of aldehyde cytotoxicity in humans (Nelson et al., 2017). The organic nature of aldehydes makes them lipid-soluble, which are difficult to excrete from the body. Aldehydes can form adducts with several biomolecules such as DNA and proteins and, therefore, disrupt their biological function and thus induce pathogenicities such as cancer, diabetes, and degenerative disease (Nelson et al., 2017).

Once cells are affected by stress, they enter a survival mode reacting to overcome this threat. In the case of aldehydes presence, affected cells have developed several systems to eliminate these molecules. One of the most important systems is aldehyde-metabolizing enzymes, which are used to convert aldehydes to less reactive and thus less-harmful products that can easily be excreted from the body. Several aldehyde-metabolizing enzymes exist such as oxidases, aldo-keto reductases, alcohol dehydrogenases, short-chain dehydrogenases/reductases, cytochrome P450 enzymes (Edenberg and McClintick, 2018; Garattini and Terao, 2012; Manikandan and Nagini, 2018; Parés et al., 2008; Penning, 2015), and aldehyde dehydrogenases (ALDHs), which have been the focus of my work.

1.8. Aldehyde dehydrogenases in health and disease

ALDHs belong to a large superfamily of proteins. Today 160 ALDH genes from different organisms have been sequenced, and studies have shown that humans possess 19 putative ALDH genes clustered in 11 families and 4 subfamilies (Muzio et al., 2012). Phylogenetic studies showed the conservative nature of ALDH protein sequences from bacteria to humans (Muzio et al., 2012). On the one hand, this highlights that the biological role conferred by ALDHs is conserved through evolution. On the other hand, it emphasizes the importance of ALDHs presence in different organisms. A typical ALDH structure contains a catalytic domain, a binding domain for co-substrates, and a homodimer domain, which allows molecules

to form dimers or sometimes tetramers (Liu et al., 1997). It has long been established that two ALDHs, which are identical in more than 40% of their protein sequences, are considered to belong to the same family, and two ALDHs that share an identity in more than 60% of their protein sequences belong to the same subfamily (Vasiliou and Nebert, 2005). In addition to their role in detoxifying aldehydes by converting them into their corresponding carboxylic acids (Vasiliou et al., 2004), ALDHs are known for their role in cell proliferation, embryonic development, metabolism of neurotransmitters and hormones, as well as absorption of ultraviolet radiation in the cornea (Vasiliou et al., 2013). ALDHs are present in several tissues such as the liver, brain, kidney, and eye, and they can be found in several subcellular localization, such as mitochondria, nucleus, cytosol, and endoplasmic reticulum (Rodríguez-Zavala et al., 2019; Stagos et al., 2010). They are either expressed in a continuous manner or after induction (Lindahl, 1992; Takimoto et al., 1992).

Several studies have established a tight link between known human diseases and mutations in ALDH genes. Among those diseases, the Sjögren-Larsson syndrome, which results from a mutation in the *aldh3A2* gene (Rizzo, 2016). Another example is the ALDH5 family, which contains a very important enzyme called the succinic semialdehyde dehydrogenase (SSDH) encoded by the *aldh5A1* gene, which is highly expressed in the human brain. This enzyme is involved in the degradation of the γ -aminobutyric acid. Once the function of this enzyme is impaired, this acid will not be degraded but accumulates, which in turn is the origin of the development of moderate to severe neurological disorders such as mental retardation and seizures (Didiášová et al., 2020). Pyridoxine-dependent seizures originate from a mutation in *aldh7A1* (Mills et al., 2006), and hyperprolinemia type II originates from a mutation in the *aldh4A1* gene (Srivastava et al., 2012). Moreover, it has been shown that the alteration in ALDH function is the origin of the development of Parkinson's and Alzheimer's diseases (Grünblatt and Riederer, 2016).

1.8.1. Aldehyde dehydrogenases (ALDHs) and cell proliferation

Besides their role in converting aldehydes into their corresponding carboxylic acids, ALDHs have been long known for their intervention in several other biological mechanisms such as the metabolism of vitamins, hormones, neurotransmitters, and cell proliferation (Vasiliou et al., 2013). ALDHs are also responsible for generating retinoic acid, which plays an important role during development (Haselbeck et al., 1999; Mic et al., 2000). Moreover, the role of ALDHs in cell proliferation has been intensively discussed (Muzio et al., 2012). Several ALDH

molecules were identified to play important roles in cell proliferation. For instance, it has been shown that ALDH3A1 is involved in the regulation of cell proliferation by being involved in the catabolism of 4-hydroxynonenal, an endogenous compound that harbors the capacity to regulate gene expression (Muzio et al., 2012). Moreover, it has been shown that ALDH1A1 is a key marker for stem cells and together with ALDH3A1, they play roles in cell proliferation (Puttini et al., 2018; Wang et al., 2013). In addition, human hematopoietic cells show a high ALDH activity compared to their progeny (Christ et al., 2007). High levels of cytosolic ALDH expression are also observed in several other progenitor/precursor cells such as myogenic cells (myoblasts) and prostate cells (Burger et al., 2009; Jean et al., 2011).

1.8.2. ALDHs and drug resistance

The link between ALDH activity and drug resistance goes back to the finding that ALDHs can break down and metabolizing cyclophosphamide, a teratogen, which exerts a cytotoxic effect on the developing embryo. It is also used as chemotherapy in anticancer treatment (Domeyer and Sladek, 1980; Mirkes et al., 1991). ALDHs are an important factor in cancer biology by controlling the proliferation of cancer stem cells and thus, ALDHs are used as markers of these cells. Furthermore, a high expression of ALDH is strongly linked with the resistance of certain cancer cells to drug treatments (Pors and Moreb, 2014). This is the case for hematopoietic stem cells (HSCs), which have a high level of expression of ALDHs. This makes them not just capable of producing long-term and multi-lineage hematopoietic colonies, but also more resistant to the anti-cancer drug cyclophosphamide (Kastan et al., 1990). In line with the same observation, it has been shown that ovarian cancer cells presenting a high ALDH activity showed resistance to cancer chemotherapy using platinum-based agents (Roy et al., 2018).

Furthermore, flatworms possess stem cells, known as neoblasts. One of the most prominent examples are neoblasts of the planarian, *Schmidtea mediterranea*, which are well known for their role in the regeneration of this organism upon injury (Scimone et al., 2014). Neoblasts are also present in the trematode *S. mansoni*, and here they contribute to the homeostatic tissue maintenance in adults, most likely contributing to the parasite's longevity (Collins and Collins, 2016). In addition, it has been shown that neoblasts present in the tegument of *S. mansoni* play an important role in the regeneration of the tegument, and thus contribute to the survival of schistosomes in the mammalian host (Collins et al., 2016).

Taken together, ALDHs are highly expressed in normal stem cells as well as cancer stem cells but also, they might be highly expressed in the neoblasts of parasites. Therefore, ALDHs are not only interesting candidates for the design of novel anti-cancer drugs but they may also be considered potential antiparasitic targets.

1.9. Disulfiram (DSF)

In 1937, the editor of the Journal of the American Medical Association (JAMA) received a letter, in which the authors described workers in a rubber factory becoming involuntary abstainers of alcohol after grinding tetraethylthiuram disulfide (later called disulfiram), a compound that they described as a cure for alcoholism. Not until 1945, this compound was characterized as a drug sensitizing organisms to adverse effects of aldehydes that the body forms upon alcohol intake (Hald and Jacobsen, 1948). From that moment on, several advances have been made in understanding DSF and its mode of action. DSF can irreversibly inhibit ALDHs *in vitro* and *in vivo* (Lipsky et al., 2001a, 2001b). It has been shown that DSF, once incorporated, is reduced *in vivo* to diethyldithiocarbamate (DDC) within 4 min (Cobby et al., 1977). Moreover, studies have shown that DSF doesn't act directly on its targets, but via its most active metabolite S-methyl-N,N-diethylthiocarbamate sulfoxide (MeDTC-SO) (Hart and Faiman, 1992, 1994). Further work also investigated the mode of action of DSF, how DSF interacts with ALDH. It was suggested that DSF can form covalent adducts with ALDHs (Kitson, 1983). Other studies suggested the existence of disulfide bridge formation within the catalytic site (Vallari and Pietruszko, 1982). Therefore, DSF may serve as a suitable candidate for treating fasciolosis via the inhibition of ALDH in the parasite.

1.10. Objectives of the study

Fasciolosis is a neglected tropical disease (NTD) with a huge impact on animal and human health. Although TCBZ is the drug of choice to fight against *F. hepatica*, several reports have provided evidence of TCBZ resistance. Therefore, it is an urgent need to find alternative drugs, especially in the absence of an efficient vaccine.

Based on the hypothesis that aldehyde dehydrogenases (ALDHs) could be a potential target for the identification of inhibitors that affect the survival of *F. hepatica*, the aims of this study were:

- 1) To investigate (*in silico*) the presence of ALDHs in *F. hepatica*.
- 2) To study the expression profile of *Fhaldhs* (by qRT-PCR), which required first the identification of suitable reference genes in two different experimental settings: the intra-mammalian stages and the *in vitro*-cultured juveniles.
- 3) To analyze the expression pattern (by *in situ* hybridization) of *Fhaldhs*.
- 4) To check out if the identified ALDHs are enzymatically active.
- 5) To examine the effect of DSF, a well-known ALDH inhibitor, on several stages of *F. hepatica*.
- 6) To investigate the effect of DSF derivatives on *F. hepatica*.
- 7) To study the effect of DSF and the most potent DSF derivatives on stem-cell proliferation, and the induction of oxidative stress.
- 8) To explore the effect of knock-down of *Fhaldhs* transcripts (by RNA interference (RNAi)) on stem-cell proliferation.

2. MATERIALS AND METHODS

2.1. Materials

2.1.1. List of liquid chemicals

Chemical	Supplier	Batch/Cat#	Application
Acetic acid	Carl Roth	3738.5	<i>In situ</i> hybridization
Betaine solution (5 M), PCR reagent	Sigma	B0300	PCR
DEPC \geq 97%	Carl Roth	K028.3	<i>In situ</i> hybridization, <i>in vitro</i> transcription, dsRNA synthesis
DMSO	Sigma	D4540	Inhibitors' solvent
Ethanol Rotipuran®	Carl Roth	9065.4	Nucleic acids precipitation
Formaldehyde solution (37%)	Carl Roth	4979.1	Fixation of samples
Glycerol	Carl Roth	7530.1	<i>In situ</i> hybridization
HCl	Carl Roth	T134.1	<i>In situ</i> hybridization
Methanol Rotipuran®	Carl Roth	4627.1	Transfer buffer for western blot, preservation of samples
PCR-H ₂ O	Carl Roth	3478.1	PCR
ROTI® Mount Fluorcare	Carl Roth	HP19.1	Mount samples on glass slides for confocal imaging
Sodium hypochlorite solution	Carl Roth	9062.3	Excystment
Xylol	Carl Roth	9713.3	<i>In situ</i> hybridization

2.1.2 List of solid chemicals

Chemical	Supplier	Batch/Cat#	Application
Agarose NEEO	Carl Roth	2267.3	Gel electrophoresis
FastRed TR salt	Sigma	F8764	<i>In situ</i> hybridization
Glycine	Carl Roth	3790.2	<i>In situ</i> hybridization
Imidazole	Sigma	56750	Washing and elution during protein purification
Maleic acid	Sigma	M0375	<i>In situ</i> hybridization
Naphtol AS phosphate	Sigma	N5625	<i>In situ</i> hybridization
Ni-NTA Superflow	QIAGEN	30410	Protein expression and purification
SigmaFast™ Protease inhibitor cocktail tablets, EDTA-free	Sigma	S8830	Protein expression and purification
Tetraethylthiuram disulfide (disulfiram)	Sigma	86720	<i>In vitro</i> test on parasites
Tris	Carl Roth	4855.2	Buffer preparation
Dithiocarbamate derivative (028)	Philipps-Universität Marburg	AG Schlitzer (Tom Gallinger)	<i>In vitro</i> test on parasites

2.1.3 Buffers and solutions

Buffer/solution	Composition	Application
Bleaching solution	1 ml NaClO (6-14% active chlorine) + 9 ml dH ₂ O	Excystment
Blocking buffer	1x TBS, 0.1% Tween-20, 5% non-fat dry milk	Blocking after transfer of proteins to the membrane
Blocking solution	7.5% heat-inactivated horse serum (Sigma) in TNT	<i>In situ</i> hybridization
Coomassie Blue staining buffer	0.16% (w/v) Coomassie Brilliantblue R250; 3 ml con. HCl.	SDS-PAGE
dNTP mix	10 mM dATP; 10 mM dCTP; 10 mM dGTP; 10 mM dTTP	PCR
Fixation solution	4% formaldehyde in PBST	Fixation for EdU staining
Hatching solution	0.6% NaHCO ₃ , 0.45% NaCl, 0.4% sodium tauroglycocholate, 0.025 M HCl, 0.4% L-cysteine	Excystment
Hybridization solution	50% deionized formamide; 10% (w/v) dextran sulfate; 5x SSC; 1 mg/ml yeast RNA in formamide; 1% Tween 20	<i>In situ</i> hybridization
10x L-Mix	Sigma; #11464221	<i>In vitro</i> transcription
Maleic acid buffer	0.1 M maleic acid; 0.15 M NaCl; DEPC H ₂ O pH 7.5	<i>In situ</i> hybridization
PBS (10x)	1.37 M NaCl; 27 mM KCl; 81 mM Na ₂ HPO ₄ ; 18 mM KH ₂ PO ₄ ; dH ₂ O ad 1 l (pH 7.4); autoclaved	Wash buffer
PBSTx	1x PBS; 0.3 % Triton X-100	Wash buffer
Ponceau S Red staining buffer (10x)	2% Ponceau S in 30% trichloroacetic acid and 30% sulfosalicylic acid.	Visualization of proteins on membrane
Proteinase K Buffer	100 mM Tris (pH 8.0), 50 mM EDTA	<i>In situ</i> hybridization
RNase Inhibitor, murine	NEB	<i>In vitro</i> transcription
10x SDS-PAGE running buffer	250 mM Tris; 1.92 M glycine; 1% SDS; in 1 L H ₂ O and pH 8.3	SDS-PAGE
Separating gel buffer	0.4% SDS; 1.5 M Tris-HCl; pH 8.8	SDS-PAGE
20x SSC	3 M NaCl; 0.3 M Na ₃ C ₆ H ₅ O ₇ ; dH ₂ O ad 1 l pH 7.0	<i>In situ</i> hybridization
Stacking gel buffer	0.4% SDS; 0.5 M Tris-HCl; pH 6.8	SDS-PAGE
Substrate buffer	100 mM Tris-HCl; DEPC H ₂ O pH 8.0	<i>In situ</i> hybridization
TAE buffer (50x)	2 M Tris; 50 mM EDTA; 5.71% acetic acid; add 1 l dH ₂ O; pH 8.0	Gel electrophoresis
10x Transcription Buffer	Sigma; #11465384001	<i>In vitro</i> transcription
Transfer buffer	25 mM Tris, 192 mM glycine, 20% methanol and 0.06% SDS in dH ₂ O; pH 8.3	Transfer of proteins

2.1.4 Media and supplements

Media/supplement	Supplier	Batch/Cat#	Application
ABAM	C.C. pro	2-18-M	Supplement for culture medium
Ampicillin	Sigma	A9518	Antibiotic used for selection in cloning (final concentration 100 $\mu\text{g/ml}$)
APS	Sigma	A3678	SDS-PAGE
Chicken serum	GIBCO	16110082	Supplement for <i>in vitro</i> culture
IPTG	Carl Roth	CN08.2	Protein expression (final concentration 0.4 mM); blue-white selection (final concentration 0.2 mM)
Kanamycin	Sigma	K4000	Antibiotic used for selection in cloning (final concentration 50 $\mu\text{g/ml}$)
LB agar	Carl Roth	5210.2	15 g in 1 L dH ₂ O and autoclave; bacterial culture
LB medium	Carl Roth	X964.2	20 g in 1 L dH ₂ O and autoclaved; Bacterial culture
TEMED	Carl Roth	2367.3	SDS-PAGE
RPMI Medium 1640 (1x)	GIBCO	11835	<i>In vitro</i> culture
X-Gal ((5-bromo-4-chloro-3-indolyl- β -D-galactopyranoside)	PEQLAB	37-2610	Cloning (final concentration 0.004%)

2.1.5 List of qRT-PCR primers and size of the PCR product

Gene	Annotation	Forward primer (5'→3')	Reverse primer (5'→3')	Product (bp)
<i>tbcd</i>	Tubulin-specific chaperone D	CAGCAGCCGCATTTCAGGA	AGCCAAATGGTCAATCATCGC	176
<i>eprs</i>	Glutamyl-prolyl-tRNA synthetase	TACACCACAACCATCGAGGC	GTGGTCAATCCCCACGAGTT	167
<i>actb</i>	Actin, cytoplasmic 1	CATGTTTGAGACCTTCAACGCT	AGATCACGCCACAGCAAGGT	189
<i>snrpa1</i>	U2 small nuclear ribonucleoprotein A'	GAGAACATGGGTAGTACATTGG	CCAGATCCTCTGCTATGCG	148
<i>gapdh</i>	Glyceraldehyde-3-phosphate dehydrogenase	GCCAATGTTTCGTTCGGAG	TCAACGACCTTCTGAGTGGC	183
<i>letm1</i>	Leucine zipper- and EF-hand-containing transmembrane protein 1	AGATGGATAAGTTAGCCGAGG	ACCTTTTGAGACGCCGTAAG	184
<i>psmb7</i>	Proteasome subunit beta type 7	TCACCAAGGATTCCACGGAG	GATCTGGCAGATCCCGAATC	171
<i>ppplcb</i>	Protein phosphatase 1 catalytic subunit beta	GCAGTTGGTACTTTGTTTTCGG	CAGGCCATACCGCATTGAG	161
<i>abl1</i>	ABL proto-oncogene 1, cytosolic tyrosine kinase	CTGCCTGTACATACTGTGCC	GTGCGGTGAGTTCATGGTTC	154
<i>abl2</i>	ABL proto-oncogene 2, cytosolic tyrosine kinase	CGTTAGCGAATCCCAATCTAG	GGTCTCTGTGTAGTGACCG	179
<i>akt1</i>	Rac-alpha serine/threonine-protein kinase	TCTCGGTGGTGGTCTAGT	TATGTACTTCGTGTCCGTAGG	142
<i>plk1</i>	Polo-like kinase 1	ATGGCTAGTAAGGACGCTGC	TGCTTTCGGAACCACTTTCC	177
<i>pkc</i>	Protein kinase C	TAAAGAGGGCATCACAGCGG	GCCAACATTTCCACGGAG	172
<i>aldh1</i>	Aldehyde dehydrogenase 1 family member A	CGTTGAGAGTCCAATTTACGAC	AACCACCTGTGACGAGACGG	188
<i>aldh2</i>	Aldehyde dehydrogenase 2	AGTGAAGCGACTGACTTTGGA	CCACAACTTATCATAGATTCCT	176
<i>sod</i>	Superoxide dismutase	TTGGCGATCTGGGAAATGTTG	GACCGAGGTCGTCTCATTT	141
<i>sodex</i>	Extracellular superoxide dismutase	CAGATACCGCATCCCGTCAT	TCTTGACCTGCGTGTACGAC	151

2.1.6 List of primers and the purpose of their usage

Purpose	Forward primer (5'→3')	Reverse primer (5'→3')
Full-length cDNA cloning primers (<i>Fhaldh1</i>)	TATACATATGATGCGCTCC ATTGTTCTG	CTCAGCGGCCGCTTA GTGGTGGTGGTGGTG GTGGGAATTCTTCTG CGAG
3'end cloning primers (<i>Fhaldh1</i>)	CTCTTGACAACGGAAAAGC TGT	TTTTTTTTTTTTTTTTT TTTTTTTAA
Full-length cDNA cloning primers (<i>Fhaldh2</i>)	TATACATATGATGCTGCCG TTGTCTGTAGTG	CTCAGCGGCCGCTCA GTGGTGGTGGTGGTG GTGGTGACCGGTTTG GTCC
<i>In situ</i> hybridization without T7 sequence (<i>Fhaldh1</i>)	CTCTTGACAACGGAAAAGC TGT	GATCAGTTGACCAAC CTCCG
<i>In situ</i> hybridization with T7 sequence (<i>Fhaldh1</i>)	TAATACGACTCACTATAGG GAGACTCTTGACAACGGAA AAGCTGT	TAATACGACTCACTA TAGGGAGAGATCAGT TGACCAACCTCCG
<i>In situ</i> hybridization without T7 sequence (<i>Fhaldh2</i>)	CTCACCTGGGCTTGTCTTC	TGATCCAAACAGTTC CTGCTC
<i>In situ</i> hybridization with T7 sequence (<i>Fhaldh2</i>)	TAATACGACTCACTATAGG GAGACTCACCTGGGCTTGT TCTTC	TAATACGACTCACTA TAGGGAGATGATCCA AACAGTTCCTGCTC
Knock-down (KD) with T7 sequence (Neomycin)	TAATACGACTCACTATAGG GAGAGTGGAGAGGCTATTC GGCT	TAATACGACTCACTA TAGGGAGACATCCTG ATCGACAAGACCG
Knock-down (KD) with T7 sequence (<i>Fhaldh1</i>)	TAATACGACTCACTATAGG GAGATCGCTGGTACTCGGA TTTTC	TAATACGACTCACTA TAGGGAGAGCCCCGA CTAGATTGTAGCA
Knock-down (KD) with T7 sequence (<i>Fhaldh2</i>)	TAATACGACTCACTATAGG GAGATGGCTGTCAAACGG CTCAC	TAATACGACTCACTA TAGGGAGAGAAATCC GCATATCGTCCTC
Sequencing primers (<i>Fhaldh1</i>)	TTCTGGCCATGTAAAGGT AGC	GATCAGTTGACCAAC CTCCG
Sequencing primers (<i>Fhaldh2</i>)	AGTGAAGCGACTGACTTTG GA	CCACAACTTATCAT AGATTCCCT

2.1.7 Bacterial strains used for cloning

Bacterial Strain	Supplier	Batch/Cat#
NEB 5-alpha competent <i>E. coli</i> (High Efficiency)	NEB	C2987H
NEB 10-beta competent <i>E. coli</i> (High Efficiency)	NEB	C3019H
LOBSTR-BL21 (DE3)-RIL	Kerafast	EC1002

2.1.8 Enzymes

Enzymes	Supplier	Batch/Cat#	Application
DNase I (RNase-free)	NEB	M0303L	dsRNA synthesis, protein purification
FIREPol® DNA Polymerase	Solis Biodyne	01-01-00500	PCR
<i>Hind</i> III	NEB	R0104S	Cloning
Lysozyme from chicken egg white	Sigma	62971	Bacteria lysis during protein expression and purification
<i>Nde</i> I	NEB	R0111S	Cloning
<i>Not</i> I	NEB	R0189L	Cloning
Proteinase K, recombinant, PCR grade	Roche	03115801001	EdU staining, <i>in situ</i> hybridization
Q5 High-Fidelity DNA Polymerase	NEB	M0491S	PCR
RNase A	Sigma	R5503	Protein purification
RNase H	NEB	M0297S	Reverse transcription
<i>Sac</i> I	NEB	R0122S	Cloning
T4 DNA Ligase	NEB	M0202S	Cloning
T7 RNA Polymerase	Sigma	11000622	<i>In vitro</i> transcription
<i>Xho</i> I	NEB	R0146S	Cloning

2.1.9 Kits and antibodies

Kit/antibody	Supplier	Batch/Cat#	Application
Monarch DNA Gel Extraction kit	NEB	T1020L	PCR product extraction from agarose gel
Monarch Total RNA Miniprep kit	NEB	T2010S	Total RNA extraction
QuantiTect Reverse Transcription kit	QIAGEN	205313	cDNA synthesis
PerfeCTa SYBR Green Super Mix	Quanta	95054	Real-time qPCR
QIAGEN PCR Cloning kit	QIAGEN	231124	Cloning
Monarch Plasmid Miniprep kit	NEB	T1010L	Extraction of plasmid from bacterial culture
Click-it™ Plus EdU Alexa Fluor™ 488 Imaging kit	Invitrogen	C10637	Detection of proliferating cells
SuperScript IV Reverse Transcriptase kit	Invitrogen	18090010	cDNA synthesis
MEGAscript RNAi kit	Invitrogen	AM1626	Double-stranded RNA (dsRNA) synthesis
Pierce ECL Western Blotting Substrate	Thermo Scientific	32132	Detection for western blot
Anti-Digoxigenin-AP, Fab-Fragment	Sigma	11093274910	<i>In situ</i> hybridization
Goat anti-Rabbit IgG (H+L) secondary antibody, HRP conjugate	Thermo Scientific	31460	Western blot
Rabbit Monoclonal anti-6x His-tag antibody	Thermo Scientific	RBM2-6402-P1	Western blot

2.1.10 Molecular weight standards

Standards	Supplier	Batch/Cat#	Application
Hyperladder™ 50 bp	Bioline	BIO-33039	DNA gel electrophoresis
Color Prestained Protein Standard, Broad Range (10-250 kDa)	NEB	P7719G	Western blot

2.1.11 Online databases and Software

Name	Website	Application
NCBI	https://www.ncbi.nlm.nih.gov/	Homology search, literature search
WormBase ParaSite	https://parasite.wormbase.org/index.html	Homology search, protein blast
SMART	http://smart.embl-heidelberg.de/	Protein domain analyses
Primer3Plus	https://www.bioinformatics.nl/cgi-bin/primer3plus/primer3plus.cgi/	Primer design
Oligo Calc-Oligonucleotide	http://biotools.nubic.northwestern.edu/OligoCalc.html	Melting temperature adjustment
Oligo Analyzer Tool	https://eu.idtdna.com/pages/tools/oligoanalyzer	Primer characteristics analyses
Image J	https://imagej.nih.gov/ij/	Videos and images analyses
Clustal Omega	https://www.ebi.ac.uk/Tools/msa/clustalo/	Alignment
Reverse complement	https://www.bioinformatics.org/sms/rev_comp.html	Reverse complement sequence search
Excel	Microsoft Excel	Statistical analysis
MEGA11	https://www.megasoftware.net/	Phylogenetic tree construction

2.2 Methods

2.2.1. Ethics statement

Animal experiments using rats or sheep as hosts were performed under the European Convention for the Protection of Vertebrate Animals used for experimental and other scientific purposes (ETS No 123; revised Appendix A). Experiments involving rats were approved by the Regional Council (Regierungspraesidium) Giessen (V54-19c20 15 h 02 GI 18/10 Nr. A16/2018). Experiments with sheep were approved by the ethics commission of the Institutional Animal Care and Use Committee (IACUC) of the German Lower Saxony State Office for Consumer Protection and Food Safety (Niedersaechsisches Landesamt für Verbraucherschutz und Lebensmittelsicherheit) under reference number 33.8-42502-05-118A336.

2.2.2. Biological samples

2.2.2.1. Newly excysted juveniles (NEJs)

Metacercariae of an Italian strain of *F. hepatica* were purchased from Ridgeway Research (UK). These larvae were attached to plastic sheets in water. To obtain NEJs, excystment was done as previously described in (Houhou et al., 2019). Briefly, the outer layer of the encysted metacercariae was mechanically removed using a scalpel followed by 3-5 min exposure to a 10% bleaching solution consisting of freshly diluted sodium hypochlorite. After several rounds of washing with H₂O, metacercariae were then incubated in a pre-warmed hatching solution for at least 1-2 h at 37°C and 5% CO₂ until NEJs started to hatch. Hatched NEJs were collected progressively in RPMI1640 medium containing 1% ABAM-solution (10,000 units penicillin, 10 mg streptomycin, and 25 mg amphotericin B per ml). The remaining unhatched metacercariae were left overnight at 37°C to allow them to hatch. On the following day, the total amount of hatched NEJs was collected for either inhibitor testing or snap-frozen at -80°C for RNA extraction purposes.

2.2.2.2. Immature and adult fluke

Immature and adult worms were harvested from livers of male Wistar rats RjHan: WI (Janvier, France) or sheep orally infected with 25-30 (for rats) or 250 (for sheep) metacercariae. Rats were sacrificed by cervical dislocation after CO₂ anesthesia, while sheep were sacrificed by

bleeding after a bolt shot. Immature flukes were collected 4 weeks post-infection, whereas adult flukes were collected 12 weeks after infection. Immature juveniles were collected from chopped pieces of the liver. In contrast, adults were collected from bile ducts. Adult worms were kept for 1 h in 0.9% NaCl or in RPMI1640 medium containing 1% ABAM-solution to allow clearance of gut contents followed by overnight incubation with RPMI1640 medium supplemented with 1% ABAM-solution and 20% chicken serum (CS). Parasites were subsequently used to test compounds during *in vitro* culture or were snap-frozen and stored at -80°C until RNA extraction.

2.2.2.3. *In vitro*-grown juveniles

To obtain *in vitro*-grown juveniles of *F. hepatica*, NEJs were incubated on day 1 post-excystment in RPMI1640 medium supplemented with 50% CS at 37°C and 5% CO₂ (McCusker et al., 2016). The medium was refreshed regularly (2-3 times per week). Juveniles were incubated at a density of 10 juveniles per ml in a 2 ml reaction vial with its lid closed. At week 4 of culture, juveniles were harvested, washed in PBS, snap-frozen in liquid nitrogen, and stored at -80°C for RNA extraction or they were used subsequently for other purposes.

2.2.3. *In silico* analyses

2.2.3.1. Identification of orthologues in *F. hepatica*

The public domain tool WormBase ParaSite, version WBPS16 (Howe et al., 2017) was used to extract all gene or protein sequences from the genome of *F. hepatica* (Centre for Genomic Research, University of Liverpool, BioProject ID PRJEB25283). For this aim, and based on *S. mansoni* ALDH sequences, I used BLASTp searches to find orthologous sequences in *F. hepatica* and the SMART analysis tool to predict protein domains (Letunic et al., 2015). After collecting all the sequences, multiple sequence alignment was done using Clustal Omega (Sievers et al., 2011).

2.2.3.2. Phylogenetic tree construction

To create a phylogenetic tree for ALDH, protein sequences of known orthologues in different species were used. Name, accession numbers, and the sources are listed in (**Table 1**). Phylogenetic analysis was done using the Molecular Evolutionary Genetics Analysis

(MEGA11) software (Tamura et al., 2021). Briefly, all the protein sequences were extracted as previously described and then aligned using Multiple Sequence Comparison by Log-Expectation (MUSCLE). A “Maximum Likelihood Tree” method was applied which was done using the Bootstrap method with 1000 bootstrap replications.

Table 1. List of proteins used for phylogenetic tree construction of ALDH including the names of the species, the Gene IDs, the accession numbers, and the web sources.

Species	Gene ID	Accession number	Source
<i>Homo sapiens</i>	ALDH2	NP_000681	NCBI*
<i>Homo sapiens</i>	ALDH1A2	NP_003879	NCBI
<i>Mus musculus</i>	ALDH2	NP_033786	NCBI
<i>Mus musculus</i>	ALDH1A2	NP_033048	NCBI
<i>Gallus gallus</i>	ALDH2	NP_001376401	NCBI
<i>Gallus gallus</i>	ALDH1A2	NP_990326	NCBI
<i>Xenopus laevis</i>	ALDH2	NP_001087022	NCBI
<i>Xenopus laevis</i>	ALDH1A2	NP_001084244	NCBI
<i>Fasciola hepatica</i>	ALDH1a	maker-scaffold10x_208_pilon-snap-gene-0.16	WormBase ParaSite
<i>Fasciola hepatica</i>	ALDH2	maker-scaffold10x_80_pilon-snap-gene-0.189	WormBase ParaSite
<i>Schistosoma mansoni</i>	ALDH2	SmALDH_022	WormBase ParaSite
<i>Schistosoma mansoni</i>	SmALDH_312	Smp_312460	WormBase ParaSite
<i>Branchiostoma floridae</i>	ALDH2	106815	JGI genome portal**
<i>Branchiostoma floridae</i>	RALDH2	XP_035666435	NCBI
<i>Petromyzon marinus</i>	ALDHm	XP_032799899	NCBI
<i>Petromyzon marinus</i>	RALDH2	XP_032805864	NCBI
<i>Aedes aegypti</i>	RALDH1m	XP_001653648	NCBI
<i>Aedes aegypti</i>	RALDH1	XP_001660495	NCBI
<i>Nematostella vectensis</i>	ALDH2	179476	JGI genome portal
<i>Nematostella vectensis</i>	ALDH1a	181421	JGI genome portal
<i>Capitella teleta</i>	ALDH2	183731	JGI genome portal
<i>Capitella teleta</i>	ALDH1a	151890	JGI genome portal
<i>Caenorhabditis elegans</i>	ALDH1J2 (alh-2)	Q9TXM0	UniProt
<i>Drosophila melanogaster</i>	ALDH1A10	Q9VLC5	UniProt
<i>Arabidopsis thaliana</i>	ALDH1A1	AAM27004	NCBI

*National Center for Biotechnology Information; **Joint Genome Institute

2.2.4. Total RNA isolation

Total RNA was isolated from parasites using the Monarch Total RNA Miniprep kit (NEB) following the manufacturer's instructions. Briefly, at least 30-40 NEJs, 5-10 *in vitro*-grown juveniles, and 1 immature fluke were incubated in 300 μ l of 1x RNA/DNA protection buffer, whereas the adult fluke (usually cut in half from anterior to posterior) was incubated in 600 μ l of RNA/DNA protection buffer. Shock-frozen samples were manually grinded using pestles. The quality and the quantity of extracted RNA were checked by electropherogram analysis using the BioAnalyzer 2100 and an Agilent RNA 6000 Pico or Nano Chip according to the manufacturer's instructions (Agilent Technologies, USA). A good RNA quality is judged by the presence of two distinct RNA peaks, which correspond to 18S and 28S RNA (**Figure 3**). Isolated RNA was directly reverse-transcribed or stored at -80°C until usage.

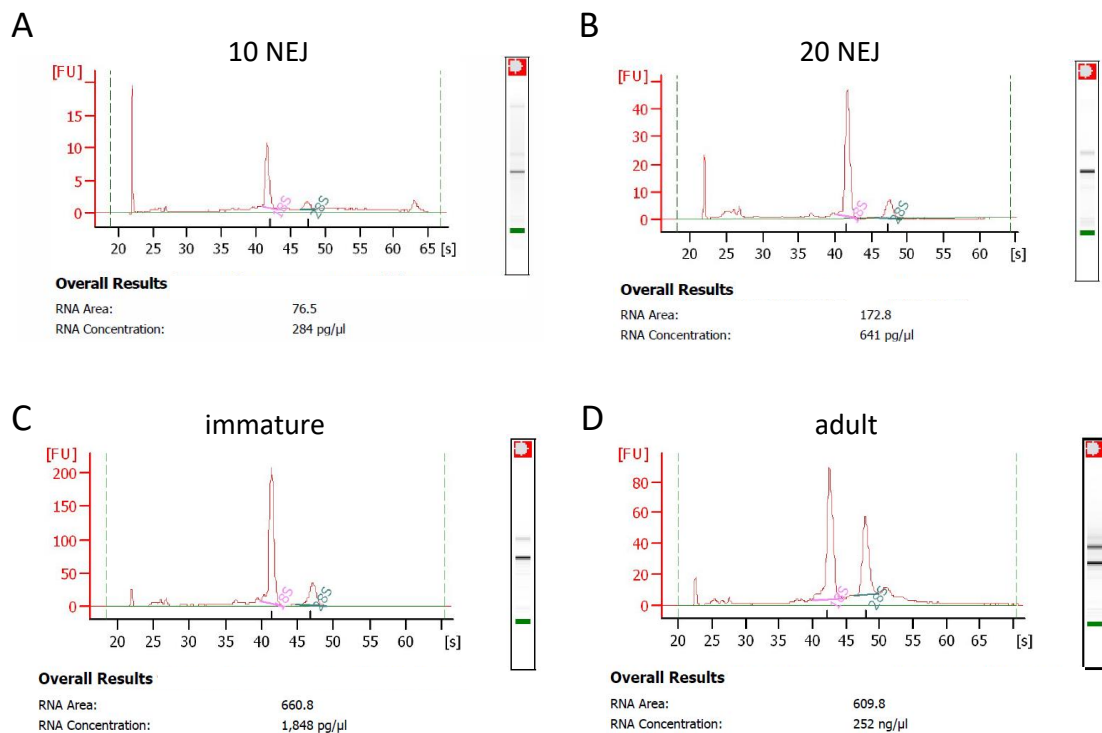


Figure 3. Quantity and quality of total RNA isolated from exemplary liver fluke samples.

Electropherogram analysis was obtained using BioAnalyzer (Agilent technologies). The diagrams show distinct RNA peaks extracted from 10 or 20 NEJs (A, B), 4-week-old immature (C), or 12-week-old adult flukes (D). Agilent RNA 6000 Nano Chip (adult) or Pico Chip (others) was used.

2.2.5. Reverse transcription

2.2.5.1. cDNA synthesis for qRT-PCR analysis

Reverse transcription of 5-10 ng of RNA was done using the QuantiTect Reverse Transcription Kit (Qiagen), which includes a genomic DNA (gDNA) removal step. In brief, incubation of RNA with 2 μ l of gDNA wipeout was done at 42°C for 2 min in a total volume of 14 μ l. Next, a mixture (6 μ l) of a Master Mix including, 5x Quantiscript RT buffer, RT primer mix, and reverse transcriptase was added to the previous reaction to get a total volume of 20 μ l. The mixture was incubated at 42°C for 30 min followed by an inactivation step of the enzyme at 95°C for 3 min. Before being used as a template in qRT-PCR, the total volume of cDNA was diluted at 1:5 or 1:10 in RNase-free water.

2.2.5.2. cDNA synthesis for cloning purposes

Total RNA isolated from adult *F. hepatica* was reverse transcribed using a superscript IV kit. For this aim, 2.5 μ g of RNA, 1 μ l of oligo(dt)₂₅ (50 μ M), and 1 μ l dNTP mix (10 mM) were mixed to a total volume of 14 μ l and incubated at 65 °C for 5 min and then on ice. To the mixture, 4 μ l of 5x first-strand buffer, 1 μ l of 0.1 M DTT, and 1 μ l of superscript IV reverse transcriptase were added and the total mixture was incubated at 50 °C for 1 h and then the enzyme was inactivated by heating at 70 °C for 15 min. 1 μ l of RNase H was incubated with the mixture at 37°C for 20 min. The mixture was finally diluted at 1:5 using RNase-free water.

2.2.6 Primer design for qRT-PCR

All primers used for qRT-PCRs were designed using the Primer3Plus software tool (Untergasser et al., 2012) and in a way, when possible, on different exons of a gene to distinguish amplification products derived from (contaminating) gDNA versus cDNA by size. Primers were designed to avoid the formation of homo or hetero dimers as well as hairpin structures. Moreover, “OligoCalc” (Kibbe, 2007) was used to check the optimal melting temperature (T_m), which was 60°C \pm 0.5°C in the salt-adjusted analysis. In addition, primers were designed to amplify a specific DNA fragment with a length between 140-200 bp. These qualities were checked using the online available tool IDT DNA oligo analysis. Primers were commercially synthesized by Integrated DNA Technologies IDT (Belgium), and they were used at a final concentration of 400 nM in a 10 μ l total reaction volume.

Before usage, qRT-PCR primers were tested for specificity and occurrence of primer dimers. This was done under standard PCR conditions using the FirePol Taq polymerase as listed below. Only primers yielding one specific product with no primer dimers were used for qRT-PCR.

Ingredients	Volume (μ l)
10x RBD buffer	5
MgCl ₂ (25 mM)	5
dNTP (20 mM)	0.5
Fire-pol	1
Forward primer (10 μ M)	2
Reverse primer (10 μ M)	2
cDNA (1:40)	2
PCR-H ₂ O	32.5

PCR program		
Cycle	Temperature	Time
1x	95°C	5'
35x	95°C	30''
	60°C	30''
	72°C	1'
1x	72°C	2'

The PCR product was purified from 2% agarose gel. The eluate served as starting material to prepare a standard curve with 1:10 dilution steps to calculate primer efficiencies (Dorak, M (Oxford: Taylor & Francis), 2008). Efficiency was considered good when it ranged between 90-100%.

2.2.7. Polymerase chain reaction

2.2.7.1. 3' Race PCR

The sequence of *Fhaldh1* available in Wormbase ParaSite appeared too long when compared to orthologues in other species. A scheme of the experimental approach for determining the actual sequence is shown (**Figure 4**). Before cloning the full cDNA length of *Fhaldh1*, I first identified the 3' end of the cDNA as follows:

Ingredients	Volume (μ l)
Q5 buffer	5
dNTP (20 mM)	1
Betaine	1.25
Q5 polymerase	1
Forward primer (10 μ M)	1
cDNA (with oligodt and 1:5)	2
DEPC-H ₂ O	12.75

PCR program		
Cycle	Temperature	Time
1x	98°C	3'
10x	95°C	20''
	65°C	20''
	72°C	1'

The forward primer (FP) is a primer that can anneal specifically to the gene body, and 65°C corresponds to its melting temperature (T_m). After this step, 1 μ l of the reverse primer (RP) was added. In this case, the RP is oligo(dt).

PCR program		
Cycle	Temperature	Time
10x	95°C	20''
	53°C	30''
	72°C	1'
22x	95°C	20''
	55°C	20''
	72°C	1'
1x	72°C	5'

53°C is the T_m of the reverse primer and 55 °C is the average T_m of both reverse and forward primers. The PCR product was purified from 2% agarose gel using Monarch DNA Gel Extraction kit and eluted in 10 μ l, and later cloned in pDrive (Qiagen) for sequencing (more description about the cloning method is provided in the cloning chapter).

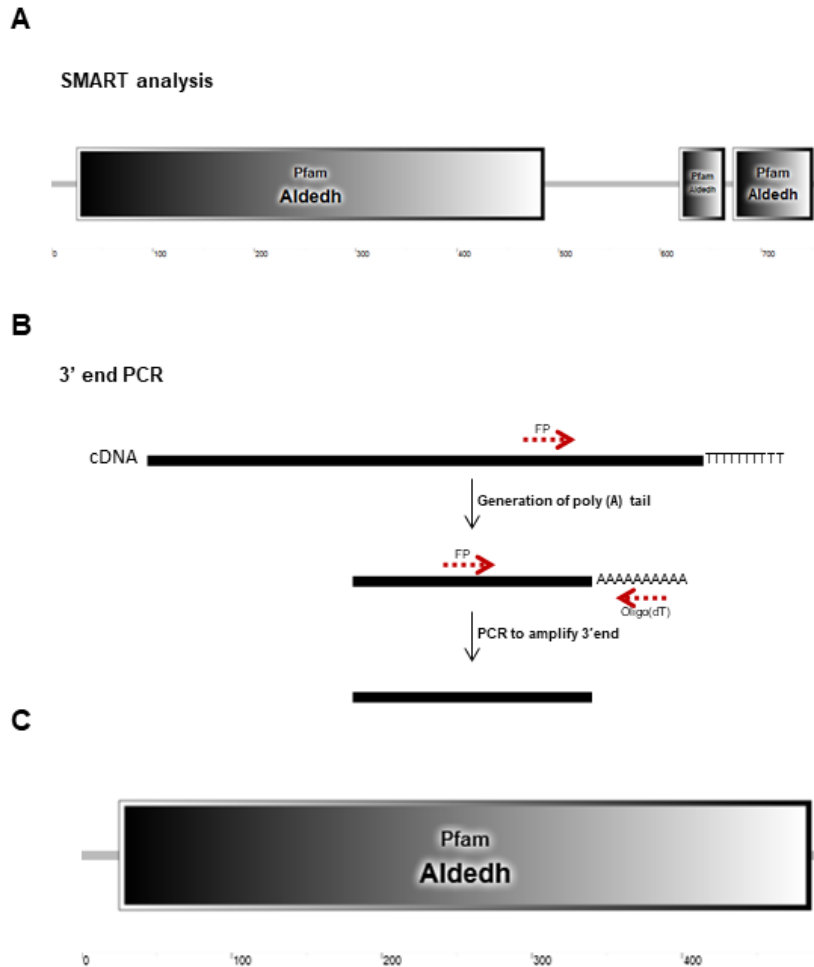


Figure 4. Cloning strategy to complete the full-length cDNA sequence of *Fhaldh1*. (A) SMART analysis shows two additional Aldehyd domains and thus a wrongly annotated sequence (the sequence found in the database is too long). (B) PCR strategy to identify the 3' end sequence of *Fhaldh1* and the completion of the sequence. (C) SMART analysis of revised *Fhaldh1* coding sequence and after confirmation by sequencing (Microsynth Seqlab, Germany).

2.2.7.2. Colony PCR

After the overnight growth of bacteria, I performed colony PCRs to confirm the presence of positive clones before extracting the plasmids. The reactions were done as follows:

Ingredients	Volume (μ l)
10x RBD buffer	2.5
MgCl ₂ (25 mM)	2.5
dNTP (20 mM)	0.25
Fire-pol	0.5
Forward primer (10 μ M)	1
Reverse primer (10 μ M)	1
PCR-H ₂ O	8.625

PCR program		
Cycle	Temperature	Time
1x	95°C	3'
35x	95°C	30''
	60°C	30''
	72°C	1'
1x	72°C	5'

Forward and reverse primers could be either those that amplify the whole sequence of the insert or those that bind and amplify a part of the cloned sequence. The PCR products were checked on 2% agarose gels. Positive colonies were inoculated in a 5 ml LB medium containing kanamycin and incubated at 37°C overnight. Subsequently, plasmids were extracted using Monarch Plasmid Miniprep kit (NEB) and then sent for sequencing (Microsynth Seqlab, Germany) to confirm cloning success.

2.2.7.3. qRT-PCR

For qRT-PCR, the 2x PerfeCTa SYBR Green SuperMix was used. The reactions were performed using the Rotorgene Q cycler (QIAGEN, Germany) under the following conditions: initial denaturation step at 95°C for 3 min, 45 cycles at 95°C for 10 sec, 60°C for 15 sec, and 72°C for 20 sec. The reaction took place in a 10 μ l total volume with 400 nM of each primer. At the end of each reaction, a melting point analysis was performed to ensure the absence of primer dimers and the presence of a single, specific product. All qRT-PCRs were performed in three to four biological replicates with three technical replicates for each sample. The expression of genes of interest (GOIs) was determined by relative quantification against the geometric mean of two selected reference genes (Houhou et al., 2019), which were “*Fheprs* and *Fhtbcd*” for *in vivo* life stages and “*Fhtbcd* and *Fhpsmb7*” for *in vitro*-grown parasite stages. Gene expression levels of different life stages were calculated using the formula: relative expression = $2^{-\Delta\Delta Ct} \times f$, with $f = 1000$ as an arbitrary factor. Fold change of gene expression levels between treated worms and control was calculated using the $2^{-\Delta\Delta Ct}$ method (Livak and Schmittgen, 2001).

2.2.8. Cloning

2.2.8.1. Cloning of PCR products with pDrive vector

Ligation of the *Fhaldh1* was done using the QIAGEN PCR cloning kit. The pDrive vector is a linear plasmid with 3'-prime U overhangs present at the truncated lacZ gene, which encodes β -galactosidase. When no PCR product is inserted, the enzyme will be expressed and will turn bacterial colonies blue in presence of X-gal and IPTG. When a PCR product is inserted, however, the gene remains truncated and thus encodes an inactive enzyme, therefore, colonies remain white. The ligation was performed in a 3:1 ratio. The ligation product was incubated at 4°C overnight. 10-beta competent *E. coli* strain (NEB) was transformed with recombinant plasmids by heat shock at 42°C for 30 sec. Next, the bacteria were plated on agar plates containing ampicillin, X-gal, and IPTG overnight at 37°C. Positive colonies (white colonies) were first subjected to colony PCR before being incubated in a 5 ml LB medium containing ampicillin at 37°C overnight for plasmid isolation (Monarch plasmid Miniprep kit; NEB). The sequencing results of several clones were analyzed to verify that the complete sequence of *Fhaldh1* was obtained.

2.2.8.2. Cloning of the PCR product in the expression vector pET-30a (+)

Once the full-length cDNA sequence of *Fhaldh1* (1488 bp) was completed, I designed a (His)₆-tagged *Fhaldh1* version into the expression vector pET-30a (+) (Merck KGaA, Darmstadt, Germany). For this aim, forward and reverse primers were designed in a way to include two different restriction sites *NotI* and *NdeI*, and a His-tag fused to the C-terminus of the protein. PCR reactions were done as follows:

Ingredients	Volume (μl)
Q5 buffer	5
dNTP (20 mM)	0.25
Q5 polymerase	0.25
Forward primer (10 μM)	1.25
Reverse primer (10 μM)	1.25
cDNA (RT with oligodt and 1:5)	1
PCR-H ₂ O	16

PCR program		
Cycle	Temperature	Time
1x	95°C	3'
5x	95°C	8''
	60°C	30''
	72°C	1'
30x	95°C	8''
	62°C	30''
	72°C	1'
1x	72°C	5'

The resulting products were purified from a 2% agarose gel and eluted in 15 μl. 1 μg of the empty plasmid as well as the PCR products were double digested using 1 μl of *NotI* and 1 μl of *NdeI* restriction enzymes. The reaction was performed in 3 μl of 3.1 buffer at 37°C for 2 h. Purification of the digestion products was done from 2% agarose gel. Ligation was run in a 3:1 ratio based on the following equation:

$$\text{ng PCR product (insert)} = (\text{bp (insert)} \times \text{molar ratio}) / \text{bp (plasmid)}$$

Ligation was performed in 20 μl containing 2 μl of T4 DNA ligase and 2 μl of T4 DNA ligase buffer. The mixture was incubated at 4°C overnight. 5-alpha competent (DH5α) *E. coli* strain was used for transformation with the ligation product, which was done by heat shock at 42°C for 30 sec. Antibiotics-free LB medium (300 μl) was added to the bacteria to let them recover at 37°C for 1 h before plating them overnight on agar plates containing kanamycin. To verify the presence of positive clones and in addition to performing colony PCR (explained above), restriction enzyme digestion was performed using 1 μl of each restriction enzyme in 3 μl cutsmart (NEB) or 2.1 buffer (NEB) in a total volume of 30 μl. The digestion was done using *XhoI* and *SacI* for *aldh1*, and *XhoI* and *HindIII* for *aldh2*. Digestion was performed at 37°C for 1h 30min, and the digestion products were checked on 2% agarose gels. Positive colonies were inoculated in a 5 ml LB medium containing kanamycin and incubated at 37°C overnight. Following plasmid isolation, the cloned sequences were confirmed by sequencing.

2.2.9. Evaluation of expression stabilities of reference genes

Four different software algorithms were used to determine the transcription stability of selected candidate reference genes: NormFinder, geNorm, BestKeeper, and the comparative Δ CT method (Andersen et al., 2004; Pfaffl et al., 2004; Silver et al., 2006; Vandesompele et al., 2002). Two separate sets of analyses were performed. On the one hand, cDNA samples from NEJs, immature and adult worms were analyzed to obtain the most stably transcribed genes for studies dealing with different life stages of the parasite. On the other hand, cDNA samples from NEJs and *in vitro*-grown juvenile worms were used to reveal the best reference genes for gene expression studies in *in vitro*-culture experiments.

The algorithm NormFinder determines intra- and inter-group variations across the different samples to calculate a stability value (M). Low variations give a low stability value, which indicates stable transcription of a gene. As input data, the calculated concentrations of qRT-PCR amplification were used (Vandesompele et al., 2002). The geNorm algorithm calculates pairwise variations of each reference gene when compared with the other genes based on relative Ct values. The stability value (M) is based on the average of these pairwise variations. Again, a stable transcription is reflected by a low M value. BestKeeper analysis was performed on raw Ct values. This algorithm assumes that stable reference genes should display similar transcription patterns, i.e., are highly correlated to each other. This is reflected by a high coefficient of correlation (r), whereby the most stably transcribed genes exhibit values closest to 1. The comparative Δ CT method compares the difference in Ct values of reference genes in pairs. The ranking is based on the variability of averaged standard deviations (Silver et al., 2006).

2.2.10. In situ hybridization

2.2.10.1. Amplification of specific target probes by PCR

PCRs were performed to amplify 300-500 bp of selected target sequences using specific primer sets. The following ingredients were used for PCR:

Ingredients	Volume (μ l)
10x Buffer B	2.5
MgCl ₂ (25 mM)	2.5
dNTP mix (20 mM)	0.25
Fire-pol. (5U/ μ l)	0.5
Forward primer (10 μ M)	1
Reverse primer (10 μ M)	1
cDNA (RT with oligodt and 1:5)	2
PCR-H ₂ O	15.25

PCR program		
Cycle	Temperature	Time
1x	95°C	1'
35x	95°C	30''
	60°C	30''
	72°C	30''
1x	72°C	6'

The PCR products were purified from 2% agarose gels. The purified PCR products (eluted in 15 μ l) were used as templates to run a second set of PCRs using primers containing the T7 promoter sequence. Each PCR reaction was performed either with the forward or the reverse primer containing the T7 sequence to generate sense and anti-sense probes.

Ingredients	Volume (μ l)
10x Buffer B	5
MgCl ₂ (25 mM)	5
dNTP mix (20 mM)	0.25
Fire-pol. (5U/ μ l)	0.5
Forward primer (10 μ M)	2
Reverse primer (10 μ M)	2
DNA (purified and 1:10)	2
PCR-H ₂ O	33.25

Two different combinations (2 PCR reactions) were used: FP+T7/RP-T7; FP-T7/RP+T7

PCR program		
Cycle	Temperature	Time
1x	95°C	1'
5x	95°C	30''
	65°C	30''
	72°C	30''
30x	95°C	30''
	60°C	30''
	72°C	30''
1x	72°C	1'

The totality of the PCR reaction was purified from 2% agarose gel and the corresponding eluate served as a DNA template for *in vitro* transcription.

2.2.10.2. RNA probes synthesis, precipitation, and purification

An amount of 500 ng of DNA was used to perform a 20 μ l *in vitro* transcription reaction:

Ingredients	Volume (μ l)
10x Transcription buffer	2
10x L-Mix	2
RNase inhibitor	0.5
T7 RNA polymerase	2
DEPC-H ₂ O	Calculated accordingly

The template volume was calculated to get a total amount of 500 ng and then adjusted by DEPC-H₂O to obtain a final volume of 20 μ l. The mixture was incubated at 27°C overnight. To remove the DNA template, 1 μ L of DNase I was added to the mixture, which was incubated at 37°C for 15 min. Precipitation of the generated probes was done by adding 3 μ l of lithium chloride (LiCl), 50 μ l of 100% EtOH and incubation at 80°C overnight. Next, the mixture was centrifuged at 10,000 x g at 4°C for 10 min. The supernatant was removed, and the RNA was resolved in 20 μ l of DEPC-H₂O. All the probes were diluted 1:1 with hybridization buffer and stored at -20°C until usage.

2.2.10.3. Preparation of the slides and hybridization of the probes

To localize the transcripts of *Fhaldh1* and *Fhaldh2*, I used a colorimetric approach of *in situ* hybridization as previously described in (Morawietz et al., 2020) with some modifications. Paraffin sections (5 μ m thickness, provided by Ariane Blohm) were treated 2x with xylol 100% at room temperature (RT) for 5 min each. Then a series of washing with decreasing EtOH percentage (100%, 90%, and 70%) was performed. Each step was done twice and at RT for 5 min. Lastly, slides were washed with DEPC-H₂O before incubation with 0.2 N HCl at RT for 20 min. Next, the slides were incubated with proteinase K buffer for 5 min, and then proteinase K was added (final concentration 1 μ g/ml) and incubated at 37°C for 20 min. Slides were washed one time with 0.2% glycine solution followed by 15 sec with pre-cooled 20% acetic acid followed by a washing step with PBS 1x and an incubation in 20% glycerol for 15 min. Slides were immersed in 2x SSC and then heated on a plate heater (70°C) for 10 min. After this step, the slides were transported on a pre-cooled metal rack at -80 °C and then incubated with 500 μ l of hybridization buffer at 55°C for 10 min. Right before adding them, the probes were denatured at 70°C for 10 min to remove secondary structures and then added to the slides (final concentration 1 ng/ μ l) and incubated at 42°C overnight. The slides were covered with cover slips.

2.2.10.4. Antibody incubation

After overnight incubation, the slides were immersed in a pre-heated 2x SSC+0.1% tween20 solution at 42°C for 15 min. A series of washing steps were applied using 1x SSC, and 0.5x SSC solutions at RT for 15 min each. Lastly, the slides were incubated with 1x maleic acid solution at RT for 5 min. 200 µl of 4% blocking solution was added to the slides and incubated at RT for 30 min. 2 µl of anti-DIG-AP antibody (1:2500) was incubated on the slides at RT for 2 h.

2.2.10.5. Signal detection

Slides were washed with 2x maleic acid solution at RT for 20 min each. Next, they were incubated 1x with substrate buffer at RT for 5 min. A mixture of developing solution was freshly prepared by dissolving 5 mg of naphthol-AS-phosphate in 100 µl DMSO and 25 mg of FastRed TR salt in 25 ml substrate buffer, mixing both compounds, and filtering the solution. Slides were incubated with 500 µl of the developing solution at dark. Once the staining signal was clear enough, the developing step was stopped with PBS and the slides were mounted using glycerol. Pictures were taken using a Leica microscope (M125 C) and a Leica camera (DMC2900; Leica, Germany).

2.2.11. Expression and purification of FhALDH in *E. coli*

2.2.11.1. Kinetics of FhALDH expression in *E. coli*

Protein expression of FhALDH was done in the LOBSTR *E. coli* strain (Kerafast) that was transformed using the vector containing the His-tagged FhALDH variant by heat shock at 42°C for 30 sec. An antibiotic-free medium (300 µl) was added to the mixture, which was incubated at 37°C for 1 h before plating on an agar plate containing kanamycin. After overnight incubation at 37°C, one colony of bacteria was used to inoculate 5 ml of LB medium containing kanamycin (1:1,000). Growth of bacteria was done overnight at 37°C with shaking at 170 rpm. The following day, the OD₆₀₀ was measured, and the bacteria solution was diluted to an OD₆₀₀ of 0.1. From this moment on, the OD₆₀₀ was checked regularly until it reached 0.6-0.8. At this point, protein expression was induced using 1 mM of IPTG, and the bacteria were left shaking at RT at 170 rpm. 1 ml of bacterial culture was collected each hour as well as right before the start of the induction. Bacteria were spun down for 2 min at 14,000 x g, the supernatant was

discarded, and the bacteria pellet was frozen at -20°C until usage. The last sample corresponded to an overnight incubation of the bacterial culture.

2.2.11.2. Expression and purification of FhALDH1 for enzyme assays

The LOBSTR *E. coli* strain was transformed as described above with the ligation product and incubated in 300 μl of an antibiotic-free medium at 37°C for 1 h before plating on an agar plate containing kanamycin. After overnight incubation, one bacterial colony served as starting material for plasmid extraction and preparation, which has been done using the Monarch kit. Briefly, a colony was inoculated in 20 ml of LB medium containing kanamycin at 37°C overnight. The next day, the OD_{600} was measured, and the bacterial solution was diluted to an OD_{600} of 0.1 right before incubation at the same temperature. The OD_{600} was followed progressively until it reached a value between 1.7-2.0. Then IPTG was added to the culture medium in a final concentration of 0.4 mM, and the bacteria were incubated at RT for 30 min to 1 h before an overnight incubation at 16°C . The following day, the bacteria were harvested by centrifuging at $8,000 \times g$ at 4°C for 15 min and then used directly or stored at -80°C until further use.

The bacteria pellet was resuspended in Tris-HCl 100 mM buffer pH 7.4 with lysozyme at a final concentration of 1 mg/ml and SigmaFast protease inhibitor cocktail tablet (final concentration 1.5 mg/ml; Sigma). The mixture was left at 4°C for 1 h with slight agitation. Next, the mixture was sonicated using a sonifier (BRANSON) for three min (1 sec on/1 sec off) at 60% of the maximum power. The whole mixture was centrifuged at $18,000 \times g$ at 4°C for 30 min. The supernatant (~ 10 ml) was incubated with 500 μl of Ni-NTA superflow beads at 4°C overnight. RNase A and DNase I (Sigma; NEB) were added to the mixture.

Protein purification was done using a column (Bio-RAD, Micro bio-spin column), where the beads were added progressively. Once all the beads were added, several elution steps followed with increasing concentrations of imidazole (10 mM-300 mM) to obtain the fraction with the highest amount of protein and the lowest impurities.

2.2.12. Protein analyses

2.2.12.1. Western blot

To confirm the protein expression of FhALDH, I used an SDS-PAGE. For this aim, a 12% separating gel and 1 mm thickness stacking gel were made. Since bacteria were used as starting material, I brought all the samples to an OD₆₀₀ of 0.05 to load equal amounts. Bacteria were resuspended in 2x SDS buffer, heated at 95°C for 5 min, and then the extract was loaded. Electrophoresis was done at 200 V for 45-50 min. Then, proteins were transferred on a nitrocellulose membrane (cut in the following size 8.5x6 cm). The transfer was done at 100 V for 1 h on ice. The success of the transfer was checked by soaking the membrane in 1x Ponceau S Red (Sigma Aldrich) staining solution and then washing several times with TBST 1x before blocking with 5% non-fat dry milk in 1x TBST 5% Milk freshly prepared and incubated at RT for 1 h on a shaker. Next, the membrane was washed 3x with TBST 1x for 10 min each and then incubated with the antibody (α -His; 1:1000) in 3% BSA at 4°C overnight. The following day, the membrane was washed 3x with 1x TBST at RT, and then the secondary antibody HRP-conjugated goat anti-rabbit IgG antibody (1:10,000) was added to the membrane and incubated with continuous shaking at RT for 1 h. Afterward, the membrane was washed 3x with TBST 1x and was then ready for signal development using an enhanced chemiluminescence reagent.

2.2.12.2. Coomassie staining

A 12% separating and 1 mm thickness stacking gels were made. 10 μ l of each protein fraction were mixed each with 6 μ l of 2x SDS loading dye and heated at 95°C for 10 min. The total volume was loaded as well as 3 μ l of unstained protein marker. Electrophoresis was performed at 100 V for the first 10 min and then at 150 V for 1 h to 1 h 30 min, or until the dye disappeared from the gel. Next, the gel was rinsed with dH₂O, immersed in Coomassie brilliant blue (Merck), and then heated in the microwave for 45 sec. Staining was done at RT overnight. Destaining was done by several washing steps with dH₂O until protein bands were clear with very less background.

2.2.13. RNA interference in *in vitro*-grown juveniles

2.2.13.1. Synthesis of dsRNA

To knock-down specific genes at the level of RNA, RNAi experiments were done using double-stranded RNA (dsRNA) on *in vitro*-grown juveniles. DsRNA was synthesized using the MEGAscript RNAi kit (Invitrogen) according to the manufacturer's instructions. The first step was the generation of a DNA template that was used for *in vitro* transcription. This was done using first a small PCR volume (25 μ l) followed by a big PCR volume (150 μ l).

Ingredients	Volume (μ l)
10x Buffer B	2.5
MgCl ₂ (25 mM)	2.5
dNTP mix (20 mM)	0.25
Fire-pol. (5U/ μ l)	0.5
Forward primer (10 μ M)	1
Reverse primer (10 μ M)	1
cDNA (1:10)	1
PCR-H ₂ O	16.25

PCR program		
Cycle	Temperature	Time
1x	95°C	1'
5x	95°C	30''
	65°C	30''
	72°C	30''
30x	95°C	30''
	60°C	30''
	72°C	30''
1x	72°C	1'

The PCR product was purified on a 2% agarose gel and eluted in 20 μ l. The purified PCR product served as a template for the big PCR, which was done as follows:

Ingredients	Volume (μ l)
10x Buffer B	15
MgCl ₂ (25 mM)	15
dNTP mix (20 mM)	1.5
Fire-pol. (5U/ μ l)	3
Forward primer (10 μ M)	6
Reverse primer (10 μ M)	6
DNA (purified and 1:10)	6
PCR-H ₂ O	97.5

PCR program		
Cycle	Temperature	Time
1x	95°C	1'
5x	95°C	30''
	65°C	30''
	72°C	30''
30x	95°C	30''
	60°C	30''
	72°C	30''
1x	72°C	1'

The primers used for PCR were designed to amplify a specific region of 400-600 bp in length, and they harbored T7 promoter sequences at their 5' and 3' ends (see chapter 2.1.6). The total PCR volume was loaded on a 2% agarose gel, purified by Monarch DNA Gel Extraction kit (NEB), and subsequently used as a template for *in vitro* transcription. An amount of 1 µg of each template DNA was used as starting material in the following reaction:

Ingredients	Volume (µl)
10x T7 reaction buffer	2
ATP	2
CTP	2
GTP	2
UTP	2
T7 enzyme mix	2
DEPC-H ₂ O	To be determined

The mixture was incubated at 37°C for 2 h. After *in vitro* transcription, the reaction product was stored at -20°C or used directly for subsequent steps. Single-stranded RNA (ssRNA) and DNA templates were digested with RNase and DNase I respectively as follows:

Ingredients	Volume (µl)
10x digestion buffer	5
dsRNA	20
DNase I	2
RNase	2
Nuclease-free H ₂ O	21

The mixture was incubated at 37°C for 1 h and 30 min. After the completion of the digestion, dsRNA was purified on a column according to the manufacturer's instructions MEGAscript RNAi kit (Invitrogen). Elution was done 2x with 50 µl preheated elution solution at 95°C. Lastly, the dsRNA was subjected to precipitation by adding 1/5 volume LiCl 4 M and 2/5 volume of 100% EtOH and incubated at -80°C overnight. The following day, the reaction was centrifuged at 4°C for 30 min at 13,000 x g, the pellet was washed with 500 µl of pre-cooled 70% EtOH, and centrifuged at 4°C for 10 min at 13,000 x g. The pellet was air-dried and resuspended in 50 µl of elution buffer. The quantity of dsRNA was measured by spectrophotometer analysis, and the quality of dsRNA was checked on 1.5% agarose gels. DsRNA was then stored at -20°C until further use.

2.2.13.2. Soaking of dsRNA by the juveniles

For RNAi experiments, 15-20 *in vitro*-grown juveniles were used per condition, and the knock-down was performed in 2 ml Eppendorf tubes. 5 µg of dsRNA was added to 50 µl of plain RPMI1640 in each condition (100 ng/µl). The mixture was incubated overnight at 37°C. The following day, 500 µl to 1 ml of RPMI1640 supplemented with 50% chicken serum was added to the culture. Fresh dsRNA was added every 2 days. The parasites remained under knock-down between 7-14 days. At the end of the culture, worms were either snap-frozen for RNA extraction or fixed with 4% PFA/PBS at RT for 4 h and dehydrated subsequently with MeOH for ultimate EdU staining analysis. In the latter case, 500 µM of EdU (from 10 mM stock) was added 48 h before the end of the culture. Thus, EdU was added together with the last added dsRNA.

2.2.14. In vitro compound testing

2.2.14.1. Testing compounds against newly excysted juveniles (NEJs)

NEJs were distributed in 3 cm dishes containing 3 ml of RPMI/1% ABAM-solution with 10 individuals per test condition. Medium-containing inhibitor was refreshed daily, and motility was assessed 24, 48, and 72 h post-treatment. Given the fact that the used inhibitors were dissolved in DMSO, this solvent was used as a control and in an amount equivalent to the highest concentration of the tested compounds. For documentation, 5 min videos with 500 ms intervals and a total of 601 frames were recorded for each condition (treated and control) using a stereomicroscope (SMZ-171-TLED from Motic, Germany) with a camera (SC30 Olympus) and followed by analysis with the wrMTrck plugin in Image J software (Schneider et al., 2012). For the analysis, the videos were uncompressed using Virtualdub64 software and saved in AVI format. Next, the videos were opened in Image J and set in greyscale 8-bit. The following screenshot shows the settings of the parameters used for the analysis of NEJs motility (**Figure 5**).

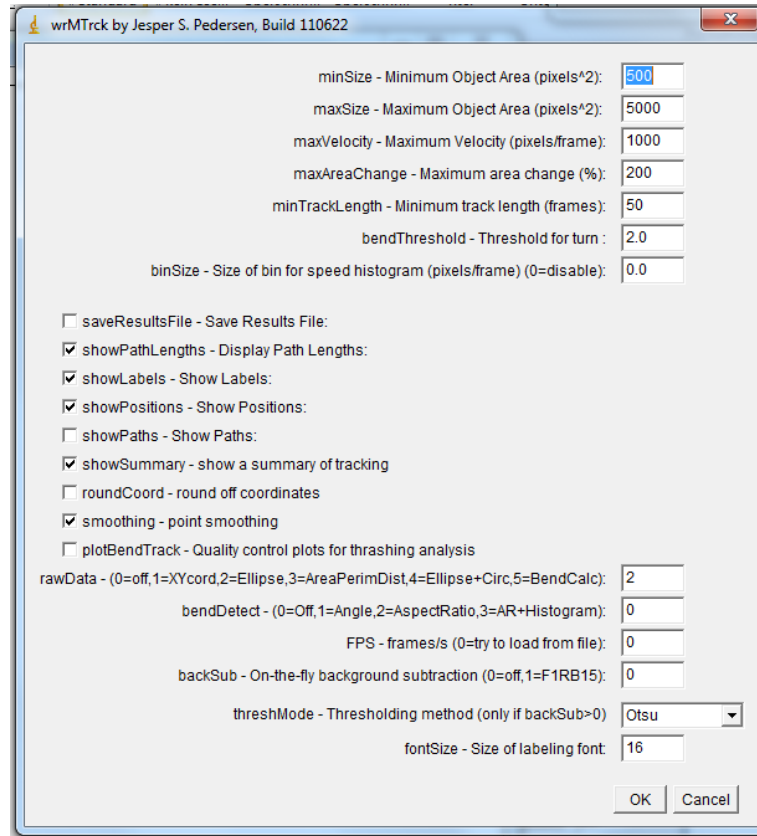


Figure 5. Motility analysis of NEJs. Screenshot showing parameters settings for the analysis of NEJs motility using wrMTrck plugin in Image J software.

2.2.14.2. Compounds against immature and adult flukes

Inhibitors were tested against immature and adult flukes. For this aim, worms were individually cultured in 12-well plates, usually 3-4 worms per condition, in 3 ml of RPMI medium, to which CS was added in a final concentration of 5% to maintain a basic survival condition. Medium and inhibitors were refreshed daily, and worm motility was assessed after 24, 48, and 72 h. Worm motility was scored with 3 for normal motility, 2 for reduced motility, 1 for minimal and sporadic movements, and 0 if flukes were dead. Images of worms as well as their motility were recorded using a stereo microscope (M125 C, Leica; SMZ-171-TLED, Motic). At the end of the experiment (after the 72 h culture), flukes were individually snap-frozen in Monarch RNA Protect Buffer and stored at -80°C until RNA extraction.

2.2.15. Analysis of cell proliferation

2.2.15.1. Samples preparation

I took advantage of the *in vitro*-grown juveniles that are small enough for a whole-mount preparation and that harbor a very good number of proliferating neoblasts (McCusker et al., 2016) easily accessible for imaging purposes. Juveniles were grown *in vitro* using RPMI medium supplemented with 50% CS. Four-weeks old juveniles were treated either with 1 μM of 028 (a test substance kindly provided by the working group of Prof. Schlitzer, Marburg; see Results) or 15 μM of DSF for 48 h. 24 h before the end of treatment and right before fixation, the medium was refreshed with newly inhibitor added as well as the thymidine analog EdU. EdU was used at a final concentration of 500 μM (prepared from 10 mM stock in PBS). The fixation was done using freshly prepared 4% PFA/PBS 0.3% Triton-100X (PBST) at RT with rotation for 4 h. Next, samples were dehydrated progressively in PBST, 50% MeOH/ PBST, and 100% MeOH at RT for 10 min each and stored at -20°C for further usage.

2.2.15.2. Staining

To visualize proliferative somatic cells (neoblasts) in *F. hepatica*, stored samples in 100% MeOH were rehydrated with 50% MeOH/PBST and washed with PBST before permeabilization with proteinase K (final concentration 5 $\mu\text{g}/\text{ml}$) at RT for 7 min. Afterward, the samples were fixed with 4% PFA/PBST at RT for 10 min followed by a washing step in PBST. A Click-iT Plus EdU Alexa Fluor 488 imaging kit (Invitrogen) was used to visualize cells that incorporated EdU during DNA synthesis (proliferating cells). The reaction takes place between a picolyl azide group harbored by the Alexa Fluor and the alkyne group harbored by EdU. This reaction is catalyzed by copper. A counter staining for the nuclei was done by incubating samples with Hoechst 33342 at RT for 20 min. Before imaging, the samples were mounted on glass slides using ROTI Mount Fluorcare (Carl Roth) and covered with cover slips.

2.2.15.3. Confocal imaging

Confocal laser scanning microscopy (CLSM) was done using a TSC SP5 microscope (Leica, Germany) and with the Leica LAS AF software. Alexa Fluor 488 was excited using an argon-ion laser at 488 nm, and Hoechst at 405 nm. Optical section thickness and background signals

were defined by setting the pinhole size to 1 Airy unit. Pictures were taken using the 20x objective with a sequential scanning, a line average of 4, and the resolution set to 1024x1024.

2.2.16. Statistical analysis

Statistical analyses were done using either a t-test or Mann-Whitney test using Excel. Error bars represent the standard error of the mean (SEM). P-values < 0.05 were considered significant.

3. RESULTS

3.1. Identification of housekeeping genes for real-time qPCR analyses in *F. hepatica*

This work is divided into two parts. In this part, I focus on the identification of stably expressed genes, which can be later used as reference genes for real-time qPCR analyses.

3.1.1. Choice of candidate reference genes

As a starting point, I chose eight different candidate reference genes to identify the most stably expressed reference genes, which subsequently will be used for normalization during the quantification of gene expression during the life cycle of the liver fluke or *in vitro* cultivation. Gene names, accession numbers as well as biological functions are summarized in (**Table 2**). Previously published transcriptome datasets and scientific literature have served as starting points for the selection of suitable reference gene candidates. In detail, β -actin (*actb*) and small nuclear ribonucleoprotein (*snrpa1*) were chosen because their stable expression has been shown in selected life stages of the liver fluke *Clonorchis sinensis* (Yoo et al., 2009). Similarly, the selection of tubulin-specific chaperone D (*tbcd*) and protein phosphatase 1 catalytic subunit beta (*ppp1cb*) was based on transcriptome analyses, which suggested a stable expression of the orthologues genes in all life stages of the blood fluke *Schistosoma mansoni* (Lu et al., 2017). In addition, we have chosen the leucine zipper and EF-hand containing transmembrane protein 1 (*letm1*) and proteasome subunit beta type-7 (*psmb7*) as candidates based on their stable expression during *in vitro* culture of *S. mansoni* (Haeberlein et al., 2019). Moreover, a previous study on different strains of *F. hepatica* indicated that the glutamyl-prolyl-tRNA synthetase (*eprs*) was stably expressed (Radio et al., 2018). Therefore, I included the corresponding orthologue. Finally, I included the well-known housekeeping gene *gapdh*, which is widely used for normalization in *F. hepatica* studies (Cwiklinski et al., 2018; McVeigh et al., 2014; Rinaldi et al., 2008). I identified the orthologues for all eight genes by BLASTp search against the genome of *F. hepatica*, and the presence of conserved protein domains was confirmed by SMART analysis (**Supplementary Figure 1**).

Table 2. Overview of candidate reference genes for the study of gene expression in *F. hepatica*.

Gene name	Gene ID	Homology (e-value) *	Protein function
<i>Fhtbcd</i>	maker-scaffold10x_815_pilon-snap-gene-1.87	Tubulin-specific chaperone D [<i>Homo sapiens</i>] (7e-177)	Cofactor D is one of four proteins involved in the pathway leading to correctly folded beta-tubulin from folding intermediates.
<i>Fheprs</i>	maker-scaffold10x_14_pilon-snap-gene-0.109	Glutamyl-prolyl-tRNA synthetase [<i>Homo sapiens</i>] (0.0)	The protein encoded by this gene is a multifunctional aminoacyl-tRNA synthetase that catalyses the aminoacylation of glutamic acid and proline tRNA species.
<i>Fhletm1</i>	maker-scaffold10x_721_pilon-snap-gene-0.10	Leucine zipper and EF-hand containing transmembrane protein 1 [<i>Homo sapiens</i>] (2e-85)	The protein functions to maintain the mitochondrial tubular shapes and is required for normal mitochondrial morphology and cellular viability.
<i>Fhactb</i>	augustus_masked-scaffold10x_269_pilon-processed-gene-0.18	Actin, cytoplasmic 1 [<i>Homo sapiens</i>] (0.0)	Actins are highly conserved proteins that are involved in cell motility, structure, integrity and intracellular signaling. The encoded protein is a major constituent of the contractile apparatus and one of the two non-muscle cytoskeletal actins that are ubiquitously expressed.
<i>Fhsnrp1</i>	maker-scaffold10x_234_pilon-snap-gene-0.20	U2 small nuclear ribonucleoprotein A' [<i>Homo sapiens</i>] (5e-72)	This gene encodes a protein which is a component of the spliceosome and it is involved in pre-mRNA splicing.
<i>Fhppp1c</i> <i>b</i>	maker-scaffold10x_238_pilon-snap-gene-0.95	Protein phosphatase 1 catalytic subunit beta [<i>Homo sapiens</i>] (0.0)	The protein encoded by this gene is one of the three catalytic subunits of protein phosphatase 1 (PP1). PP1 is a serine/threonine specific protein phosphatase known to be involved in the regulation of a variety of cellular processes.
<i>Fhpsmb7</i>	maker-scaffold10x_1452_pilon-augustus-gene-0.11	Proteasome subunit beta type-7 [<i>Homo sapiens</i>] (1e-79)	Important component of the cellular protein degradation complex
<i>Fhgapdh</i>	maker-scaffold10x_2706_pilon-snap-gene-0.15	Glyceraldehyde-3-phosphate dehydrogenase [<i>Homo sapiens</i>] (0.0)	GAPDH catalyzes the sixth step of the glycolysis by converting D-glyceraldehyde 3-phosphate to 3-phospho-D-glyceroyl phosphate

3.1.2. RNA quality of parasite samples and performance of qRT-PCR primers

I aimed to identify stably expressed genes for the intra-mammalian stages or the “*in vivo*”, (NEJs, 4-week-old immature flukes, 12-week-old adults), and *in vitro*-cultured NEJs (called 4-week-old juveniles) vs. non-cultured NEJs (**Figure 6**).

After total RNA isolation, the good integrity of RNA samples was shown by the presence of 18S and 28S peaks in the electropherograms from BioAnalyzer analysis (**Figure 3**, Materials and Methods chapter). An efficient qPCR analysis relies on specific and efficient primers. Therefore, I checked the specificity of the designed primers by PCR. The results showed the presence of one single band in each tested case, which reflected one specific amplification product of the expected size for each candidate reference gene. Moreover, the absence of unspecific products and primer-dimer formation as well as the absence of genomic DNA (gDNA) were checked by melt-curve analysis. The efficiencies of amplification for all designed primer pairs for qRT-qPCR ranged between 90-100%. I assessed the expression levels of the eight candidate reference genes by determining the Ct values for each sample. With average Ct values of 15.27 to 27.63, all candidate genes were within the range of acceptable and potential reference gene expression levels ($15 < Ct < 30$). *gapdh* turned out to be the most abundantly transcribed gene. In contrast, *ppp1cb* showed the lowest transcript levels.

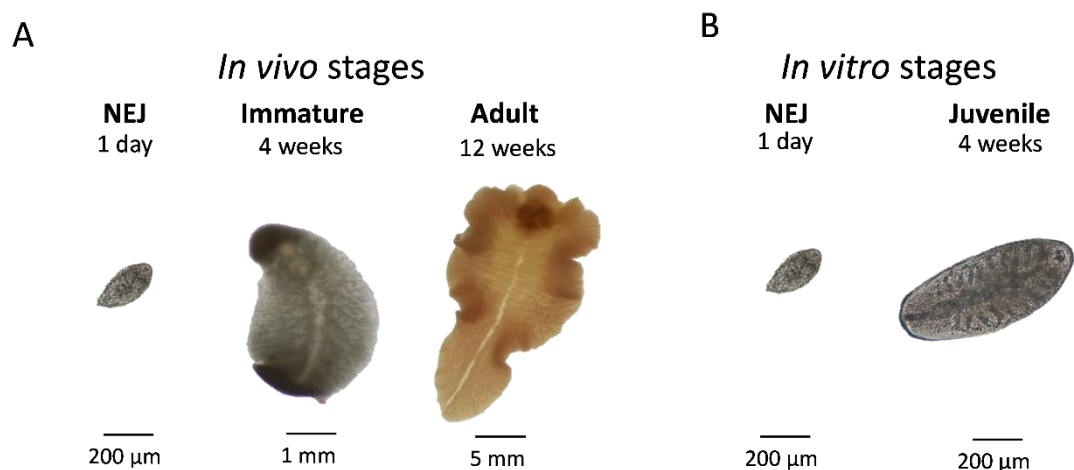


Figure 6. Different life stages of *F. hepatica*. (A) Intra-mammalian stages: newly excysted juvenile (NEJ), immature and adult worms. (B) *In vitro* stages: NEJ and *in vitro*-cultured juvenile.

3.1.3. Identification of the most stable reference genes

To identify the most stably expressed reference genes, 4 algorithms were used: NormFinder, geNorm, BestKeeper, and the comparative ΔCt method. These algorithms use different input data (as explained in Material and Methods), and they were used to evaluate the expression stability of eight candidate genes. The reference gene candidate, which shows the most stable transcript profile, is the one that exhibits a low stability value (NormFinder, geNorm, ΔCt method) or has a high coefficient of correlation (BestKeeper) (for more details see Materials and Methods chapter).

3.1.3.1. Identification of the most stably transcribed reference genes in intra-mammalian stages

Firstly, I determined the expression (= transcript level) stability of the selected candidate genes between the three different fluke stages, which led to a ranking using each of the algorithms (**Figure 7; Supplementary Table 1**).

The stability value M is obtained using different algorithms. A good reference gene (a stably expressed gene) is defined as one that exhibits an M value below 1 in heterogeneous cells or among a set of tissues (Vandesompele et al., 2002). In other words, the lower the M value is, the more stably expressed (transcribed) is the gene. On the one hand, NormFinder identified the tRNA-synthetase *Fheprs* and the proteasome subunit *Fhpsmb7* as the top two candidates, whereas *Fhgapdh* was the least stably expressed gene (**Figure 7A**). In contrast, the geNorm algorithm identified the tubulin chaperone *Fhtbcd* and *Fheprs* as the two best reference genes and *Fhgapdh* as the less stably expressed gene (**Figure 7B**). BestKeeper identified *Fhtbcd* and the actin *Fhactb* as the best reference genes and the protein phosphatase subunit *Fhppp1cb* as the worst (**Figure 7C**). Using the fourth and last algorithm, the ΔCt method, *Fheprs* and *Fhtbcd* appeared as the most stably and *Fhgapdh* as the least stably expressed genes (**Figure 7D**).

Since heterogeneous rankings resulted from these different algorithms, I established, by assigning the numbers 1-8 to each stability coefficient, a global ranking, which considered the used algorithms. Here, rank 1 refers to the most stable gene and 8 to the least stable one. Based on this ranking, I created the geometric mean of these ranks for each gene. The result showed that the glutamyl-prolyl-tRNA synthetase *Fheprs* and tubulin-specific chaperone D *Fhtbcd* appeared to be the most stable reference genes for this study, thus the most suitable ones for comparisons of intra-mammalian fluke stages. The commonly used housekeeping gene

Fhgapdh was revealed as the least suitable one among the eight selected genes. Ranking according to the average calculated rank was as follows: *Fheprs* < *Fhtbcd* < *Fhpsmb7* < *Fhactb* < *Fhsnrpa1* < *Fhletm1* < *Fhppp1cb* < *Fhgapdh* (**Figure 9A**).

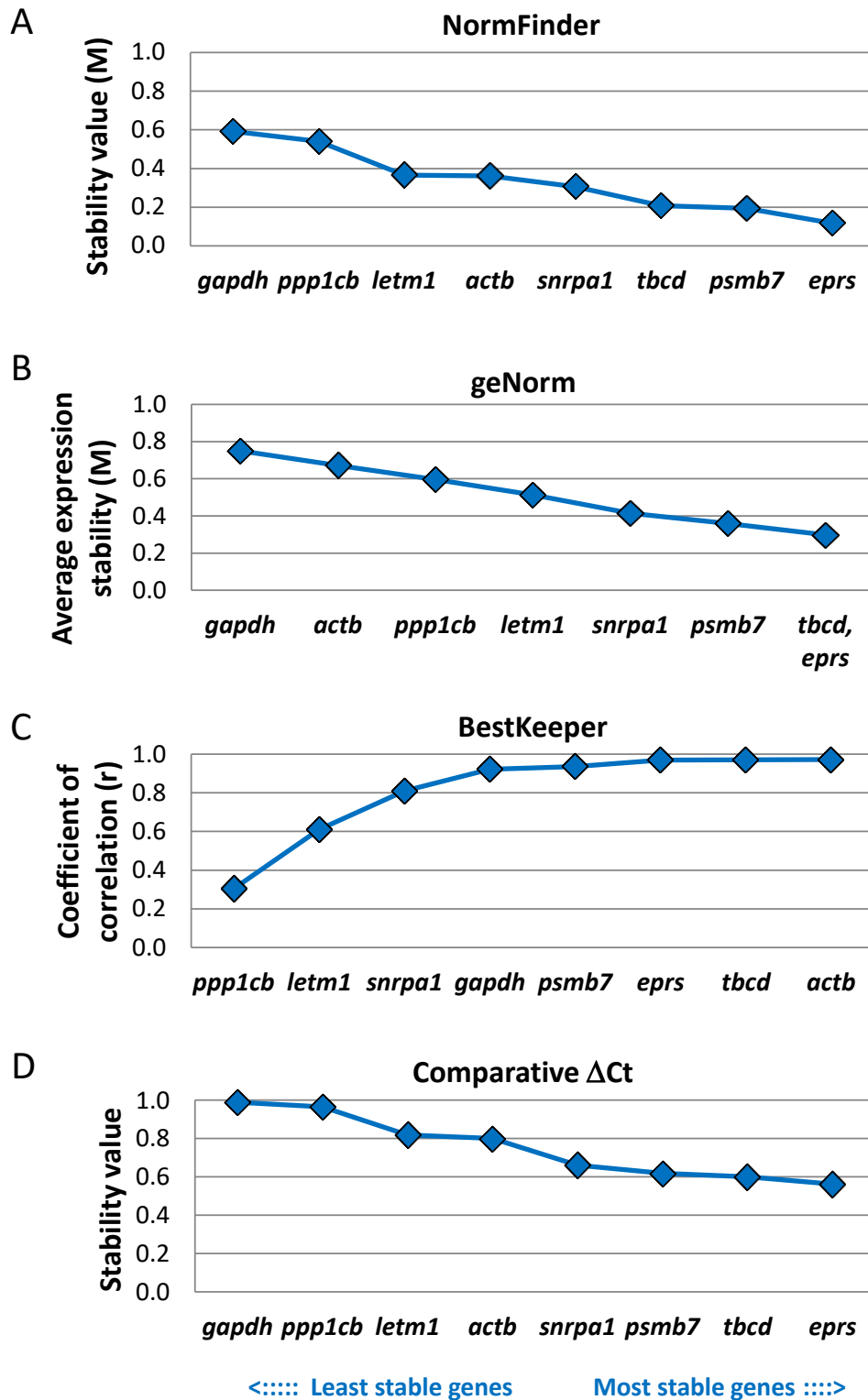


Figure 7. Ranking of eight candidate reference genes in the three different intra-mammalian life stages of *F. hepatica*. Four algorithms were used to calculate the stability of the expression of the eight chosen candidate reference genes within the intra-mammalian stages, i.e., NEJ, immature, and adult worms. NormFinder (A), geNorm (B), BestKeeper (C)

and the comparative Δ CT method (D). The most stably expressed gene is shown on the far right, whereas the least stable gene is shown on the far left.

3.1.3.2. Identification of the most stably expressed reference genes during *in vitro* culture of juvenile flukes

Having access to an *in vitro* model of a parasitic organism allows performing studies addressing scientific questions such as gene expression changes during the growth and maturation of juveniles as well as the characterization of gene function by RNA interference (RNAi) (Cwiklinski et al., 2018; McCammick et al., 2016; McVeigh et al., 2014). Therefore, it was of great importance to identify stably expressed reference genes of *F. hepatica*, for which *in vitro* cultivation of different life stages is possible. To obtain *in vitro*-grown juveniles, NEJs were cultured on day 1 post-excystment in RPMI1640 medium supplemented with 50% CS and collected 4 weeks post-excystment (McCusker et al., 2016). We used the same approach as we did for the *in vivo* analysis. The result of each ranking for each algorithm is shown in (**Figure 8; Supplementary Table 2**).

Fhtbcd and *Fhpsmb7* were identified as the two most stably expressed genes using NormFinder, BestKeeper, and the comparative Δ CT method (**Figure 8A, C, and D**). geNorm identified *Fhtbcd* and *Fheprs* as the most suitable reference genes followed by *Fhpsmb7* (**Figure 8B**). Concerning the genes, which were most unstably expressed, we identified *Fhppp1cb* (by geNorm and Δ CT method) and *Fhgapdh* (by NormFinder and BestKeeper).

Like the global ranking performed for the *in vivo* analysis, the global ranking based on the geometric mean of individual ranks revealed that *Fhtbcd* and *Fhpsmb7* as the most stably expressed reference genes. The average calculated ranks were as follows: *Fhtbcd* < *Fhpsmb7* < *Fheprs* < *Fhsnrpa1* < *Fhactb* < *Fhletm1* < *Fhppp1cb* < *Fhgapdh* (**Figure 9B**).

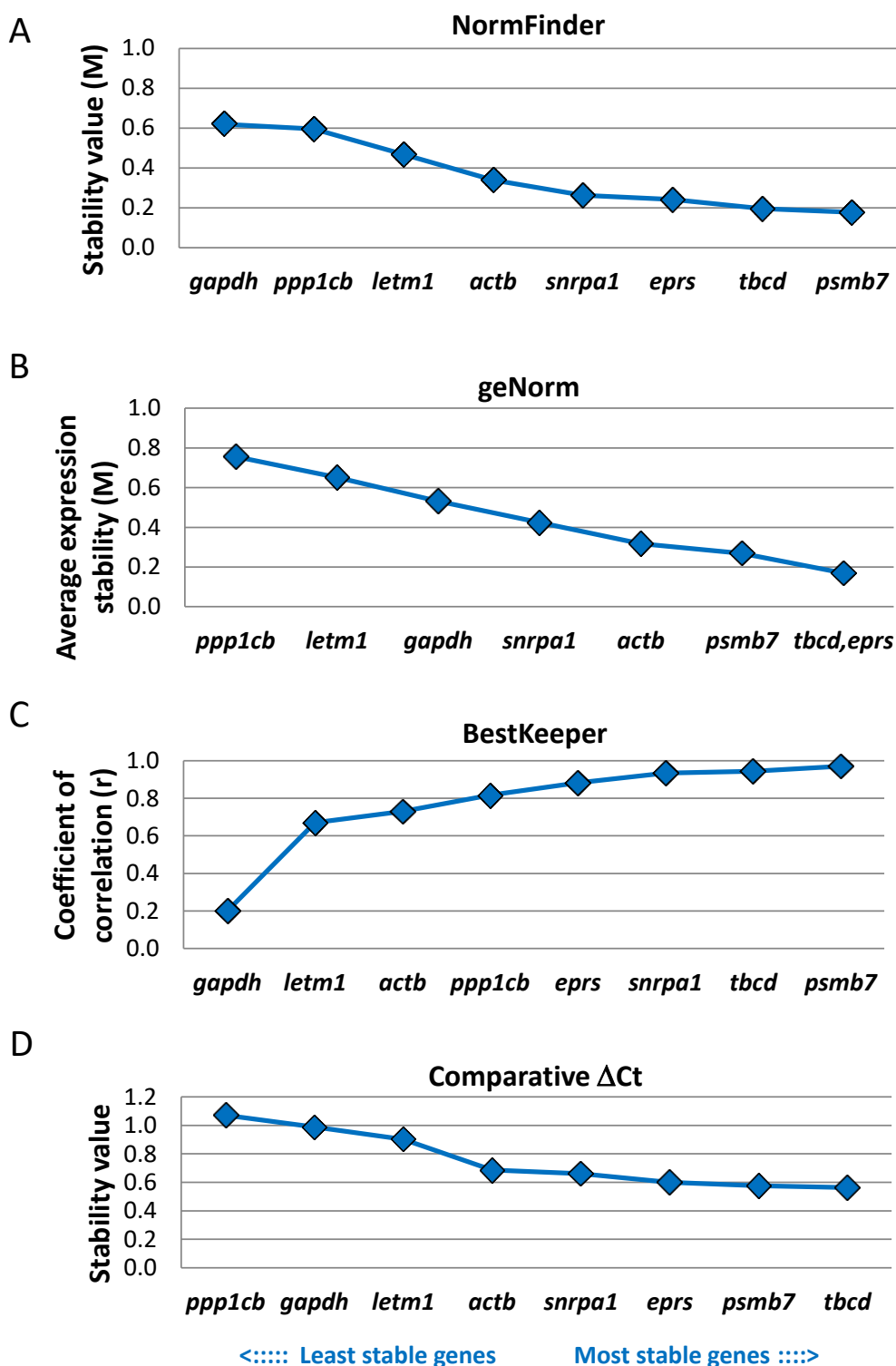


Figure 8. Ranking of eight candidate reference genes during *in vitro* culture of *F. hepatica*. Using NormFinder (A), geNorm (B), BestKeeper (C), and the comparative Δ CT method (D), the stability expression was evaluated between NEJs (day 1) and 4 weeks old *in vitro* juveniles (day 28). The most stably expressed gene is shown on the far right, whereas the least stable gene is shown on the far left.

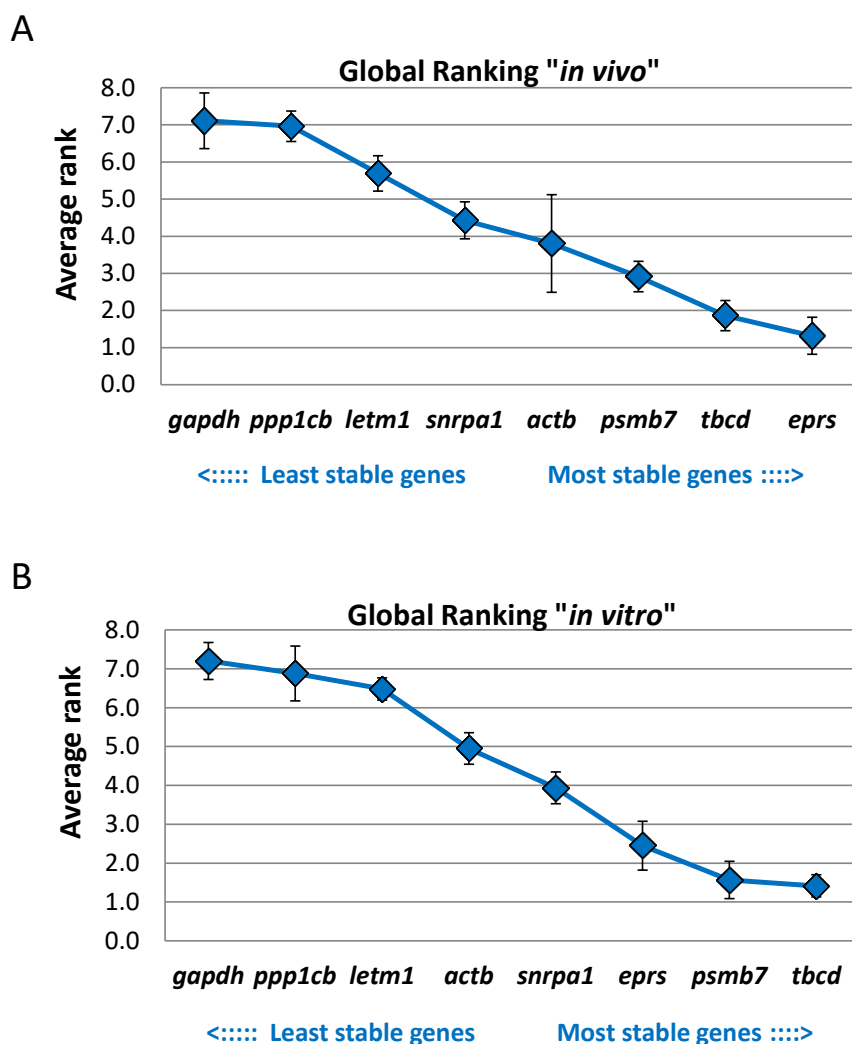


Figure 9. Average ranking of expression stability of eight candidate reference genes in *F. hepatica*. A number (from 1 to 8) was assigned to each stability coefficient obtained from four algorithms. The mean rank with SEM is shown for (A) the analysis of three intra-mammalian stages (NEJ, immature and adult flukes), and (B) the analysis of *in vitro*-cultured juveniles (NEJ before and after 28 days in culture). The most stably expressed gene is shown on the far right, whereas the least stable gene is shown on the far left.

3.1.3.3. Expression profiles of the best and worst reference genes

To strengthen these results, I performed a relative quantification of top-ranked genes, which were among the most stably expressed genes (Fheprs for *in vivo* studies and Fhpsmb7 for *in vitro* studies), and the last ranked gene, which represented the less stably expressed gene (Fhgapdh). To this end, I normalized their expression (Fheprs for *in vitro* and Fhpsmb7 for *in vivo* and Fhgapdh in both cases) to the geometric mean of the most stably expressed reference

genes *in vitro* (*Fhtbcd* and *Fhpsmb7*) and *in vivo* (*Fhtbcd* and *Fheprs*). *Fhgapdh* showed a significant upregulation in both cases, while *Fheprs* and *Fhpsmb7* showed a very stable expression (**Figure 10**). This analysis revealed that *Fhgapdh* is not always a reliable housekeeping gene that can be used for real-time qPCR analyses. This result is in line with previous studies in different models that have shown the fluctuations in *Fhgapdh*'s expression (González-Bermúdez et al., 2019; de Jonge et al., 2007).

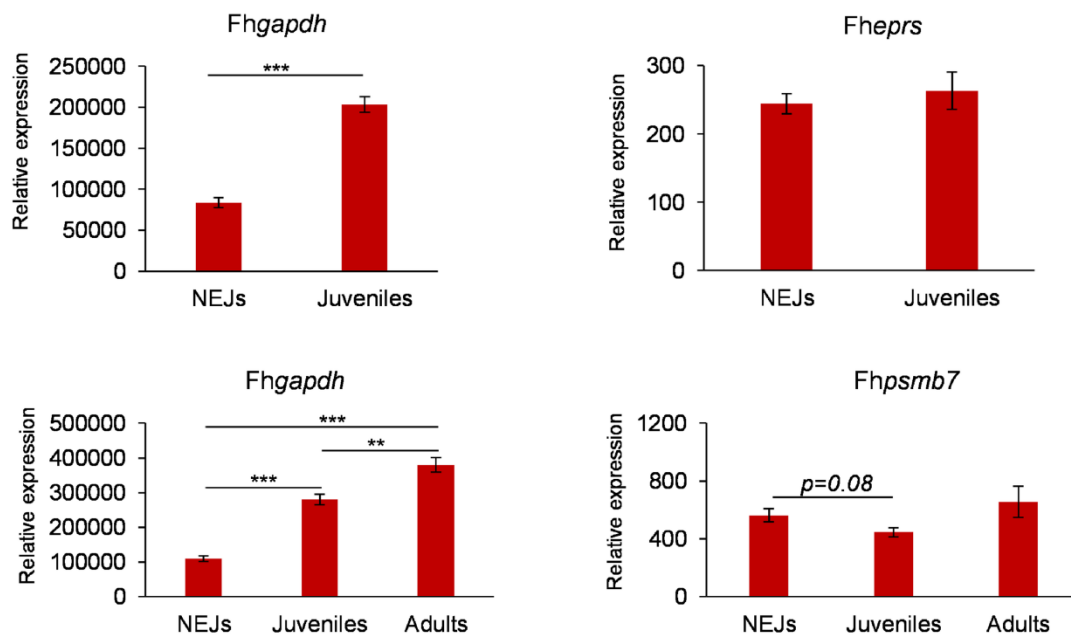


Figure 10. Relative expression levels of stably and least stably expressed reference gene candidates in *F. hepatica*. Relative quantification was based on normalization against the geometric mean of the two most stably expressed reference genes (A) *in vitro*, *Fhtbcd*, *Fhpsmb7*, and (B) *in vivo*, *Fhtbcd* and *Fheprs*. *Fhgapdh* was previously shown to be the least stably expressed gene; *Fheprs* (A) and *Fhpsmb7* (B) were among the three most stably expressed genes. Average values of 3-4 biological replicates with SEM are shown. Significant differences are indicated with ** $p < 0.01$ and *** $p < 0.001$ (t-test).

3.1.4. Using the identified reference genes to study the expression of selected target genes in different fluke stages

As interesting genes for transcript profiling, I selected kinases, which are critical enzymes acting in signal transduction pathways to control diverse cellular processes during development. Among these processes are cell growth and differentiation, proliferation, and apoptosis (Paul and Mukhopadhyay, 2004). Moreover, the importance of kinases as potential

anthelmintic targets in parasitic flatworms has been discussed (Gelmedin et al., 2015; Giuliani et al., 2018). For example, the tyrosine-protein kinase ABL1 and the polo-like kinase 1 have been studied in the past as potential targets in schistosomes, tape worms, and filariae (Beckmann and Grevelding, 2010; Hemer and Brehm, 2012; O'Connell et al., 2015; Schubert et al., 2014). Other kinases such as the protein kinases B (also called Akt) and C have been investigated as potential targets in *S. mansoni* (Guidi et al., 2015; Morel et al., 2014; Ressurreição et al., 2014). To date, no study has investigated the role of the kinases in the biology of *F. hepatica* and as a potential target against the liver fluke. To be a good target, a selected kinase should be expressed in different stages. In other words, shedding the light on kinase expression in all life stages is relevant when new concepts are designed for drug development to fight fasciolosis. In addition, reliable gene expression quantification is of great importance when functional analyses are performed, for example, knockdown experiments.

By BLAST analyses, I identified the following five kinase genes that were used for further investigation: *Fhplk1*, *Fhabl1*, *Fhabl2*, *Fhakt1*, and *Fhpkc* (accession numbers and a brief description of the function of these kinases are presented in **(Table 3)**). To confirm their identity, the presence of conserved kinase domains was analyzed by SMART (**Supplementary Figure 2**).

Table 3. Overview of genes of interest for the study of gene expression in *F. hepatica*.

Gene of interest	Gene ID	Homology (e-value) *	Protein function
<i>Fhabl1</i>	maker-scaffold10x_1995_pilon-snap-gene-0.46	ABL proto-oncogene 1, non-receptor tyrosine kinase [<i>Homo sapiens</i>] (2e-119)	Protein tyrosine kinase involved in a variety of cellular processes, including cell division, adhesion, differentiation, and response to stress
<i>Fhabl2</i>	maker-scaffold10x_873_pilon-snap-gene-0.69	ABL proto-oncogene 2, non-receptor tyrosine kinase isoform e [<i>Homo sapiens</i>] (2e-135)	Protein tyrosine kinase with a role in cytoskeletal rearrangements through its F-actin- and microtubule-binding sequences
<i>Fhakt1</i>	maker-scaffold10x_205_pilon-augustus-gene-0.40	Rac-alpha serine/threonine-protein kinase [<i>Homo sapiens</i>] (9e-137)	The serine/threonine-protein kinase AKT1 is also known as protein kinase B. AKT kinases regulate processes such as metabolism, proliferation, cell survival, and growth.
<i>Fhpkc</i>	maker-scaffold10x_608_pilon-snap-gene-0.5	Protein kinase C iota [<i>Homo sapiens</i>] (0.0)	A serine/threonine protein kinase involved in cell survival, differentiation and polarity. It plays a role in microtubule dynamics in the early secretory pathway.
<i>Fhplk1</i>	maker-scaffold10x_784_pilon-snap-gene-0.36	Polo-like kinase 1 [<i>Homo sapiens</i>] (0.0)	This serine/threonine protein kinase is highly expressed during mitosis and performs several important functions throughout the M phase of the cell cycle.

I quantified the expression of the selected kinases *in vivo* and *in vitro* using the geometric mean of the two most stably expressed reference genes, *Fheprs* and *Fhtbcd* for the *in vivo* and *Fhpsmb7* and *Fhtbcd* for *in vitro* analyses (**Figure 11** and **Figure 12**). The *in vivo* results showed that all selected kinases were expressed throughout the life cycle of the fluke with *Fhabl1* and *Fhpkc* as the most abundantly transcribed genes. Moreover, the expression profiles of *Fhabl1*, *Fhabl2*, *Fhpkc*, and *Fhakt1* were similar to the respective expression profiles in the youngest stage (NEJs) concerning the level of transcripts, which decreases progressively during growth and maturation. On the contrary, *Fhplk1* appears to be low abundantly transcribed in NEJs, and it is upregulated during growth reaching an expression peak in the adult stage (**Figure 11**). The expression of these kinases during the *in vitro* maturation of NEJ to immature flukes mimics the expression profile of the intra-mammalian stages (**Figure 12**). In summary, different kinases are expressed throughout the life cycle of the liver fluke, and the expression during *in vitro* culture mimics one of the intra-mammalian stages.

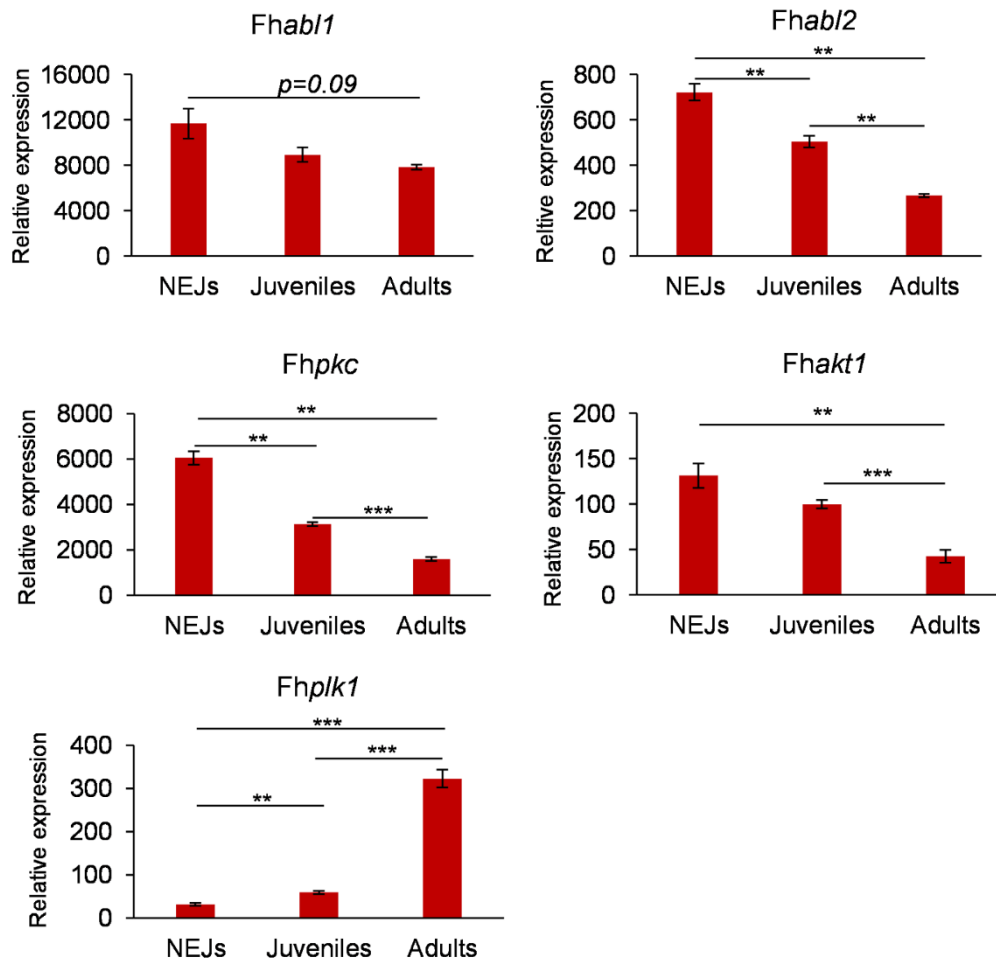


Figure 11. Relative expression levels of kinases in three different intra-mammalian life stages of *F. hepatica*. Expression data from NEJs, 4-week-old immature and 12-week-old adult worms that were normalized against the geometric mean of the two most stably expressed reference genes (*Fheprs* and *Fhtbcd*). Average values of 3-4 biological replicates with SEM are shown. Significant differences are indicated with ** $p < 0.01$, *** $p < 0.001$ (t-test). *Fhbl1*, tyrosine-protein kinase Abl1; *Fhbl2*, tyrosine-protein kinase Abl2; *Fhpkc*, protein kinase C iota; *Fhakt1*, Rac-alpha serine/threonine-protein kinase 1; *Fhplk1*, polo-like kinase 1.

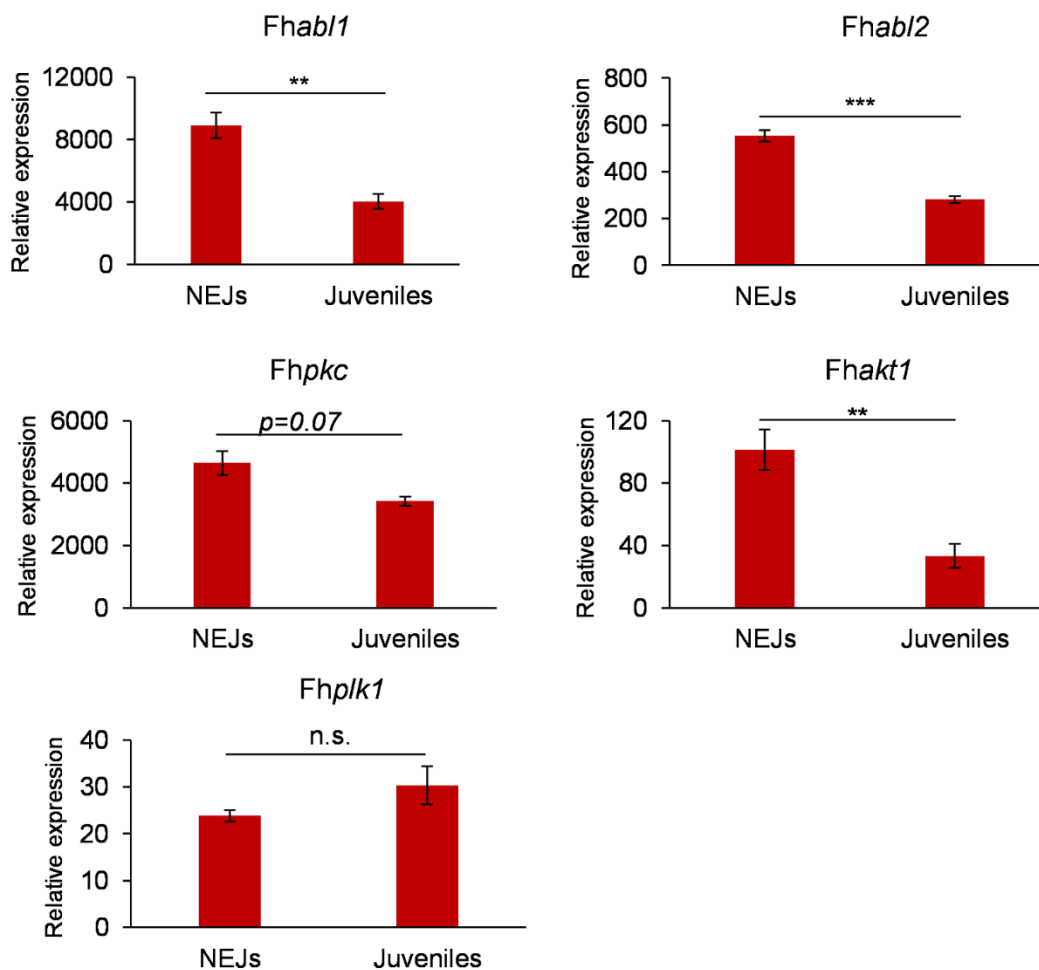


Figure 12. Relative expression levels of kinases during *in vitro* culture of juvenile *F. hepatica*. Expression data from NEJs and juvenile worms that have grown for 4 weeks in a serum-rich medium *in vitro*. Analysis was based on the normalization against the geometric mean of the two most stably expressed reference genes (*Fhtbcd* and *Fhpsmb7*). Average values of 3-4 biological replicates with SEM are shown. Significant differences are indicated with ** $p < 0.01$, *** $p < 0.001$ (t-test). n.s., not significant. *Fhabl1*, tyrosine-protein kinase Abl1; *Fhabl2*, tyrosine-protein kinase Abl2; *Fhpkc*, protein kinase C iota; *Fhakt1*, Rac-alpha serine/threonine-protein kinase 1; *Fhplk1*, polo-like kinase 1.

3.2. Identification of aldehyde dehydrogenases (ALDHs) in *F. hepatica* and evaluation of their suitability as drug targets

The focus of this chapter is the identification and characterization of genes predicted to encode aldehyde dehydrogenases (ALDH), which due to their important roles in several biological processes could represent targets for drug repurposing or drug design against *F. hepatica*. Among these roles is the involvement in retinoic acid synthesis, a critical morphogen for the establishment of body plans as well as the development of several organs and limbs (Cunningham and Duester, 2015; Koop et al., 2010), and roles as aldehyde scavengers, i.e., helping cells to eliminate reactive aldehydes by oxidation into their corresponding carboxylic acids, thus protecting the cells and subsequently the organism from death (Singh et al., 2013).

3.2.1. Identification of ALDH1 and ALDH2 orthologues in *Fasciola hepatica*

According to literature research, no previous study has addressed the role of ALDHs in the liver fluke. Therefore, I started this project partly by the identification of two aldehyde dehydrogenase gene orthologues in *F. hepatica*. Based on the available protein sequence from the related trematode *S. mansoni* (SmALDH_312 (Harnischfeger J, Beutler M, Salzig D, et al., 2021); and SmALDH_022 (data not shown)) and using Blastp analyses, I detected ALDH orthologues in the liver fluke. SMART analysis showed the presence of the Aldedh domain, thus confirming the nature of this enzyme. However, the sequence of one of the orthologues was not complete because the 3'-part was wrongly annotated. In other words, the sequence was too long when compared to other ALDH protein sequences from other species. This part was cloned by a PCR-based 3'-RACE approach, whose identity was confirmed by sequencing (**Figure 4**, Materials and Methods chapter). To verify the identity of both orthologues, I performed a phylogenetic analysis based on amino acid sequences and generated a tree using ALDH sequences from vertebrates and invertebrates extracted from published data. Species names, gene IDs, accession numbers, and sources are listed in (**Table 1**; Materials and Methods chapter). The obtained result substantiated my assumption that one of the orthologues belongs to the ALDH1 family, and here to the subgroup of cytosolic ALDHs, whereas the second orthologue belongs to the ALDH2 family which localizes in the mitochondria (**Figure 13**). Therefore, in the subsequent parts, I will refer to the cytosolic orthologue from *F. hepatica* as FhALDH1 and to the mitochondrial one as FhALDH2. Moreover, the multiple sequence

alignment of FhALDH1 together with the sequences from the other species to which each of the orthologues belongs showed the conservative nature of the catalytic domain (**Figure 14**).

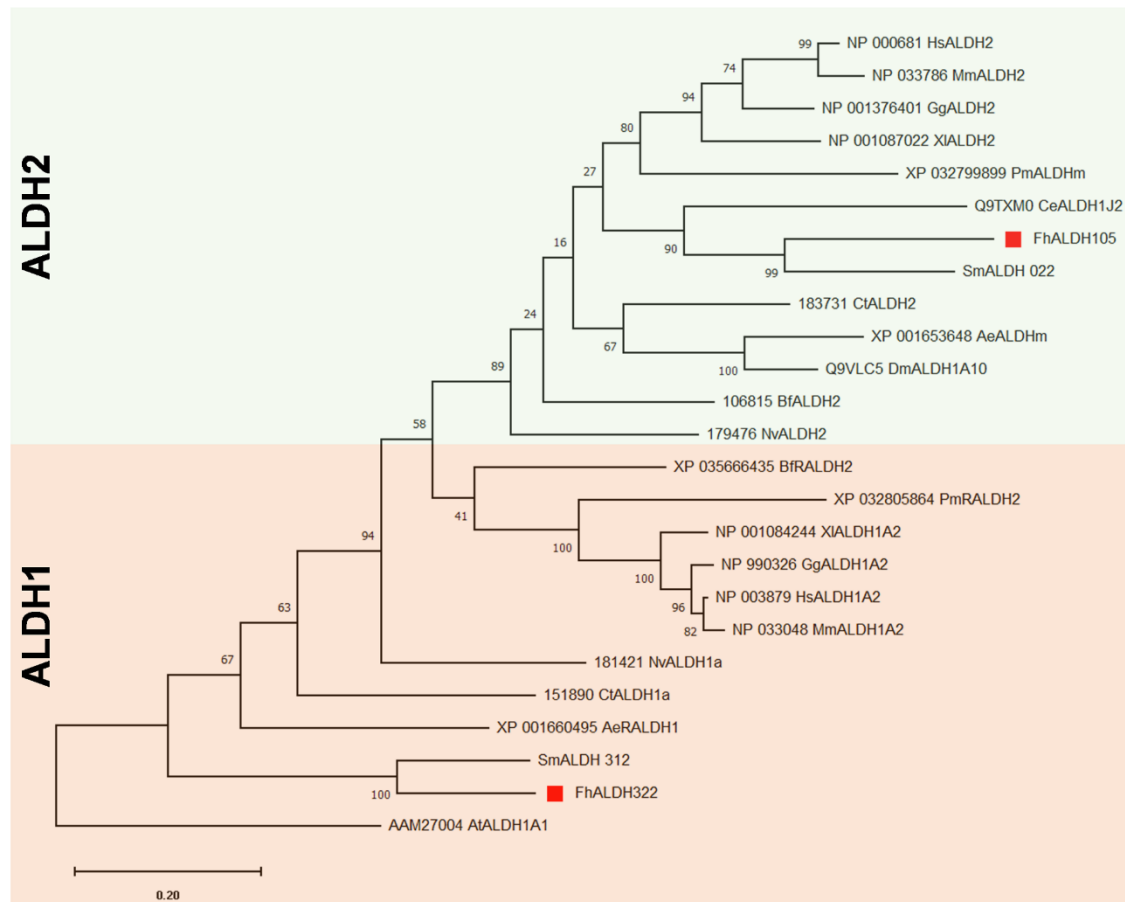


Figure 13. Phylogram of a phylogenetic tree analysis of FhALDH1 and FhALDH2. FhALDH1 is referred to as its former gene ID FhALDH322 and FhALDH2 as its former gene ID FhALDH105. At each node, there is an indication of the posterior probabilities. Bf: *Branchiostoma floridae*; Pm: *Petromyzon marinus*; Xl: *Xenopus laevis*; Gg: *Gallus gallus*; Hs: *Homo sapiens*; Mm: *Mus musculus*; Nv: *Nematostella vectensis*; Ct: *Capitella teleta*; Ae: *Aedes aegypti*; Sm: *Schistosoma mansoni*; Fh: *Fasciola hepatica*; Ce: *Caenorhabditis elegans*; Dm: *Drosophila melanogaster*; and At: *Arabidopsis thaliana*. The ALDH sequence from *Arabidopsis thaliana*, ALDH1A1, was used as an outgroup.

```

HsALDH1A2      GVCGQIIPWNFPLLMFAWKIAPALCCGNTVVVVKPAEQTPLSALYMGALIKEAGFPPGVIN 237
MmALDH1A2      GVCGQIIPWNFPLLMFTWKIAPALCCGNTVVVVKPAEQTPLSALYMGALIKEAGFPPGVN 237
GgALDH1A2      GVCGQIIPWNFPLLMFAWKIAPALCCGNTVVVVKPAEQTPLSALYMGALIKEAGFPPGVN 237
XlALDH1A2      GVCGQIIPWNFPLLMFAWKIAPALCCGNTVVVVKPAEQTPLTALYMGALIKEAGFPPGVN 237
BfRALDH2       GVCGAIIPWNFPLMMAVWKLAPALCAGCTVVLKPAEQTPLSALYLAALIKEAGFPPGVN 222
PmRALDH2       GVCGQIIPWNFPLLMFIWKIAPALSCGNTVVVVKPAEQTPLTALHVGALIAEAGFPPGVN 239
CtALDH1a       GVCGCIIPWNFPAMMFVYKIAPALATGNTIVIKPAEQTPLSALYLAALIKEAGFPPGVN 210
AeRALDH1       GVVGQIIPWNYPLLMLAWKWPALAAGCTIVMKPAEQTPLTALYMC SLVKEAGFPPGVN 209
SmALDH_312     GVVACITPWNYPFFLSVLKGTPLCAGCTVVLKPAEQTPLSALYLAALIKEAGFPPGVN 211
NvALDH1a       GLVGAITPWNFPLNMA SVKIAPALACGNVVLKPAEQTPLTALYFCALVKEAGFPAGV 214
FhALDH322      GVVLGITPWNYPFFLAMLKVAPSLCAGCTIVLKPAEQTPLSAIYLGSLVCEAGFPPGVN 215
* : * * * * * : * * . * . : : : * * * * * : : : * * * * * * . *

HsALDH1A2      ILPGYGPTAGAAIASHIGIDKIAFTGSTE V GKLIQEAAGRSNLKRVTLELGGKSPNIIFA 297
MmALDH1A2      ILPGYGPTAGAAIASHIGIDKIAFTGSTE V GKLIQEAAGRSNLKRVTLELGGKSPNIIFA 297
GgALDH1A2      ILPGFGPIVGA AIASHV GIDKIAFTGSTE V GKLIQEAAGRSNLKRVTLELGGKSPNIIFA 297
XlALDH1A2      ILPGYGPTAGAAIASHIGIDKIAFTGSTE V GMFIQEAAGRSNLKRVTLELGGKSPNIIFA 297
BfRALDH2       IVPGYGPTAGAAI SEHMDIQKVAFTGSTE V GKLIQQAAGKSNLKRVSLELGGKSP TIVFP 282
PmRALDH2       IVPGFGPTAGAAI VQHPDIDKIAFTGSTE V GKLIQE EAGKSNLKRVTLELGGKSP IIVFA 299
CtALDH1a       VVPGFGPTAGAAI SSHPEIRKIAFTGSTE V GKVM EAAAQSNLKKVTLELGGKSP LIIMP 270
AeRALDH1       MVPGYGPTAGNAITMHPDIRKVAFTGSTE V GKIVMA-GAASN LKKVSLLELGGKSP LVICD 268
SmALDH_312     VICGYGETTGEAL THHPDVRAISFTGSTE V GQLIMK-AAATN I KHVKLELGGKSP LIILA 270
NvALDH1a       VIPGYGPTAGAAI TTHLDIDKVSFTGSTE V GRLIQEASAKSNLKRRTLELGGKSP NIVFA 274
FhALDH322      ILPGYGETTGASLCVHPDIRVISFTGSTE V GQLIMK-AAATN I KHVKLELGGKSP LIIFA 274
: : * : * . * : : * : : * * * . * * : . . : * : : * * * * * : :

HsALDH1A2      DADLDYAVEQAHQGVFFNQGCC TAGSRI FVEESIYEEFVRRSVERAKRRVVGSPFDPTT 357
MmALDH1A2      DADLDYAVEQAHQGVFFNQGCC TAGSRI FVEESIYEEFVKRSVERAKRRIVGSPFDPTT 357
GgALDH1A2      DADLDYAVEQAHQGVFFNQGCC TAGSRI YVEESIYEEFVRRSVERAKRRVVGSPFDPTT 357
XlALDH1A2      DADLDYAVEQAHQGVFFNQGCC TAGSRTFVEDSIYEEFVRRSVERAKRRIVGSPFDPTT 357
BfRALDH2       DADLDFAVEEAHQALFFNMGMQCTAGSR TYVHEDIYDEFVVRKSV ERAKSRTVGD PFDPRN 342
PmRALDH2       DADLDAAVEQAHQGVFFNQGCC TAGSRVYVEDPVYDEFVRRSAQRARVRRVGH PFCPST 359
CtALDH1a       DANLDEALAVSHMGVFFYNGQVC IASSR L FVHEDIYDDFVRKSV ELAKKKCVGDPFDLKM 330
AeRALDH1       DVDVN EAAQIAYTGVFENMGQCC IAATR T FVQEGIYDAFVQKATELAKGRKVG NPFVSQGI 328
SmALDH_312     DADIEKASEVAHEATMVNHGQCC VAGTR I FVQAPIYDQMVEK LKLAEQRKVGD PFDVSDT 330
NvALDH1a       DSDMDYAVEMAHEALFFNQGCC SAGSR T FVQDTIYDEFVVKKSVKRAKARTVGD PFDSDS-V 333
FhALDH322      DADFEAAAQTAHEATMVNHGQCC VAGTR I FVESPIYDKMVNRLKELAEARKVGD PFDAGDT 334
* : : * : : : * * * * * : * : * : * : * : * : * : * : * * *

```

Figure 14. Multiple sequence alignment. Clustal omega was used to generate a multiple sequence alignment for FhALDH1 among several ALDH protein sequences. In yellow, catalytic residues (active site), in green (NAD binding site). Symbols below all the sequences describe the similarities in the amino acids across the sequences at each position and define them as being identical (*), highly similar (:) or less similar (.). Bf: *Branchiostoma floridae*; Pm: *Petromyzon marinus*; Xl: *Xenopus laevis*; Gg: *Gallus gallus*; Hs: *Homo sapiens*; Mm: *Mus musculus*; Nv: *Nematostella vectensis*; Ct: *Capitella teleta*; Ae: *Aedes aegypti*; Sm: *Schistosoma mansoni*; Fh: *Fasciola hepatica*.

3.2.2. Expression pattern of Fhaldh1 and Fhaldh2 during life stages of the liver fluke

To unravel the gene expression patterns of *Fhaldh1* and *Fhaldh2* during the intra-mammalian life cycle stages, real-time qPCR analyses were performed. To this end, cDNA was reverse transcribed from total RNA isolated from newly excysted juveniles (NEJs), immature, and adult flukes. The normalization of gene expression was based on the set of reference genes

(*Fhtbcd* and *Fheprs*) previously identified as the most stably expressed reference genes *in vivo* (Houhou et al., 2019). The result showed a significant increase in the transcript level of *Fhaldh1* during the growth of the parasite with a peak in the adult stage (**Figure 15A**). On the other hand, *Fhaldh2* showed a lower expression when compared to *Fhaldh1*, and its expression remained stable through the life cycle of the parasite (**Figure 15B**). Moreover, I investigated the transcript localization of both genes on paraffin sections of adult worms by *in situ* hybridization using a specific anti-sense probe coupled with digoxigenin. No signal was detected for *Fhaldh2* (data not shown). On the contrary, an accumulation of *Fhaldh1* transcripts in several tissues was detected, including the intestine, the ovaries, the uterus, and the testis (**Figure 15C**).

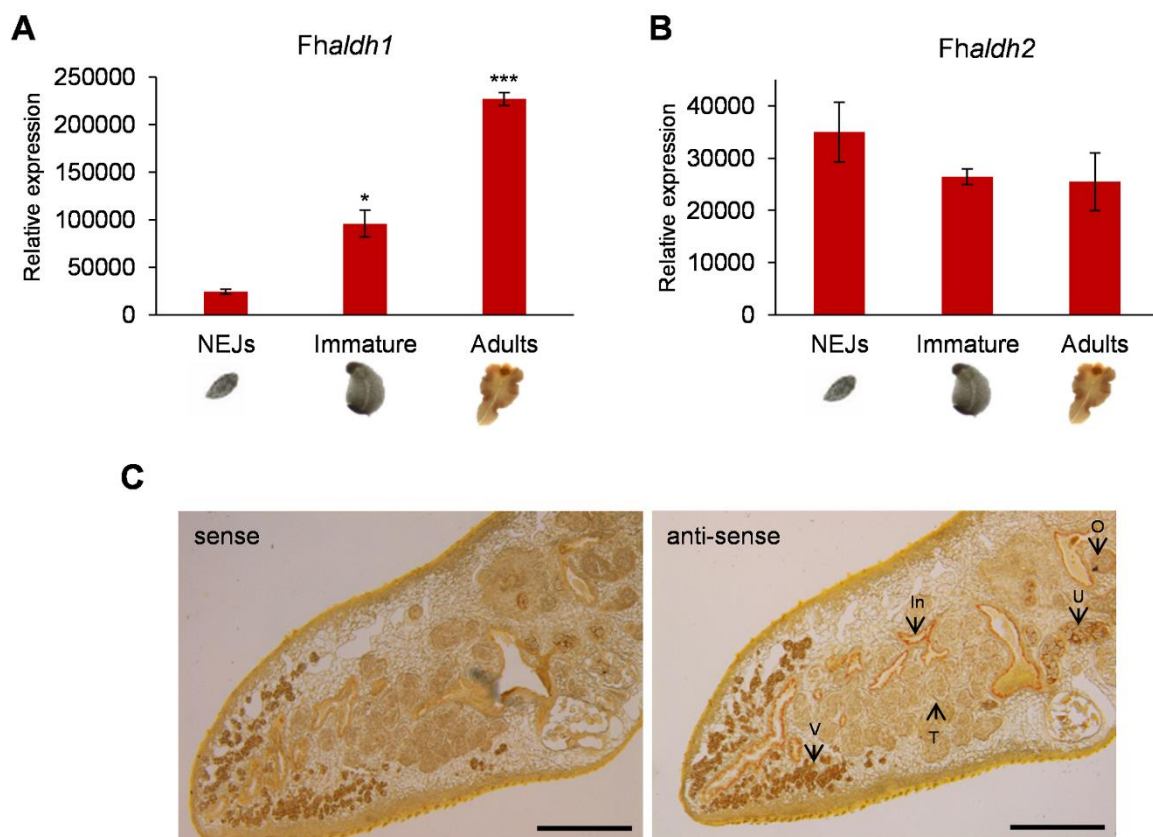


Figure 15. Expression of two *Fhaldh* orthologues of *F. hepatica*. (A) and (B) qRT-PCR analyses show the transcript levels of *Fhaldh1* and *Fhaldh2* throughout the life cycle. The relative quantification was done by normalization against the geometric mean of the two most stably expressed reference genes previously established in the intra-mammalian stages (*Fhtbcd* and *Fheprs*). Average values of 3-4 biological replicates with SEM are shown. Significant differences are indicated with * $p < 0.05$ and *** $p < 0.001$ (t-test). (C) Localization of *Fhaldh1* transcripts by *in situ* hybridization (ISH) in the intestine, vitellarium, uterus, ovary, and testis.

Here, paraffin sections on adult flukes were used. An anti-sense probe coupled with digoxigenin was used for detection. As a negative control, a sense probe was used. No signals were identified for *Fhaldh2* (not shown). (V: Vitellarium; In: intestine; U: uterus; O: ovary; T: Testis). Scale bars = 500 μm .

3.2.3. Expression of the FhALDHs orthologues

3.2.3.1 Recombinant expression of two ALDHs orthologues of *F. hepatica*

Both orthologues were cloned for recombinant expression of the corresponding proteins. To this end, I cloned His-tagged *Fhaldh1* and *Fhaldh2* variants and expressed these in the *E. coli* LOBSTR-strain. After induction with IPTG, I collected the bacteria at regular time points and then loaded the lysates on an SDS-PAGE as a basis for Western blot analyses to check protein expression using an α -His antibody (**Figure 16**). In both cases, the results obtained show that protein expression succeeded. The amounts of the recombinant proteins increased over time with peaks at 5 h in each case. Compared to FhALDH2, there was less background for FhALDH1. However, the yield of FhALDH2 protein was higher compared to FhALDH1.

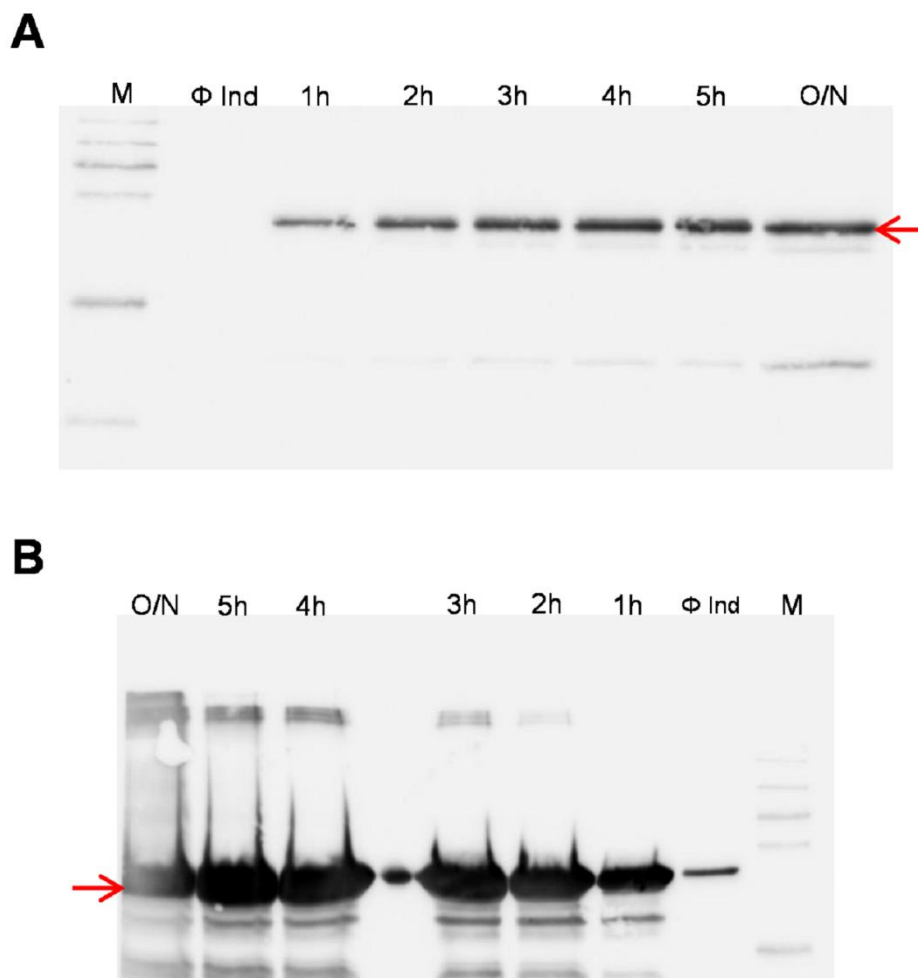


Figure 16. Protein expression of both ALDHs orthologues. Western blot analyses of lysates of *E. coli* LOBSTR using an α -His antibody (A) Protein expression of FhALDH1. (B) Protein expression of FhALDH2. In both cases, the amounts of protein were highest after 5 h of induction (time points indicated). The expected molecular weight of FhALDH1 is 54 kDa and the one for FhALDH2 is 58 kDa. Φ Ind= without induction. M = protein weight marker.

3.2.3.2 Expression of the ALDH1 orthologue

Because of the higher impurities of recombinant FhALDH2, I first focused on the purification of FhALDH1 as a prerequisite to establishing an enzyme assay. After induction of protein expression and purification using Ni-NTA beads (QIAGEN), Coomassie-blue staining showed the expressed form of FhALDH1 (54 kDa) (**Figure 17A**). An enzyme assay was established to evaluate whether the recombinant enzyme was active. ALDHs are known to oxidize aldehydes into their corresponding carboxylic acids using NAD⁺ (nicotinamide adenine dinucleotide) as

a cofactor, which in turn is converted into NADH (Marchitti et al., 2008). In this assay, I determined the accumulation of NADH in the medium by measuring its absorption at 340 nm. The concentration of NADH increased over time (**Figure 17B**), which reflected the successful conversion of an aldehyde into a carboxylic acid. Thus, an enzyme assay was successfully established, which confirmed the enzymatic activity of FhALDH1.

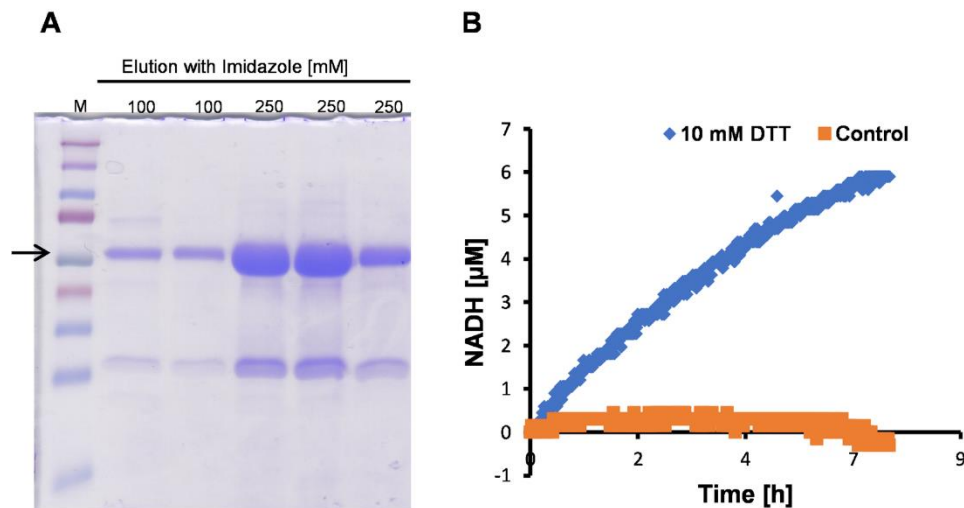


Figure 17. FhALDH1 protein expression, purification, and enzymatic activity. (A) A Coomassie-blue-stained gel showing the purified FhALDH1 eluted with increasing concentrations of imidazole. M = protein weight marker. (B) The activity of the enzyme was tested by the increased absorption of NADH at 340 nm by the conversion of acetaldehyde into acetic acid. The enzyme showed an activity when 10 mM of the reducing agent DTT was added, as shown before for an *S. mansoni* ALDH orthologue (Harnischfeger J, Beutler M, Salzig D, et al., 2021). A control reaction was set up using FhALDH1 without DTT.

3.2.4. Treatment of the intra-mammalian liver fluke stages with disulfiram

Disulfiram (DSF) is a well-established drug known for its role in inhibiting ALDH in humans (Deitrich and Erwin, 1971; Lam et al., 1997; Lipsky et al., 2001a). In the context of finding inhibitors against ALDH that may affect the vitality of *F. hepatica*, I tested the effect of DSF on all intra-mammalian stages including NEJs, immature, and adult flukes *in vitro*. DSF at 20 μM was lethal to NEJs. Furthermore, I observed an enlargement of the worm bodies which became darker (**Figure 18A and B**). On the contrary, no obvious phenotype was observed in immature and adult flukes. The motility of the immature flukes was only affected when they were treated with a higher DSF concentration, i.e., 100 μM (**Figure 18C and D**).

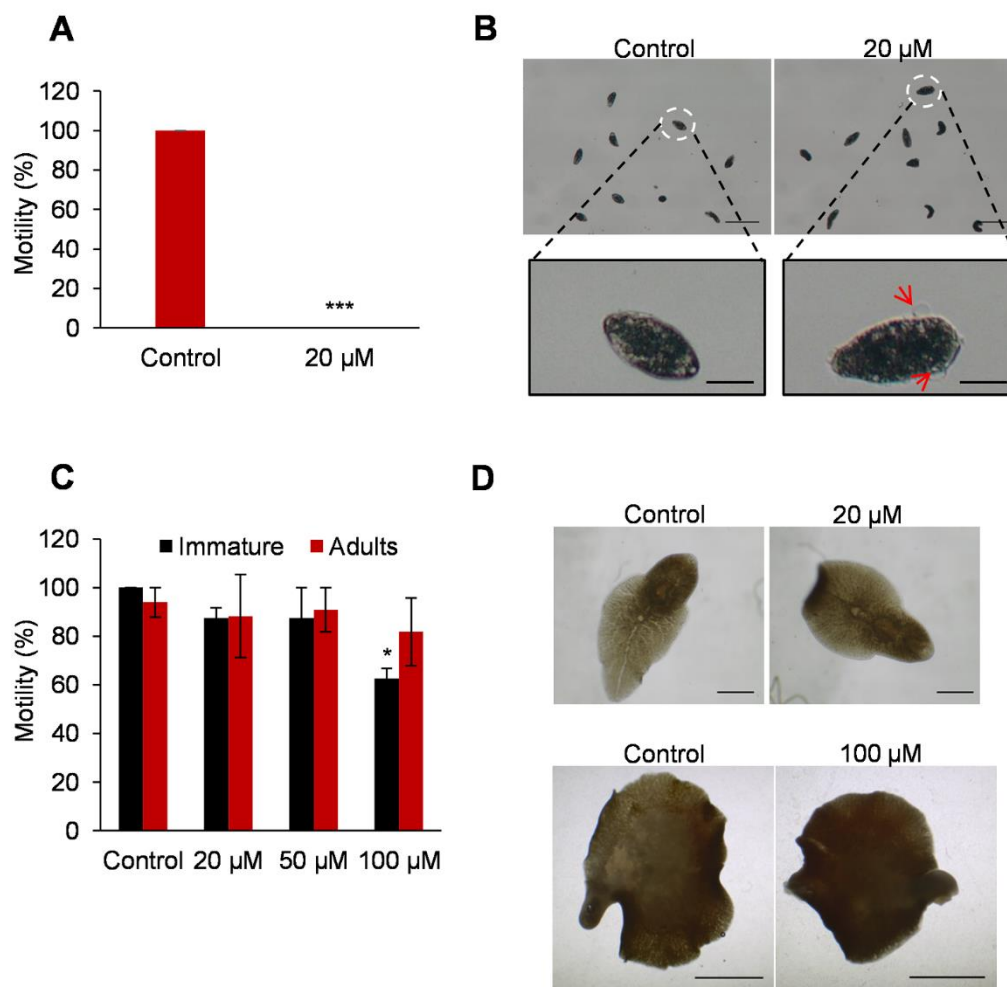


Figure 18. Effect of disulfiram (DSF) on intra-mammalian stages of *F. hepatica*. (A) Motility analysis of NEJs after 72 h treatment with 20 μ M DSF. (B) Bright-field microscopy shows the morphological changes of NEJs treated with 20 μ M DSF. The individuals marked by an interrupted white circle are shown also in higher magnification. (C) Relative motility of immature and adult flukes treated with 20, 50, and 100 μ M of DSF compared to control flukes. Immature flukes showed a reduction in their motility only after treatment with 100 μ M DSF. No effect was observed with 12-week-old flukes. (D) Bright-field microscopy showing no obvious phenotypic effects on immature and adult flukes treated with 20 and 100 μ M DSF, respectively. Average values of the motility of 18-20 NEJs, 8 immature flukes, and 12 biological replicates (with SEM) of two independent experiments (for NEJs and immature flukes) and three independent experiments (for adult flukes) are shown. Scale bars: for NEJs 500 μ m (whole) and 100 μ m (zoom). For immature fluke, scale bar = 1 mm, and for adults, scale bar = 5 mm. Significant differences are indicated with *** $p < 0.001$ (Mann-Whitney test).

3.2.5. Treatment of adult flukes with chemically synthesized derivatives of disulfiram

Provided by cooperation partners who work on new compounds with anti-parasitic effects, several compounds were generated by chemical derivatization of DSF and provided to me for *in vitro* testing (**Figure 19A**). I started screening the best derivatives by testing their activity against adult flukes, which are considered the most problematic and disease-causing stage. For this aim, 9 derivatives were pre-selected based on low cytotoxicity against a human cell line (cooperation with the working groups of Prof. Schlitzer and Prof. Grünweller, Philipps University, Marburg). These derivatives were tested against adult flukes *in vitro*, and fluke motility was assessed after 72 h. Five of nine derivatives exhibited a significant reduction of worm motility upon treatment with 100 μM , respectively (**Figure 19B**). One derivative (028) was of great interest because the reduction of worm motility was even more pronounced, and a similar effect was also observed with a lower concentration (50 μM , data not shown). Based on these results, I focused my attention on this derivative for subsequent experiments.

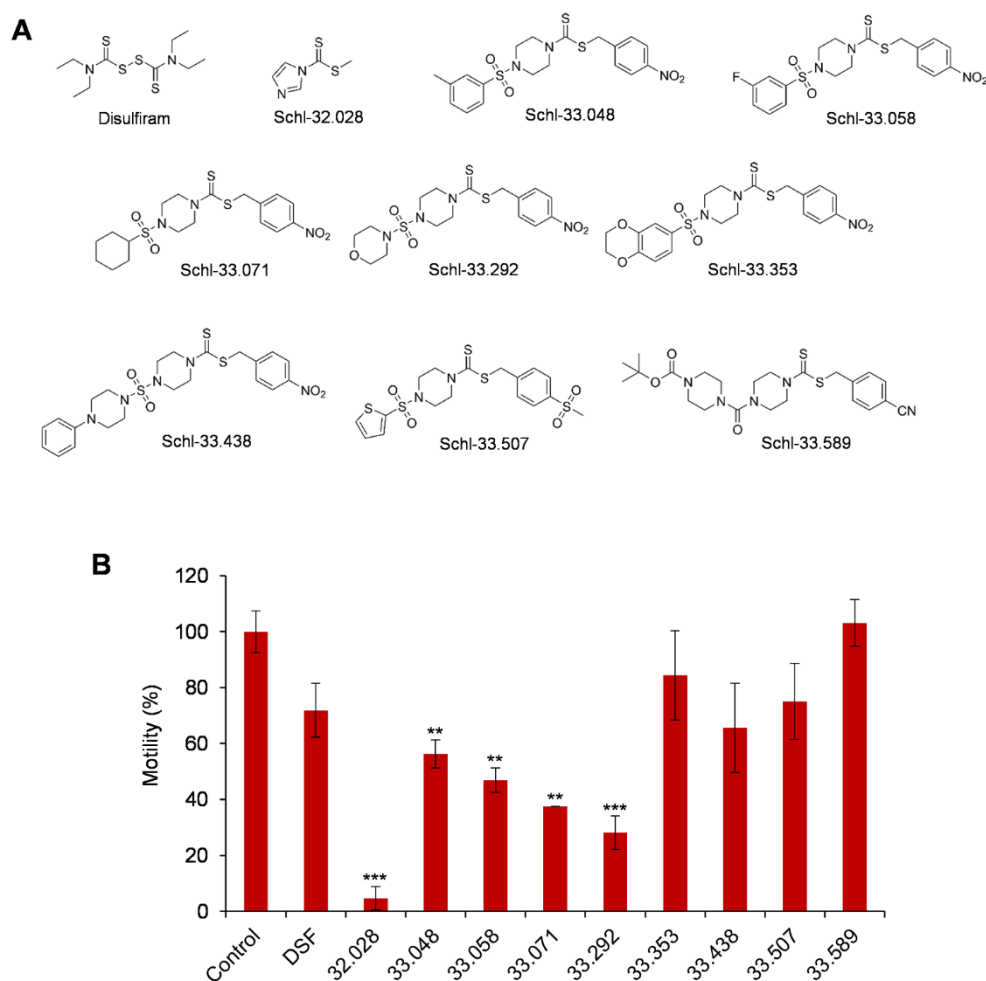


Figure 19. Effect of disulfiram derivatives on the motility of 12-week-old flukes. (A) Chemical structures of 9 disulfiram derivatives (provided by Tom Gallinger, working group Prof. Schlitzer, Philipps University Marburg) have been used in addition to DSF. (B) Motility analysis of adult flukes upon treatment with 100 μ M each. Five derivatives caused a significant reduction of the motility after 72 h treatment compared to control flukes. Especially one inhibitor, 028, resulted in a remarkable decrease in motility. Average values of the motility of 4-12 adults (with SEM) of two independent experiments are shown. A significant difference is indicated with ** $p < 0.01$, and *** $p < 0.001$ (Mann-Whitney test).

3.2.6. Treatment of NEJs and immature flukes with compound 028

The effect of 028 treatment on adults motivated me to test its effect also on the younger fluke stages, NEJs, and immature flukes. Surprisingly, 2 μ M of 028 showed a lethal effect on NEJs. NEJs were floating with the destruction of their bodies (**Figure 20A** and **Figure 20B**). This highlights the potency of this derivative compared to DSF (NEJs died upon treatment with 20

μM). Furthermore, this finding mirrored the effect of the anti-fasciolosis drug triclabendazole (TCBZ) (NEJs died when treated with $2\ \mu\text{M}$ of TBZ (**Supplementary Figure 3**)). Moreover, immature and adult flukes showed a significant reduction in motility when they were treated with only $20\ \mu\text{M}$ and $50\ \mu\text{M}$ of 028 respectively (**Figure 20C**). These flukes shortened in size, they accumulated tegument bubbles, and they became darker compared to the control (**Figure 20D**).

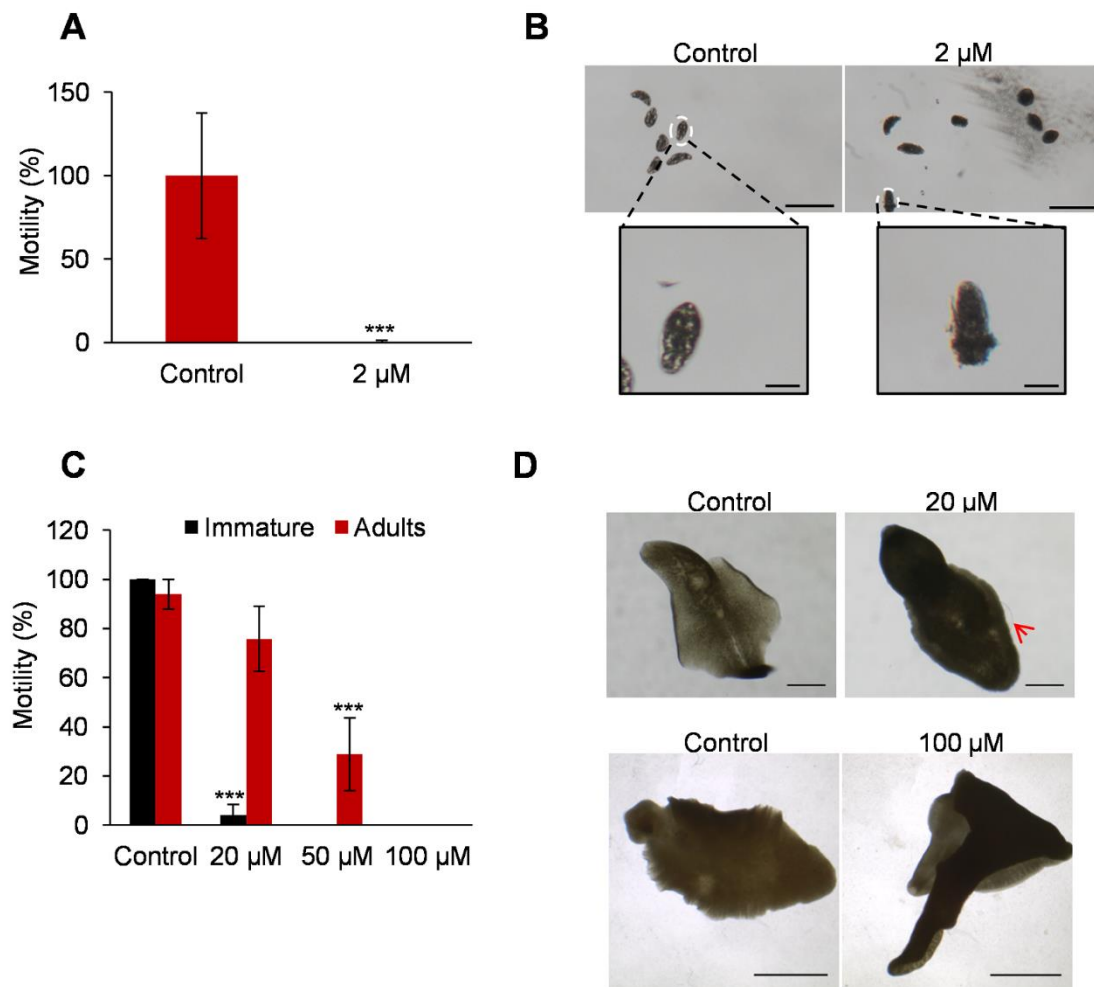


Figure 20. Effect of compound 028 on intra-mammalian stages of *F. hepatica*. (A) A significant reduction of NEJs motility was observed after treatment with $2\ \mu\text{M}$ of compound 028. (B) Morphological damage occurred in NEJs treated with $2\ \mu\text{M}$ of 028 as shown by bright-field microscopy. A closer look at damaged and intact NEJs (highlighted in white circles) is shown in higher magnification. (C) Motility analysis of immature and adult flukes treated with 20 , 50 , and $100\ \mu\text{M}$ of 028. Immature flukes showed a significant reduction in motility when treated with $20\ \mu\text{M}$ 028. Adults exhibited a significant reduction of motility upon treatment with $50\ \mu\text{M}$ 028. (D) Phenotypic effects on immature and adult flukes were observed by bright-field microscopy. The arrow indicates a tegument bubble in an immature fluke. Average values

of the motility of 10-20 NEJs, 6 immature flukes, and 11-12 biological replicates (with SEM) of two independent experiments (for NEJs and immature flukes) and three independent experiments (for adult flukes) are shown. Scale bars: for NEJs 500 μm (whole) and 100 μm (zoom). For immature fluke, scale bar = 1 mm, and for adults, scale bar = 5 mm. Significant differences are indicated with *** $p < 0.001$ (Mann-Whitney test).

3.2.7. Effects of DSF and 028 on oxidative stress-related genes

Resistance to chemotherapeutic agents has been associated with an increase in the expression of human aldehyde dehydrogenase *Hsaldh1a1* as well as the expression of ROS-inactivating enzymes in cancer cells (Lei et al., 2019; Yokoyama et al., 2016). To get insights if a similar mechanism of resistance that may occur in *F. hepatica*, first qRT-PCR analyses were performed for selected genes with predicted functions in oxidative stress management (Morawietz et al., 2020). To this end, I used sub-lethal concentrations of DSF and 028, which failed to affect the vitality of the parasite, i.e., DSF 100 μM , 028 20 μM . I observed a significant upregulation of transcript levels of two of the selected genes, which code for superoxide dismutase (*Fhsod* and *Fhsodex*) as well as *Fhaldh1* when compared to control worms (**Figure 21**). In contrast, 028 treatment induced an increase in the expression of only one gene, *Fhsodex*. Interestingly, there was no change in the expression level of *Fhsodex*, *Fhsod*, and *Fhaldh1* upon TCBZ treatment.

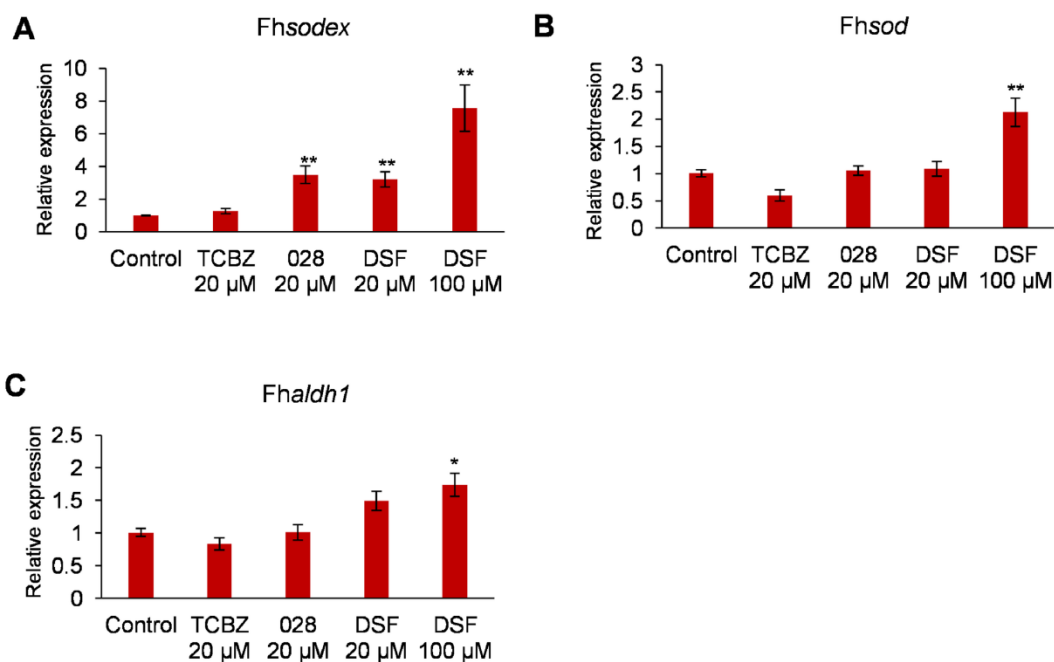


Figure 21. Expression of oxidative stress-related genes by DSF and 028 in adult *F. hepatica*. Expression analysis of *Fhsodex* (A), *Fhsod* (B), and *Fhaldh1* (C) by adult flukes after treatment with sub-lethal concentrations of DSF, 028, and TCBZ for 72 h. For the normalization of qPCR data, the geometric mean of the two most stably *in vivo*-expressed reference genes, *Fhtbcd* and *Fheprs*, was used. Average values of 3-4 biological replicates (with SEM) from one experiment are shown. Significant difference is indicated with * $p < 0.05$ and ** $p < 0.01$ (t-test).

3.2.8. Compound 028 possibly affects stem cell self-renewal

Another aspect of the ALDH1 family is its implication in the proliferation of cancer stem cells and also its role as a stemness marker (Duan et al., 2016; Mao et al., 2013; Moreb, 2008). Therefore, I intended to analyze the effects of sub-lethal concentrations of DSF and 028 on the self-renewal of stem cells. For this purpose, I used 4-week-old juveniles grown *in vitro* as a basis for my experiments because of the easy access to proliferating cells compared to other stages (McCusker et al., 2016). First, using qRT-PCR I confirmed that the expression of *Fhaldh1* and *Fhaldh2* in the *in vitro*-grown flukes mimics the expression in the *in vivo*-grown juveniles (**Figure 22A** and **Figure 22B**). Next, these juveniles were subjected to treatment with disulfiram or 028 for 48 h, and EdU was added to the culture medium 24 h before collection of the samples. CLSM images were then taken to assess the presence or absence of proliferating cells. The results showed the complete loss of EdU-positive cells in flukes treated with 1 μ M

of compound 028 compared to the control, which showed EdU-positive cells distributed throughout the worm body (**Figure 22C**). On the contrary, worms treated with DSF even at 15 μM showed no significant change in EdU-positive cells compared to the control (**Figure 22C**).

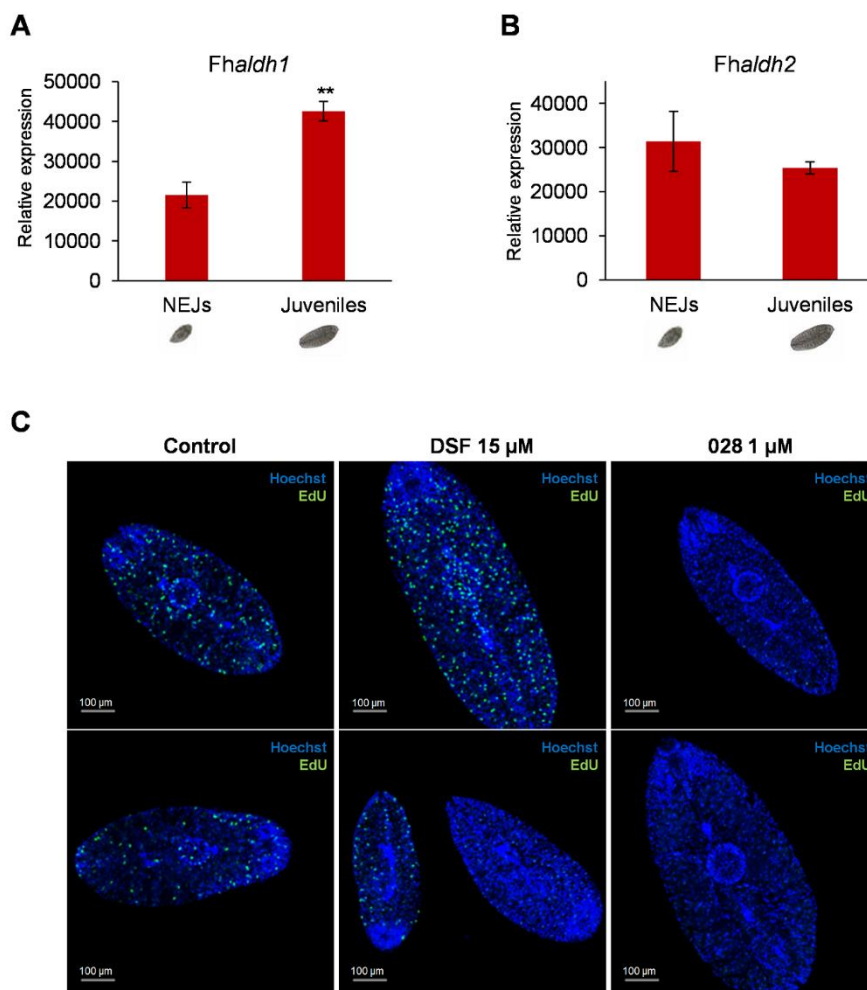


Figure 22. Transcript profiles of *Fhaldh1* and *Fhaldh2* and effects of compound 028 on stem-cell renewal in 4-week-grown juveniles. (A) qRT-PCR analyses showed a significant increase in *Fhaldh1* expression between NEJs (day 1 post-ecystment) and 4-weeks *in vitro* grown juveniles (day 28 post-ecystment), whereas no significant difference was shown for *Fhaldh2*. For the normalization of the qPCR data, the geometric mean of the two most stably *in vitro* expressed reference genes, *Fhtbcd* and *Fhpsmb7* were used. Average values of 3-4 biological replicates (with SEM) are shown. A significant difference is indicated with ** $p < 0.01$ (t-test). (B) CLSM images showing control juveniles displaying EdU-positive cells in the entire body (in green; Hoechst staining in blue). Such cells are absent when worms were treated with 1 μM of compound 028. In contrast, no significant differences were observed between untreated control worms and worms treated with 15 μM DSF. Scale bars correspond to 100 μm .

3.2.9. Knock-down (KD) of both *Fhaldh* orthologues and testing effects on cell proliferation

Based on the known roles of ALDHs in cell proliferation and cancer stem cells, I intended to check if ALDHs may also play roles in cell proliferation in *F. hepatica*. For this aim, I performed KD approaches by RNAi against *Fhaldh1* and *Fhaldh2* and investigated cell proliferation by EdU staining. Single KDs of each gene showed no effects (data not shown). Therefore, I performed a double KD approach for 14 days. Real-time qPCRs showed a KD efficiency of 90% for *Fhaldh1* and 75% for *Fhaldh2* (**Figure 23A**). It appeared that the worms showed a reduced size following KD. Although the number of EdU+ cells seemed to be reduced in treated worms compared to the control, which could be a consequence of their reduced size, this seems not to be a significant difference (**Figure 23B**).

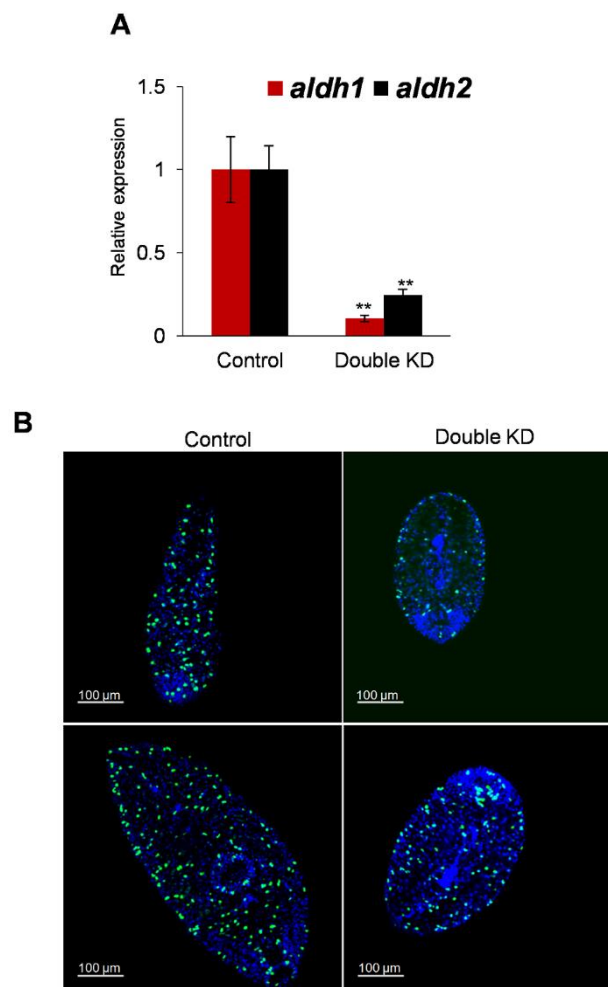


Figure 23. Effect of *Fhaldhs* knock-down on cell proliferation in 4 weeks *in vitro*-grown juveniles. (A) qRT-PCR shows a significant reduction of both *Fhaldhs* transcripts upon KD. (B) Analysis of the effect of KD on the size of the worms and proliferating cells by EdU

staining. The sizes of worms seem to be reduced after treatment as well as the number of EdU+ cells, although this seems not to be significant. Average values of 2 biological replicates with SEM are shown. A significant difference is indicated with ** $p < 0.01$ (t-test). Scale bars correspond to 100 μm .

4. DISCUSSION

4.1. Identification of housekeeping genes for real-time qPCR analyses in *F. hepatica*

4.1.1. A stably expressed reference genes for more reliable qRT-PCR analyses

Studying gene expression in all life stages of the liver fluke *F. hepatica* is of great importance for several reasons. On the one hand, gene expression studies can be relevant as part of anthelmintic drug development and drug target characterization, since a potent drug can target a protein(s) expressed in all mammalian parasite stages. On the other hand, analysis of gene expression is considered a well-established and reliable method to quantify gene expression during *in vitro* culture, which is a crucial step e.g., validation of gene expression following knockdown (KD) approaches by RNAi. Among others, members of signalling pathways can be considered potential drug targets. Among these are kinases, which are one of the largest superfamilies of proteins. Kinases are involved in several biological processes such as cell proliferation, cell differentiation, and dorsal-ventral polarity (Hanks and Hunter, 1995). To get more insights into the role of kinases in the biology of *F. hepatica*, one aspect of the analysis is the determination of kinases' expression during the life cycle of the liver fluke. However, the absence of a stably expressed housekeeping gene for normalization makes an accurate expression analysis by qRT-PCR impossible.

One aim of this work was to identify the most stably expressed genes among eight reference gene candidates selected from previous studies in *F. hepatica*, *S. mansoni*, and the liver fluke *Clonorchis sinensis* (Cwiklinski et al., 2018; Haeberlein et al., 2019; Lu et al., 2017; Radio et al., 2018; Yoo et al., 2009). A comparison of expression stability was performed for the eight candidate genes and in two different experimental settings, the intra-mammalian life stage, and the *in vitro* culture of juvenile flukes. Because a slight divergent ranking of the selected genes was expected among the four algorithms due to the different types of input data and data processing used by different algorithms (DeLorenzo and Moon, 2018; Haeberlein et al., 2019), a global ranking based on the results of all algorithms was performed.

As defined by Butte et al., housekeeping genes are defined as being constitutively expressed to maintain e.g., cellular function (Butte et al., 2001). These genes are required to be stably expressed under several experimental conditions. Traditionally, *gapdh* is among the well-

known housekeeping genes used for qRT-PCR quantification in the trematode *F. hepatica* (Cwiklinski et al., 2018; McVeigh et al., 2014; Rinaldi et al., 2008). However, for human cells, it has been reported that the expression of *gapdh* is two-fold higher in the invasive T1C3 melanoma cells than in noninvasive 1C8 cells (Goidin et al., 2001). In addition, *gapdh* showed poor expression stability in the comparison between metacercariae and adults of the oriental liver fluke *Clonorchis sinensis* (Yoo et al., 2009). Moreover, *gapdh* was among the least stably expressed genes in a study on the related trematode *S. mansoni* (Haeberlein et al., 2019). These results indicated the possibility that *gapdh* may not represent a reliable housekeeping gene.

My experiments showed that the transcript level of *Fhgapdh* appeared to be significantly upregulated during the maturation of the fluke (*in vitro* and *in vivo*). This is of particular interest since, as discussed above, *gapdh* is currently a standard gene used for normalization of gene expression in *F. hepatica* research (Cwiklinski et al., 2018; McVeigh et al., 2014; Rinaldi et al., 2008). Based on my results, *gapdh* might not be a reliable reference gene for comparison of gene expression by qRT-PCR. This finding confirmed similar findings in other organisms used for lab studies (Haeberlein et al., 2019; Yoo et al., 2009) indicating that reference genes should be carefully selected and not just based on other studies in a related or non-related species.

4.1.2. Two different sets of reference genes for two different experimental settings

I found out that in the three intra-mammalian stages, the glutamyl-prolyl-tRNA synthetase *Fheprs* and tubulin-specific chaperone D *Fhtbcd* were most stably expressed. In *in vitro*-cultured parasites, *Fhtbcd*, and the proteasome subunit beta type-7 *Fhpsmb7* were the most stably expressed genes among the eight selected ones. Previous studies showed that the tubulin-specific chaperone TBCD is a microtubule-destabilizing protein that plays a role in the beta-tubulin folding, and thus microtubule assembly. Its action is, among others, very crucial since microtubules are involved in essential and specialized cellular functions such as cell division, intracellular transport, and cell motility (Martín et al., 2000; Tian et al., 2010). The glutamyl-prolyl-tRNA synthetase EPRS belongs to the family of aminoacyl-tRNA synthetases, which play a vital role in protein synthesis by charging tRNAs with their corresponding amino acids (Katsyv et al., 2016). The proteasome subunit beta type-7 PSMB7 is part of the 20S and 26 complexes, and thus it is involved in the degradation of most intracellular proteins. The proteasome plays a key role in the maintenance of protein homeostasis, stress response, cell division, and signal transduction (Bard et al., 2018; Rivett et al., 1997). Since protein

translation, protein degradation, and microtubule assembly are key mechanisms that contribute to the well-being of the cell as well as cell homeostasis, independently of the developmental stage of the fluke, it was not surprising to find *tbcd*, *eprs*, and *psmb7* to be the most stably expressed genes in this study. In a previous related study on *S. mansoni*, it has been shown that the ranking was in part like the one found for the *in vitro*-cultured liver flukes. Here the orthologue for *psmb7*, *Smpsmb7*, ranked also second-best during *in vitro* culture of adult worms, and *Smgapdh* was among the least stably expressed genes (Haeberlein et al., 2019). In contrast to the result found in schistosomes, which identified *letm1* as the most stable gene in adults, the *F. hepatica* orthologue was among the least stably expressed genes. In a meta-analysis on schistosomes, heterogenous rankings were also obtained for *tbcd* and *ppp1cb*: both genes were stably expressed in different life stages of *S. mansoni*, while in *F. hepatica*, only *tbcd* was (Lu et al., 2018). Altogether, the most stably expressed reference genes among the tested candidates in *F. hepatica* are genes belonging to the family of tRNA synthetases, proteasome subunits, and the microtubule machinery.

4.1.3. Kinases as important drug target analyses

In the context of fighting NTD such as fasciolosis, I focused on kinase genes as potential drug targets because of their importance to the cell and their intervention in several processes. In addition, kinases are discussed as druggable targets in other helminth species but also in protozoan parasites (Arendse et al., 2021; Efstathiou and Smirlis, 2021; Gelmedin et al., 2015; Hemer and Brehm, 2012; Kaur and Goyal, 2022; O'Connell et al., 2015). Therefore, I checked the expression of some selected kinases in the two experimental settings, intra-mammalian stages and the *in vitro* cultured flukes. It is important to note that kinases in the liver fluke have been largely neglected in research until now. Phosphofruktokinase seemed to be the only kinase of *F. hepatica* studied as a potential target (Mansour and Mansour, 1962; Schulman et al., 1982a), but was not further followed because of the suboptimal *in vivo* efficacy of a phosphofruktokinase inhibitor (MK-401) (Schulman et al., 1982b). In addition, kinases were either studied as vaccine candidates as this was the case for phosphoglycerate kinase (Wesołowska et al., 2016) or used as a marker to distinguish the hybrid species of *Fasciola* spp. as this is the case of phosphoenolpyruvate carboxykinase (Shoriki et al., 2016).

To get more insights on kinases of *F. hepatica* as a part of anthelmintics research, I identified five orthologues of kinase genes in *F. hepatica*. These kinases have been studied in several organisms, such as *S.mansoni*, *Echinococcus multilocularis*, and filaria (Beckmann and

Greveling, 2010; Hemer and Brehm, 2012; Morel et al., 2014; O'Connell et al., 2015; Ressurreição et al., 2014; Schubert et al., 2014). To analyze their expression patterns *in vivo* and *in vitro*, I quantified their transcript levels by qRT-PCR and normalized this against the newly characterized reference genes. My analyses revealed that these kinases were transcribed in all intra-mammalian stages of *F. hepatica*. In addition, interesting transcript profiles were detected throughout development. For instance, the potential polo-like kinase 1 orthologue *Fhplk1* followed an exponential expression pattern, which reached its peak at the adult stage in my analysis. This result might suggest that *Fhplk1* plays a particular role in later stages of development. Previous studies in *S. mansoni* have shown a similar pattern for the ortholog *Smplk1*, which was mainly found in germinal cells of adults. Furthermore, *Smplk1* KD experiments by RNAi strongly affected egg production and gonad morphology (Guidi et al., 2015; Long et al., 2010). In contrast to the *Fhplk1* expression pattern, orthologues of the two Abl kinases and two serine/threonine-protein kinases exhibited peaks of expression in NEJs, and then the expression decreased as the flukes became more and more mature. In other organisms, these kinases are, amongst others, involved in the regulation of polarity, stem-cell differentiation, cytoskeleton organization, morphogenesis, transcription, translation, cell proliferation, and apoptosis (Shaha et al., 2022; Stergiou et al., 2021; Wu et al., 2021). Thus, these kinases might play important roles during the early growth and development of flukes, which still has to be substantiated in functional studies in the future. In addition, these kinases were found to be expressed in all intra-mammalian stages, which is a prerequisite for any novel target in *F. hepatica*, because new and effective compounds should preferably be able to hit all developmental stages in the final host, as does the current gold standard TCBZ (Kelley et al., 2016). Whether the significant difference in mRNA expression levels between the parasite stages, which has been found for most kinases, will lead to a difference in susceptibility to target inhibition remains an open question for future investigation. As a first step towards the validation of a given gene as a drug target, a KD using RNAi should be achieved. For this aim, *in vitro*-cultured juveniles are needed that are more easily manipulated than larger stages, and it should be considered that according to our findings, kinase transcript levels significantly change during 4 weeks of culture. Furthermore, for all studied kinases, inhibitor treatment *in vitro* has revealed anthelmintic effects also on other parasitic flatworms, where the kinase inhibition induces several morphological and physiological effects, such as pairing stability, attachment, egg-laying, metastasis within the host, and pathological alterations of the gastrodermis, which finally leads to the death of the parasite (Beckmann and Greveling, 2010; Hemer and Brehm, 2012; Morel et al., 2014; Ressurreição et al., 2014; Schubert et al., 2014).

In *F. hepatica*, it has been already shown that imatinib (an ABL-TK inhibitor) and BI2536 (a PLK1 inhibitor) affect adult and immature flukes *in vitro*. Both inhibitors had a lethal effect on immature flukes. In addition, BI2536 significantly affected egg production by adults, whereas imatinib killed some of the adult flukes and significantly affected the motility of others (Morawietz et al., 2020). Previous results on kinases inhibitors in other parasitic systems as well as the data provided here, shed the lights on the possibility of kinases involvement in the developmental program of several parasites, and thus a solid basis for future work on this class of potential target molecules.

4.1.4. A solid basis for future gene expression analyses in *F. hepatica*

Taken together, for future expression analyses by qRT-PCR in *F. hepatica*, I propose using the glutamyl-prolyl-tRNA synthetase *Fheprs* and tubulin-specific chaperone D *Fhtbcd* as reference genes for studies dealing with the different intra-mammalian fluke stages. Beyond that, I suggest using *Fhtbcd* and the proteasome subunit beta type-7 *Fhpsmb7* for studies on *in vitro*-cultured juvenile flukes, such as for RNAi experiments. Especially for inter-stage comparisons, these new reference genes have the potential to replace the traditional housekeeping gene *gapdh*, which has been used in many *Fasciola* studies to date (Cwiklinski et al., 2018; McVeigh et al., 2014; Rinaldi et al., 2008), but turned out to be differentially expressed during fluke development in my analysis (Houhou et al., 2019). I also propose the validation of the suitability of reference genes once different experimental setups are used, such as extended drug treatment studies. Using the newly defined reference genes from this study, I quantified the expression of kinase orthologues in all relevant intra-mammalian life stages important for drug targeting, which revealed distinct expression patterns throughout development pointing to interesting biological functions. These results together with previous proteomic studies on the liver fluke (Di Maggio et al., 2016; Robinson et al., 2009) might open the door for more detailed analyses of the roles of kinases in the biology of *F. hepatica* and to validate these signalling molecules as potential anthelmintic targets.

4.1.5. Are kinases the end of the story or just the beginning?

To fight disease, one must fight its causes. Fighting fasciolosis means fighting *F. hepatica* by inhibiting its survival, growth, and/or development. In the fight against a devastating parasite, all factors should be envisaged that exert a crucial role(s) in the biology of the liver fluke.

Among these are kinases, as shown before for related parasites such as *S. mansoni*, *S. haematobium*, and *S. japonicum* (Grevelding et al., 2018; Stroehlein et al., 2015; Wu et al., 2021). The take-home message from the first part is that my results provided a solid base for real-time qPCR analyses to check the expression of any gene of interest in *F. hepatica*, including kinases and ALDHs as discussed next.

4.2. Identification of aldehyde dehydrogenases (ALDHs) in *F. hepatica* and evaluation of their suitability as drug targets

4.2.1. Why are aldehyde dehydrogenases (ALDHs) interesting molecules to study in the context of fighting NTDs?

Fighting parasites is a long and complicated journey (Alum et al., 2010; Artis, 2006; Kandoth and Mitchum, 2013). To find a potent new drug, we need to understand the basic biology of the parasites, which can be extremely complex: starting from reproduction, growth, invasion of hosts, overcoming the host's immune system, to drug resistance. A basic and important principle of cell biology is the detoxification of reactive molecules such as aldehydes. Once they accumulate, aldehydes are considered a major threat to the cells because these organic compounds are highly reactive species capable of forming adducts with DNA and proteins, and thus alter their biological functions and cause pathologies (Nelson et al., 2017). Cells have developed several strategies to eliminate accumulating aldehydes. Among the most important ones are “aldehydes scavengers” or aldehyde dehydrogenases (ALDHs) (Singh et al., 2013).

4.2.2. Presence of ALDHs in *F. hepatica* and the conserved nature of their key domains

ALDHs belong to a big superfamily, which is one of the ancient protein families that exists from archaeal species to the higher eukaryotes (Sophos and Vasiliou, 2003). Members of the ALDH superfamily are not exclusively expressed in a certain type of tissue, but they are widely distributed. Among other tissues, they can be found in the liver, brain, kidney, and eye. Moreover, ALDHs are found in different organelles of a cell such as the nucleus, cytosol, mitochondria, and endoplasmic reticulum (Rodríguez-Zavala et al., 2019; Stagos et al., 2010). While *H. sapiens* has 19 ALDHs, *A. thaliana* has 14 ALDHs, *C. elegans* has 13, and 6 annotated ALDHs exist in the yeast *S. cerevisiae*. In contrast, not much is known so far about the occurrence of ALDHs in *F. hepatica* (Singh et al., 2013; Vasiliou and Nebert, 2005). To shed the light on FhALDHs, it was a crucial first step to identify orthologues in the liver fluke and analyze to which ALDH family they belong. Blastp analysis of the ALDH sequences from the related trematode, the blood fluke, *S. mansoni*, allowed us to find two corresponding orthologues in the genome of *F. hepatica* that we first named FhALDH105 and FhALDH322. The numbers 105 and 322 come from the last three digits of the old gene ID, which belong to the genome version PRJEB6687(FhALDH105: BN1106_s3402B000105 and FhALDH322: BN1106_s645B000322). The phylogenetic analysis has shown that both orthologues belong to

two different clusters. While FhALDH105 appeared in a cluster of known ALDH2 proteins, which are mitochondrial ALDHs, FhALDH322 belongs to a cluster of ALDH1 proteins, which are cytosolic (Muzio et al., 2012). Moreover, the multiple sequence alignment showed the highly conserved nature of the catalytic residues between *F. hepatica* and other species. The ALDH1 orthologue of *F. hepatica* shared similar amino acids with the other orthologues at more than 55% of the aa residues, and the ALDH2 orthologue of *F. hepatica* shared more than 63% of the aa residues (data not shown). Altogether, these results highlight on the one hand the conserved nature of this enzyme between species, and on the other hand, it points out the importance of these domains (catalytic and binding domains) for the enzyme action. Altogether, my result showed the existence of two different ALDH orthologues in the liver fluke, and based on my phylogenetic analysis, the nomenclature of FhALDH1 for the cytosolic ALDHs and FhALDH2 for the mitochondrial one was introduced. Computational-based methods such as the deep learning based alignment-free method (DeepFam) for protein family modeling and prediction would help uncovering, to which subfamily the identified ALDH1 belongs (Seo et al., 2018).

4.2.3. Analyzing the expression profiles of Fhaldhs

To investigate the expression profiles of these orthologues during development and the *in vitro* growth of the parasite, RT-qPCR analyses were performed showing that Fhaldh1 was more abundantly expressed than Fhaldh2 throughout the life cycle of *F. hepatica*. Furthermore, the expression of the Fhaldh1 orthologue followed an exponential pattern with a peak of transcripts observed in the adult stages compared to the younger ones. This might reflect the importance of this orthologue particularly for the adult stage. This was substantiated by the presence of these transcripts in several tissues as revealed by *in situ* hybridization, signals were detected in the intestine, uterus, ovary, vitellarium, and testis. Several studies in other organisms also showed the localization of ALDH transcripts in several tissues. For instance, studies in mice demonstrated that ALDH1a1 is highly expressed in the small and large intestine (Alnouti and Klaassen, 2008) and the ovary, while ALDH1a2 is highly expressed in gonads followed by the uterus. It is also important to point out that ALDH1b1 is found in the intestine in a subset of cells as putative stem cells lining the intestine crypt and used as a potential marker for colorectal tumors (Singh et al., 2015; Wang et al., 2021). The presence of Fhaldh1 transcripts in ovaries, testicles, and uterus suggests the involvement of this orthologue in reproduction. This assumption is supported by previous studies showing that ALDH1a2 was the main enzyme

involved in retinoic acid biosynthesis, which is crucial for spermatogenesis (Kasimanickam, 2016; Khanehzad et al., 2021). Moreover, it has been previously shown that the missense mutation ALDH1A3 C174Y leads to a decrease in the fecundity in *C. elegans* by 50% (Wong et al., 2021).

The absence of *Fhaldh2* transcript detection by colorimetric *in situ* hybridization might be explained by the low level of transcription level of this orthologue compared to the level of *Fhaldh1*. This is in line with the results of qRT-PCR analyses indicating that *Fhaldh2* is low-abundantly expressed. ALDH2 is an important enzyme mainly present in the mitochondria and is mainly required for the detoxification reaction by converting aldehydes to their corresponding carboxylic acids (Muzio et al., 2012). Moreover, it has been shown that ALDH2 deficiency can promote skeletal muscle atrophy in mice (Kasai et al., 2022). Therefore, it is important to use other methods, which are technically more sensitive such as fluorescent *in situ* hybridization, to detect if this gene is ubiquitously expressed or tissue-specifically, which might also highlight an important role in the biology of the liver fluke. Spatial and single-cell transcriptomics could also help elucidate the expression patterns and levels of both orthologues. Indeed, preliminary data of our lab have shown that both *Fhaldhs* orthologues are expressed in several tissues and to different extents. Furthermore, both genes were found to be highly expressed in neoblasts-like cells (Oliver Puckelwaldt, Svenja Gramberg; ongoing work, unpublished data), which is in line with knowledge about the potential function of ALDHs also in cell proliferation including stem-cell activities (Muzio et al., 2012).

4.2.4. Is FhALDH1 capable of oxidizing aldehydes?

ALDHs are known for their capacity to oxidize aldehydes into their corresponding carboxylic acids in the presence of a cofactor, nicotinamide adenine dinucleotide (NAD), which in turn is converted to NADH (Marchitti et al., 2008). Therefore, and next to the *in silico* findings, I wanted to confirm if the identified orthologues harbor this capacity. Both orthologues were successfully expressed as recombinant enzymes in *E. coli*, however, since the expression of FhALDH1 was purer, I decided to focus attention on this orthologue for the subsequent biochemical analyses. It has been described that adding the reducing agent dithiothreitol (DTT), which can prevent the loss of enzyme activity by oxidation of the sulfhydryl groups, to the assay was able to boost the enzyme activity (Harnischfeger J, Beutler M, Salzig D, et al., 2021). The level of NAD conversion reached 6 μ M of NADH after 7 h, which was lower when compared to the activity of *S. mansoni* orthologue (~10 μ M). Although these results confirmed

that FhALDH1 was active, further optimization of the enzyme assay is needed. This may include adjusting the pH, temperature, and concentration of substrates and cofactors. Moreover, it has been shown that several ALDHs have different affinities to different aldehydes, which means that testing different aldehydes can help optimize the activity of the enzyme (Orywal and Szmitkowski, 2017; Yin et al., 1993; Yoshida et al., 1992). The knowledge of substrate preferences could help to reveal the potential biological roles of FhALDH1. The recombinant form of FhALDH1 can be used in the future as a basis for in-depth biochemical characterization, but also the screening of potential inhibitors.

4.2.5. Effect of the ALDH-inhibitor DSF on *F. hepatica*

In this study, I identified two ALDH orthologues in *F. hepatica* and confirmed the activity of one of these orthologues in an enzymatic assay. Next, I investigated whether ALDHs may represent suitable targets against *F. hepatica*, which could help on the way of establishing new drugs against *Fasciola*. Since the qRT-PCR results showed the expression of both orthologues in all intra-mammalian stages, both ALDHs may be targets of a drug that can target all mammalian life stages. For experimental validation, I tested disulfiram (DSF), a known drug that can irreversibly inhibit ALDHs (Lipsky et al., 2001a, 2001b).

DSF strongly affected the motility of NEJs and killed these juvenile parasites at 20 μ M, but DSF failed to exert effects on older stages (immature and adult flukes), even when the tested concentration was as high as 100 μ M. This indicates the sensitive nature of NEJs to DSF action, whereas later stages are more resistant to its action. The reason why DSF affects NEJs but doesn't affect later stages (immature and adult flukes) remains unclear at this stage of the analysis. A possible explanation is the differences in the metabolic activities between these stages. It has been shown that younger stages of *Plasmodium falciparum*, the ring stages, have decreased metabolic activities. Moreover, the older stages (schizont stage) showed an increased capacity for protein synthesis and protein turnover, which may contribute to artemisinin resistance, an antimalarial drug, by overcoming the protein damage caused by oxidative stress (Mok et al., 2011). More studies in *P. falciparum* have referred to the resilience of some stages to the artemisinin to the drug half-life as well as stage-specific lag time (Klonis et al., 2013). Therefore, it could be possible that earlier developmental stages of *F. hepatica* have metabolic activities and protein turnover which make them more sensitive to DSF action compared to older stages. Furthermore, it is well known that ALDHs are not the exclusive target of DSF and that DSF can target several signalling pathways (Han et al., 2015; Zha et al., 2014).

Therefore, it might be possible that those DSF targets are highly expressed in younger stages compared to the older ones, which makes younger stages more vulnerable to DSF action.

4.2.6. Chemical derivatization for a more potent inhibitor

Collaborators at the Phillips-University Marburg (Tom Gallinger, AG Schlitzer) have developed dithiocarbamate derivatives by chemical derivatization of the DSF core structure. Five of the tested inhibitors showed strong effects on adult flukes, causing a significant reduction in their motility when treated with 100 μM . One particular inhibitor (028) has shown an even stronger reduction in adult motility, which was affected even when the adults were treated with 50 μM 028. When compared with DSF, 028 was 10x more efficient and caused lethality at 2 μM compared to 20 μM of DSF under the same conditions. In addition, immature flukes were killed when treated with 20 μM 028, whereas no effect has been observed in the same stage when treated with the same concentration of DSF. It is important to note that 028 failed to show any cytotoxicity against a human cell line at 100 μM , a concentration at which adult flukes were killed. These results suggest that 028 could be a potential candidate for further development towards a drug, and as such an alternative for the well-established anti-fasciolosis drug triclabendazole.

4.2.7. Why might DSF be less potent against liver flukes compared to 028?

4.2.7.1. Possibilities of different targets and/or different pharmacodynamic modeling

Several explanations could help understand why DSF and its derivative have different efficiency when it comes to anti-parasitic action. Previous studies have shown that NPL4, a subunit of the p97/VCP segregase, is a DSF target in cancer cells (Skrott et al., 2017, 2019). Moreover, DSF can inhibit the O6-methylguanine-DNA methyltransferase in brain tumor cells and mouse brains (Paranjpe et al., 2014). Furthermore, an *in vitro* study on rat and human glutathione S-transferase isoenzymes has shown that these enzymes are DSF targets (Ploemen et al., 1996). In addition, it has been shown that DSF can inhibit triosephosphate isomerase and carbamate kinase in the flagellated parasitic microorganism, *Giardia duodenalis* (Castillo-Villanueva et al., 2017; Galkin et al., 2014). Taken together and given what is already known about the broad range of DSF's action, 028 might have even a broader range of action which

might explain its efficiency compared to the one of DSF. These targets might also have different expression profiles throughout the developmental stages of *F.hepatica*.

In addition, the differences in the efficiency of both inhibitors might also be explained by different pharmacodynamic properties. Theoretically, the relationship between the concentration of a given inhibitor and the effect is usually non-linear, which means that doubling the concentration of the inhibitor doesn't mean a stronger effect. It depends on several other factors. For instance, drug affinity to its receptor site, inhibitors half-life, and binding-rebinding mechanisms (Salahudeen and Nishtala, 2017; Vauquelin and Charlton, 2010). Therefore, DSF and 028 might follow different paths once taken by the fluke.

4.2.7.2. A possible counter-regulatory mechanism

The low efficiency of DSF in older stages might be explained by the induction of counter-regulatory gene expression in the parasite to escape DSF-mediated toxic effects. It has been shown that hematopoietic and leukemic stem cells with ALDH activity were highly resistant to the anti-cancer drug cyclophosphamide (Hilton, 1984; Kastan et al., 1990). In addition, tumor endothelial cells showed an increase in the expression of ALDH, which positively correlated to drug resistance as well as tumor progression (Hida et al., 2017). Previous studies have reported the involvement of ALDH1A1 in the acquisition of a stemness phenotype in tumor cells, which is why a high ALDH1A1 expression level is seen as a putative marker of cellular resistance to chemotherapeutic agents (Ciccione et al., 2020). Moreover, lung adenocarcinoma cells harboring a high level of ALDH1A1 expression are resistant to erlotinib, and this mechanism takes place via the induction of several proteins including ALDH1A1 itself (Lei et al., 2019). Besides elevated ALDH levels, malignant cells can achieve drug resistance by enhancing ROS metabolism (Butler et al., 2013; Gorrini et al., 2013). Lei et al. have shown that ALDH1A1 confers erlotinib resistance by facilitating the ROS-RCS metabolic pathway, which is associated with chemotherapy resistance (Lei et al., 2019). To investigate whether this could be an explanation of *F. hepatica* resistance of older stages to DSF action, qPCR data showed a significant up-regulation of *Fhaldh1* as well as *Fhsod* in adult worms when treated with 100 μ M of DSF. This finding suggests that a high concentration of DSF might trigger a cellular resistance mechanism, which can be manifested by an up-regulation of *Fhaldh1* and *Fhsod*, a response that has been shown in resistant cancer cells.

4.2.8. Co-therapy efficacy of DSF together with other drugs

Co-therapy is an option when it comes to enhancing the efficacy of a specific treatment. For instance, the antimalarial action of chloroquine can be potentiated when given with other drugs known to reduce cellular glutathione levels (Deharo et al., 2003). Moreover, it has already been shown that DSF together with copper Cu (II) act together to enhance the anti-tumor activity of imatinib in a dose-dependent way (Hassan et al., 2018). It has been shown that auranofin, a deubiquitinase inhibitor, and DSF provoke anti-tumor effects *in vitro* and *in vivo* when administered together (Huang et al., 2016). Furthermore, the DSF-copper combination inhibits several drug resistance-related targets in cancer such as ALDHs, NF- κ B, and MAPK pathways (Li et al., 2020). In addition, it has been shown that DSF facilitates the passage of copper across the blood-brain barrier and that the DSF-copper combination therapy in the mouse model may be an effective treatment for Menkes disease, which is characterized by copper deficiency (Bhadhprasisit et al., 2012). Although in this work DSF alone failed to show an effect on immature and adult worms, this doesn't rule out the importance of using this drug. Ongoing work on *S. mansoni* has already shown that adult flukes died when treated with the DSF-copper combination (Mandy Beutler, unpublished data). Therefore, it is worth for future work to try whether the DSF-copper combination may also enhance the effect of DSF on older stages of *F. hepatica*. Furthermore, future studies might clarify the question by co-treating liver flukes with DSF and triclabendazole to reveal whether the anthelmintic effects are attenuated or rather potentiated by DSF.

4.2.9. Stem cells as an important drug target

It has been long known the presence in the planarian *Schmidtea mediterranea*, a free-living platyhelminth, the only dividing cells in the adults are stem-like cells called "neoblasts". These cells are pluripotent with the capacity to proliferate and give rise to different progenitor cell types (Scimone et al., 2014). By actively dividing and replacing the missing parts, neoblasts also play important roles during regeneration upon injury of the planarian. Studies have expanded ever since to Platyhelminthes. It has been shown that neoblasts also exist in *S. mansoni* where they play roles in the differentiation into mesoderm-derived muscle cells and endoderm-derived gut cells. Moreover, they play a crucial role in conferring longevity in the definitive host (Wendt and Collins, 2016). Moreover, neoblasts-like cells constitute the only undifferentiated cells in *Echinococcus multilocularis* where they play an important role in larvae growth inside the host (Kozioł et al., 2014). Given the importance of stem cells in the

biology of Platyhelminthes, affecting stem cells can influence worm survival. Thus, stem cells constitute important targets for drug design. For instance, the inhibition of the polo-like kinase 1 in *Echinococcus multilocularis* (EmPLK1), using the specific inhibitor BI 2536, led to mitotic arrest and thus the inactivation of the germinative cells which lead to the arrest of the parasite proliferation and metacystode formation in the host (Schubert et al., 2014). In addition, the venom from the bug *Rhynocoris iracundus* affected stem-cell proliferation in different male tissues in *S. mansoni*, such as parenchyma and testes, which led to an antischistosomal activity (Tonk et al., 2020). Moreover, harmonine, an antimicrobial alkaloid from the harlequin ladybird *Harmonia axyridis*, reduced the number of proliferating cells in reproductive organs in *S. mansoni* such as ovaries and testes, as well as the number of proliferating parenchymal neoblasts (Kellershohn et al., 2019).

Previous reports have established a link between ALDH and a stem cell identity in normal and cancer stem cells. Studies have highlighted a strong link between the proliferation of stem cells and a high expression of ALDHs particularly ALDH1A1 and ALDH1A3 (Muzio et al., 2012; Vassalli, 2019). Therefore, I hypothesized that ALDH might also be involved in cell proliferation in *F. hepatica*. Indeed, the treatment of juvenile worms with the inhibitor 028 reduced the number of EdU-positive cells. This effect is much more pronounced when using 1 μ M 028, whereas when treated with 15 μ M DSF, juveniles didn't show a significant difference in the number of EdU+ cells. This result strongly suggests a negative influence of 028 on stem-cell renewal in *F. hepatica*. However, this result doesn't show sharp evidence of whether the stem cells were arrested after the uptake of 028, or whether the administration of 028 led to their death. In case of cell cycle arrest, removing 028 before adding EdU to the culture medium would lead to a recommencement of cell proliferation.

4.2.10. Hurdles in genetic validation of ALDH as a target

To gain more insight into whether the effects observed after DSF or 028 treatment may be mediated through inhibition of FhALDH, I knocked down the transcripts of both identified *Fhaldhs* in the *in vitro*-grown juveniles via RNAi and evaluated the effect after 14 days. A KD would ideally mimic an inhibitor's effect and thus contribute to genetic target validation. My preliminary data showed that the double KD of both orthologues in *F. hepatica* was successful as shown by the significantly decreased level of the transcripts of both orthologues through qRT-PCR analysis. KD worms showed a reduction in EdU+ cells, and thus a reduction in the number of proliferating cells. It is important to note that these are preliminary data, in which a

low replicate number was used (one experiment with 3-4 replicates). Therefore, to gain more insights into the effect of *Fhaldhs* KD, it would be necessary to reproduce these experiments as well as to perform quantification methods (such as “IMARIS for cell biologists” (Bitplane, Switzerland) to reveal if the ratio of juvenile size/EdU+ cell was affected or not. It is also important to note that the size of the *in vitro*-treated juveniles was reduced when compared to the control juveniles. This result suggests that ALDHs can also play a role in the growth and development of the parasite. In line with this observation, it has been already shown that ALDHs play a role in positively triggering the growth of normal and tumor cells. For instance, the RNA-binding protein Sam68 (*Khdrbs1*) was shown to modulate the expression of *Aldh1a3* via the regulation of its pre-mRNA 3'-end processing, and that *Khdrbs1*^{-/-} neural progenitor cells showed a decrease in ALDH1A3 and ALDH activity (ALDH isoform not specified), which resulted in the reduced cortical expansion (La Rosa et al., 2016). In addition, it was shown that the very primitive human mammary cells had low expression/activity of ALDHs and then these ALDHs were upregulated at the point of commitment to the luminal lineage (Eirew et al., 2012). This highlights the role of ALDHs in the proliferation/differentiation balance. In cancer cells, it was shown that inhibition of ALDH1A3 suppressed the growth of mesenchymal glioma cancer stem-like cells (Mao et al., 2013).

Although the knockdown efficiency was 90% for *Fhaldh1* and 75% for *Fhaldh2*, several factors might explain the lack of an obvious phenotype in the juveniles upon double KD. For instance, the KD was stopped after 14 d. A longer incubation time might enhance the observed phenotype. In addition, dsRNA at a concentration of 100 ng/μl was used, so it might be interesting to see if an increase in the amount of dsRNA as well as the number of replicates will increase the observed effect. In addition, the lack of an obvious phenotype could be explained by the presence of several FhALDHs, which exert a redundant function, and that the KD of the identified orthologues is not enough to generate an obvious phenotype in juveniles. Although the soaking method is well established, it is worth trying other methods of dsRNA delivery such as electroporation and checking whether a fast and more effective phenotype can be observed. In the meantime, western blot analysis would be crucial to detect if the KD succeeded to abolish ALDHs at the protein level. In addition, the Aldefluor technique would help to check if the activity of ALDHs was reduced after KD (Moreb et al., 2012). Finally, an overview of the downstream effects of interference with *aldhs* expression could be achieved by a whole transcriptome analysis to see what kind of genes are up or downregulated.

In this regard, apart from targeting ALDHs themselves, targeting factors upstream or downstream of ALDH might also be considered. For instance, it has been shown that BRD4, which belongs to the bromodomain and extra-terminal (BET) protein family, is capable of inducing the expression of *aldh1A1* via a super-enhancer element and its associated enhancer RNA, and that a BET inhibitor can target ALDH expression and activity in epithelial ovarian cancer, which is considered as a kind of clinical strategy against ovarian cancer (Yokoyama et al., 2016).

4.3. Conclusion

In conclusion, I identified, cloned, overexpressed, and characterized two ALDH orthologues in the liver fluke *Fasciola hepatica*, FhALDH1, and FhALDH2, using bioinformatics, molecular, and biochemical approaches. To my knowledge, this is the first study that sheds light on the ALDH-enzyme superfamily in liver flukes. Furthermore, I established two different sets of housekeeping genes to be used in two different experimental settings: the intra-mammalian stages (Fheprs and Fhtbcd) and the *in vitro*-cultured juveniles (Fhtbcd and Fhpsmb7). These housekeeping genes allowed the accurate quantification of Fhaldh transcript levels and represent a solid basis for future characterization of any gene of interest in *F. hepatica*. Moreover, I found Fhaldh transcripts throughout the life stages. Fhaldh1 reached a peak in the adult stages, in which its transcripts accumulate in the intestine and reproductive organs. In collaboration with the group of Prof. Schlitzer (Phillips University Marburg), I discovered that 028, a novel small-molecule inhibitor, in contrast to DSF exerted a more potent antiparasitic effect on all stages of *F. hepatica*. This effect was explained by the observed suppression of cell proliferation. Future work should investigate whether 028 can directly inhibit FhALDHs, and/or further molecules and whether this DSF derivative shows antiparasitic activity also in animal models. For substantiating their target potential, extended knockdown analyses are needed to shed more light on the role of Fhaldhs in the biology of *Fasciola hepatica*.

5. SUMMARY/ZUSAMMENFASSUNG

5.1. Summary

Fasciolosis is caused by liver flukes such as *Fasciola hepatica* and *Fasciola gigantica* and is considered a neglected tropical disease (NTD) with a tremendous impact on human and animal health. Triclabendazole (TCBZ) represents, due to its wide range of action, today's most effective drug against liver flukes. However, *F. hepatica* has developed resistance against TCBZ, and in the absence of an effective vaccine, it is of great importance to find alternative anthelmintic drugs.

Several protein families could serve as targets for therapeutic intervention. This work followed the hypothesis that aldehyde dehydrogenases (ALDHs) represent druggable targets in *F. hepatica*. So far, this is the first study focusing on ALDHs in this parasite. I identified two ALDH orthologues in the liver fluke using *in silico* analyses and based on the corresponding sequences of aldehyde dehydrogenases (ALDHs) in the related trematode *Schistosoma mansoni*. After the sequence of *Fhaldh1* was completed by 3'-RACE PCR, I cloned the coding sequences of both *Fhaldh1* and *Fhaldh2*, I determined the expression of these two genes by quantitative realtime-PCR. To this end, I first identified two sets of reference genes for two groups of worms that are of relevance for different experimental settings: *in vitro*-cultured worms and the intra-mammalian stages. The new reference genes were successfully applied to quantify the expression also of other druggable targets including various protein kinases. Both *Fhaldh* orthologues were expressed in all life stages of the parasite. *Fhaldh1* transcripts were localized in the reproductive organs as well as in the intestine as revealed by *in situ* hybridization. The successful expression of recombinant FhALDH1 allowed the setting up of an enzyme assay, which showed that this enzyme harbors the capacity of converting aldehydes into their corresponding carboxylic acids. While disulfiram (DSF), a well-known anti-cancer drug targeting ALDHs, was active against juvenile stages *in vitro*, it was inactive against immature and adult flukes. On the contrary, all three developmental stages were killed by a DSF derivative, the dithiocarbamate 028, at concentrations of 2, 20, and 50 μM , respectively, an activity that resembled the activity of TCBZ in the *in vitro* assay. Both compounds triggered the expression of oxidative stress-related genes. However, only 028 showed the capacity to abolish cell proliferation in juvenile flukes, which points to an impairment of cell-cycle control.

A preliminary result of a double knockdown of both orthologues pointed to a possible role of ALDHs in controlling the growth of juvenile *F. hepatica*.

Altogether, this work identified and characterized to some extent two ALDH orthologues of *F. hepatica* by *in silico* analyses as well as molecular and biochemical approaches. Furthermore, this work provides the first evidence that targeting ALDHs could be considered a novel strategy in the fight against *F. hepatica*. These results provide the basis to continue investigating the role(s) of ALDHs in the biology of *F. hepatica* in more detail in future studies and developing ALDH inhibitors as anthelmintic drugs.

5.2. Zusammenfassung

Fasziolose wird durch Leberegel wie *Fasciola hepatica* und *Fasciola gigantica* verursacht und gilt als vernachlässigte Tropenkrankheit (NTD) mit enormen Auswirkungen auf die Gesundheit von Mensch und Tier. Triclabendazol (TCBZ) ist aufgrund seines breiten Wirkungsspektrums das derzeit wirksamste Medikament gegen den Leberegel, jedoch sind Resistenzen gegen TCBZ weit verbreitet. In Ermangelung eines wirksamen Impfstoffs ist es von großer Bedeutung, neue alternative Anthelminthika gegen *F. hepatica* zu finden.

Mehrere Proteinfamilien könnten als Ziel für die Wirkstoffentwicklung dienen. In dieser Arbeit lag der Schwerpunkt auf Aldehyddehydrogenasen (ALDHs). Bisher ist dies die erste Studie, die sich auf ALDHs in *F. hepatica* konzentriert. Basierend auf entsprechenden ALDH-Sequenzen des verwandten Trematoden *Schistosoma mansoni* identifizierte ich zunächst *in silico* zwei Orthologe des Leberegels, FhALDH1 und FhALDH2. Nachdem beide *aldh*-Gene kloniert waren, wurde die Expression dieser Gene quantitativer Realtime-PCR (qRT-PCR) quantifiziert. Hierfür identifizierte ich zunächst zwei Sätze von Referenzgenen für zwei Wurmgruppen, die in verschiedenen experimentellen Ansätzen von Relevanz sind: *in vitro*-kultivierte Würmer und die pathogenen Stadien im Endwirt. Mithilfe dieser neuen Referenzgene gelang es, auch die Expression weiterer potenzieller Wirkstoffziele, diverser Proteinkinasen, erfolgreich zu quantifizieren. Die *Fhaldh*-Orthologe wurden in allen Lebensstadien des Parasiten exprimiert und in-situ-Hybridisierung zeigte, dass *Fhaldh1*-Transkripte sowohl in den Fortpflanzungsorganen als auch im Darm lokalisiert sind. Nach erfolgreicher Expression von rekombinantem FhALDH1 belegte ein von mir etablierter Enzymassay, dass dieses Enzym die Fähigkeit besitzt, Aldehyde in ihre entsprechenden Carbonsäuren umzuwandeln. Während Disulfiram (DSF), ein bekanntes Krebsmedikament

und ein ALDH-Inhibitor, gegen juvenile *F. hepatica in vitro* aktiv war, wurden keine Effekte gegen immature und adulte Egel beobachtet. Alle drei Stadien wurden hingegen durch das Dithiocarbamat 028, ein DSF-Derivat, in Konzentrationen von 2, 20 bzw. 50 μM abgetötet. Damit verhielt sich 028 ähnlich aktiv wie TCBZ in den in-vitro-Assays. Während beide Substanzen die Expression von Genen induzierten, die mit oxidativem Stress assoziiert sind, zeigte nur 028 die Fähigkeit, Zellproliferation in juvenilen Egel vollständig zu unterbinden. Dies weist auf eine Störung der Kontrolle des Zellzyklus hin. Vorläufige Daten nach gleichzeitigem Knockdown beider Orthologe deuteten auf eine mögliche Rolle von ALDHs bei der Wachstumskontrolle juveniler *F. hepatica* hin.

Insgesamt wurden in dieser Arbeit zwei ALDH-Orthologe in *F. hepatica* identifiziert und durch *in silico*- Analysen sowie molekularbiologische und biochemische Methoden zum Teil charakterisiert. Die Resultate dieser Arbeit geben erste Hinweise darauf, dass das Targeting von ALDHs als neue Strategie im Kampf gegen *F. hepatica* in Betracht gezogen werden könnte. Diese Resultate liefern die Grundlage zur weiteren Erforschung der Rolle von ALDHs in der Biologie von *F. hepatica* sowie zur Entwicklung von ALDH-Inhibitoren als neue Anthelminthika.

6. REFERENCES

- Adell, T., Martín-Durán, J.M., Saló, E., and Cebrià, F. (2015). Platyhelminthes. In *Evolutionary Developmental Biology of Invertebrates 2: Lophotrochozoa (Spiralia)*, A. Wanninger, ed. (Vienna: Springer Vienna), pp. 21–40.
- Agatsuma, T., Arakawa, Y., Iwagami, M., Honzako, Y., Cahyaningsih, U., Kang, S.Y., and Hong, S.J. (2000). Molecular evidence of natural hybridization between *Fasciola hepatica* and *Fasciola gigantica*. *Parasitol Int* 49, 231–238. [https://doi.org/10.1016/s1383-5769\(00\)00051-9](https://doi.org/10.1016/s1383-5769(00)00051-9).
- Alnouti, Y., and Klaassen, C.D. (2008). Tissue distribution, ontogeny, and regulation of aldehyde dehydrogenase (Aldh) enzymes mRNA by prototypical microsomal enzyme inducers in mice. *Toxicol Sci* 101, 51–64. <https://doi.org/10.1093/toxsci/kfm280>.
- Alum, A., Rubino, J.R., and Ijaz, M.K. (2010). The global war against intestinal parasites—should we use a holistic approach? *Int J Infect Dis* 14, e732–738. <https://doi.org/10.1016/j.ijid.2009.11.036>.
- Alvarez, L.I., Solana, H.D., Mottier, M.L., Virkel, G.L., Fairweather, I., and Lanusse, C.E. (2005). Altered drug influx/efflux and enhanced metabolic activity in triclabendazole-resistant liver flukes. *Parasitology* 131, 501–510. <https://doi.org/10.1017/S0031182005007997>.
- Alvarez Rojas, C.A., Jex, A.R., Gasser, R.B., and Scheerlinck, J.-P.Y. (2014). Techniques for the diagnosis of *Fasciola* infections in animals: room for improvement. *Adv Parasitol* 85, 65–107. <https://doi.org/10.1016/B978-0-12-800182-0.00002-7>.
- Andersen, C.L., Jensen, J.L., and Ørntoft, T.F. (2004). Normalization of real-time quantitative reverse transcription-PCR data: a model-based variance estimation approach to identify genes suited for normalization, applied to bladder and colon cancer data sets. *Cancer Res* 64, 5245–5250. <https://doi.org/10.1158/0008-5472.CAN-04-0496>.
- Anderson, R.M., Mercer, J.G., Wilson, R.A., and Carter, N.P. (1982). Transmission of *Schistosoma mansoni* from man to snail: experimental studies of miracidial survival and infectivity in relation to larval age, water temperature, host size and host age. *Parasitology* 85 (Pt 2), 339–360. <https://doi.org/10.1017/s0031182000055323>.
- Arendse, L.B., Wyllie, S., Chibale, K., and Gilbert, I.H. (2021). Plasmodium kinases as potential drug targets for malaria: challenges and opportunities. *ACS Infect Dis* 7, 518–534. <https://doi.org/10.1021/acsinfecdis.0c00724>.
- Artis, D. (2006). New weapons in the war on worms: identification of putative mechanisms of immune-mediated expulsion of gastrointestinal nematodes. *Int J Parasitol* 36, 723–733. <https://doi.org/10.1016/j.ijpara.2006.02.011>.
- Bard, J.A.M., Goodall, E.A., Greene, E.R., Jonsson, E., Dong, K.C., and Martin, A. (2018). Structure and function of the 26S proteasome. *Annu Rev Biochem* 87, 697–724. <https://doi.org/10.1146/annurev-biochem-062917-011931>.

- Beckmann, S., and Grevelding, C.G. (2010). Imatinib has a fatal impact on morphology, pairing stability and survival of adult *Schistosoma mansoni* *in vitro*. *Int J Parasitol* *40*, 521–526. <https://doi.org/10.1016/j.ijpara.2010.01.007>.
- Beesley, N.J., Caminade, C., Charlier, J., Flynn, R.J., Hodgkinson, J.E., Martinez-Moreno, A., Martinez-Valladares, M., Perez, J., Rinaldi, L., and Williams, D.J.L. (2018). Fasciola and fasciolosis in ruminants in Europe: Identifying research needs. *Transbound Emerg Dis* *65 Suppl 1*, 199–216. <https://doi.org/10.1111/tbed.12682>.
- Bennett, C.E. (1977). *Fasciola hepatica*: development of excretory and parenchymal systems during migration in the mouse. *Exp Parasitol* *41*, 43–53. [https://doi.org/10.1016/0014-4894\(77\)90128-x](https://doi.org/10.1016/0014-4894(77)90128-x).
- Bhadhprasit, W., Kodama, H., Fujisawa, C., Hiroki, T., and Ogawa, E. (2012). Effect of copper and disulfiram combination therapy on the macular mouse, a model of Menkes disease. *J Trace Elem Med Biol* *26*, 105–108. <https://doi.org/10.1016/j.jtemb.2012.05.002>.
- Burger, P.E., Gupta, R., Xiong, X., Ontiveros, C.S., Salm, S.N., Moscatelli, D., and Wilson, E.L. (2009). High aldehyde dehydrogenase activity: a novel functional marker of murine prostate stem/progenitor cells. *Stem Cells* *27*, 2220–2228. <https://doi.org/10.1002/stem.135>.
- Butler, E.B., Zhao, Y., Muñoz-Pinedo, C., Lu, J., and Tan, M. (2013). Stalling the engine of resistance: targeting cancer metabolism to overcome therapeutic resistance. *Cancer Res* *73*, 2709–2717. <https://doi.org/10.1158/0008-5472.CAN-12-3009>.
- Butte, A.J., Dzau, V.J., and Glueck, S.B. (2001). Further defining housekeeping, or “maintenance,” genes Focus on “A compendium of gene expression in normal human tissues”. *Physiol Genomics* *7*, 95–96. <https://doi.org/10.1152/physiolgenomics.2001.7.2.95>.
- Cabada, M.M., Lopez, M., Cruz, M., Delgado, J.R., Hill, V., and White, A.C.J. (2016). Treatment failure after multiple courses of triclabendazole among patients with fascioliasis in Cusco, Peru: A Case Series. *PLoS Negl Trop Dis* *10*, e0004361. <https://doi.org/10.1371/journal.pntd.0004361>.
- Castillo-Villanueva, A., Rufino-González, Y., Méndez, S.-T., Torres-Arroyo, A., Ponce-Macotela, M., Martínez-Gordillo, M.N., Reyes-Vivas, H., and Oria-Hernández, J. (2017). Disulfiram as a novel inactivator of *Giardia lamblia* triosephosphate isomerase with anti-giardial potential. *Int J Parasitol Drugs Drug Resist* *7*, 425–432. <https://doi.org/10.1016/j.ijpddr.2017.11.003>.
- Christ, O., Lucke, K., Imren, S., Leung, K., Hamilton, M., Eaves, A., Smith, C., and Eaves, C. (2007). Improved purification of hematopoietic stem cells based on their elevated aldehyde dehydrogenase activity. *Haematologica* *92*, 1165–1172. <https://doi.org/10.3324/haematol.11366>.
- Ciccone, V., Morbidelli, L., Ziche, M., and Donnini, S. (2020). How to conjugate the stemness marker ALDH1A1 with tumor angiogenesis, progression, and drug resistance. *Cancer Drug Resistance* *3*, 26–37. <https://doi.org/10.20517/cdr.2019.70>.
- Cobby, J., Mayersohn, M., and Selliah, S. The rapid reduction of disulfiram in blood and plasma. *J Pharmacol Exp Ther*. 1977 Sep;202(3):724-31. PMID: 197231.

- Collins, J.J. (2017). Platyhelminthes. *Current Biology* 27, R252–R256. <https://doi.org/10.1016/j.cub.2017.02.016>.
- Collins, J.N.R., and Collins, J.J. 3rd (2016). Tissue degeneration following loss of *Schistosoma mansoni cbp1* is associated with increased stem cell proliferation and parasite death *in vivo*. *PLoS Pathog* 12, e1005963. <https://doi.org/10.1371/journal.ppat.1005963>.
- Collins, J.J. 3rd, Wendt, G.R., Iyer, H., and Newmark, P.A. (2016). Stem cell progeny contribute to the schistosome host-parasite interface. *Elife* 5, e12473. <https://doi.org/10.7554/eLife.12473>.
- Cribb, T.H., Bray, R.A., Olson, P.D., and Littlewood, D.T.J. (2003). Life cycle evolution in the digenea: a new perspective from phylogeny. *Adv Parasitol* 54, 197–254. [https://doi.org/10.1016/s0065-308x\(03\)54004-0](https://doi.org/10.1016/s0065-308x(03)54004-0).
- Cunningham, T.J., and Duester, G. (2015). Mechanisms of retinoic acid signalling and its roles in organ and limb development. *Nat Rev Mol Cell Biol* 16, 110–123. <https://doi.org/10.1038/nrm3932>.
- Cwiklinski, K., Dalton, J.P., Dufresne, P.J., La Course, J., Williams, D.J., Hodgkinson, J., and Paterson, S. (2015). The *Fasciola hepatica* genome: gene duplication and polymorphism reveals adaptation to the host environment and the capacity for rapid evolution. *Genome Biol* 16, 71. <https://doi.org/10.1186/s13059-015-0632-2>.
- Cwiklinski, K., O'Neill, S.M., Donnelly, S., and Dalton, J.P. (2016). A prospective view of animal and human fasciolosis. *Parasite Immunol* 38, 558–568. <https://doi.org/10.1111/pim.12343>.
- Cwiklinski, K., Jewhurst, H., McVeigh, P., Barbour, T., Maule, A.G., Tort, J., O'Neill, S.M., Robinson, M.W., Donnelly, S., and Dalton, J.P. (2018). Infection by the helminth parasite *Fasciola hepatica* requires rapid regulation of metabolic, virulence, and invasive factors to adjust to its mammalian host. *Mol Cell Proteomics* 17, 792–809. <https://doi.org/10.1074/mcp.RA117.000445>.
- Dalton, J.P., Neill, S.O., Stack, C., Collins, P., Walshe, A., Sekiya, M., Doyle, S., Mulcahy, G., Hoyle, D., Khaznadji, E., et al. (2003). *Fasciola hepatica* cathepsin L-like proteases: biology, function, and potential in the development of first generation liver fluke vaccines. *Int J Parasitol* 33, 1173–1181. [https://doi.org/10.1016/s0020-7519\(03\)00171-1](https://doi.org/10.1016/s0020-7519(03)00171-1).
- Dawes, B. (1959). Penetration of the liver-fluke, *Fasciola hepatica* into the snail, *Limnaea truncatula*. *Nature* 184(Suppl 17), 1334–1335. <https://doi.org/10.1038/1841334a0>.
- Deharo, E., Barkan, D., Krugliak, M., Golenser, J., and Ginsburg, H. (2003). Potentiation of the antimalarial action of chloroquine in rodent malaria by drugs known to reduce cellular glutathione levels. *Biochem Pharmacol* 66, 809–817. [https://doi.org/10.1016/s0006-2952\(03\)00396-4](https://doi.org/10.1016/s0006-2952(03)00396-4).
- Deitrich, R.A., and Erwin, V.G. Mechanism of the inhibition of aldehyde dehydrogenase *in vivo* by disulfiram and diethyldithiocarbamate. *Mol Pharmacol*. 1971 May;7(3):301-7. PMID: 4328422.

- DeLorenzo, D.M., and Moon, T.S. (2018). Selection of stable reference genes for RT-qPCR in *Rhodococcus opacus* PD630. *Sci Rep* 8, 6019. <https://doi.org/10.1038/s41598-018-24486-w>.
- Di Maggio, L.S., Tirloni, L., Pinto, A.F.M., Diedrich, J.K., Yates Iii, J.R., Benavides, U., Carmona, C., da Silva Vaz, I.J., and Berasain, P. (2016). Across intra-mammalian stages of the liver fluke *Fasciola hepatica*: a proteomic study. *Sci Rep* 6, 32796. <https://doi.org/10.1038/srep32796>.
- Didiášová, M., Banning, A., Brennenstuhl, H., Jung-Klawitter, S., Cinquemani, C., Opladen, T., and Tikkanen, R. (2020). Succinic semialdehyde dehydrogenase deficiency: An update. *Cells* 9. <https://doi.org/10.3390/cells9020477>.
- Dietrich, C.F., Kabaalioglu, A., Brunetti, E., and Richter, J. (2015). Fasciolosis. *Z Gastroenterol* 53, 285–290. <https://doi.org/10.1055/s-0034-1385728>.
- Dixon, K.E. (1966). The physiology of excystment of the metacercaria of *Fasciola hepatica* L. *Parasitology* 56, 431–456. <https://doi.org/10.1017/s0031182000068931>.
- Domeyer, B.E., and Sladek, N.E. (1980). Metabolism of 4-hydroxycyclophosphamide/aldophosphamide *in vitro*. *Biochem Pharmacol* 29, 2903–2912. [https://doi.org/10.1016/0006-2952\(80\)90035-0](https://doi.org/10.1016/0006-2952(80)90035-0).
- Dorak, M (Oxford: Taylor & Francis) (2008). Real-time PCR.
- Duan, J.-J., Cai, J., Guo, Y.-F., Bian, X.-W., and Yu, S.-C. (2016). ALDH1A3, a metabolic target for cancer diagnosis and therapy. *Int J Cancer* 139, 965–975. <https://doi.org/10.1002/ijc.30091>.
- Edenberg, H.J., and McClintick, J.N. (2018). Alcohol dehydrogenases, aldehyde dehydrogenases, and alcohol use disorders: A critical review. *Alcohol Clin Exp Res* 42, 2281–2297. <https://doi.org/10.1111/acer.13904>.
- Efstathiou, A., and Smirlis, D. (2021). Leishmania protein kinases: Important regulators of the parasite life cycle and molecular targets for treating leishmaniasis. *Microorganisms* 9. <https://doi.org/10.3390/microorganisms9040691>.
- Eirew, P., Kannan, N., Knapp, D.J.H.F., Vaillant, F., Emerman, J.T., Lindeman, G.J., Visvader, J.E., and Eaves, C.J. (2012). Aldehyde dehydrogenase activity is a biomarker of primitive normal human mammary luminal cells. *Stem Cells* 30, 344–348. <https://doi.org/10.1002/stem.1001>.
- Fairweather, I. (2011). Reducing the future threat from (liver) fluke: realistic prospect or quixotic fantasy? *Vet Parasitol* 180, 133–143. <https://doi.org/10.1016/j.vetpar.2011.05.034>.
- Feron, V.J., Til, H.P., de Vrijer, F., Woutersen, R.A., Cassee, F.R., and van Bladeren, P.J. (1991). Aldehydes: occurrence, carcinogenic potential, mechanism of action and risk assessment. *Mutat Res* 259, 363–385. [https://doi.org/10.1016/0165-1218\(91\)90128-9](https://doi.org/10.1016/0165-1218(91)90128-9).
- Galkin, A., Kulakova, L., Lim, K., Chen, C.Z., Zheng, W., Turko, I.V., and Herzberg, O. (2014). Structural basis for inactivation of *Giardia lamblia* carbamate kinase by disulfiram. *J Biol Chem* 289, 10502–10509. <https://doi.org/10.1074/jbc.M114.553123>.

- Garattini, E., and Terao, M. (2012). The role of aldehyde oxidase in drug metabolism. *Expert Opin Drug Metab Toxicol* 8, 487–503. <https://doi.org/10.1517/17425255.2012.663352>.
- Gelmedin, V., Dissous, C., and Grevelding, C.G. (2015). Re-positioning protein-kinase inhibitors against schistosomiasis. *Future Med Chem* 7, 737–752. <https://doi.org/10.4155/fmc.15.31>.
- Giuliani, S., Silva, A.C., Borba, J.V.V.B., Ramos, P.I.P., Paveley, R.A., Muratov, E.N., Andrade, C.H., and Furnham, N. (2018). Computationally-guided drug repurposing enables the discovery of kinase targets and inhibitors as new schistosomicidal agents. *PLoS Comput Biol* 14, e1006515. <https://doi.org/10.1371/journal.pcbi.1006515>.
- Goidin, D., Mamessier, A., Staquet, M.J., Schmitt, D., and Berthier-Vergnes, O. (2001). Ribosomal 18S RNA prevails over glyceraldehyde-3-phosphate dehydrogenase and beta-actin genes as internal standard for quantitative comparison of mRNA levels in invasive and noninvasive human melanoma cell subpopulations. *Anal Biochem* 295, 17–21. <https://doi.org/10.1006/abio.2001.5171>.
- González-Bermúdez, L., Anglada, T., Genescà, A., Martín, M., and Terradas, M. (2019). Identification of reference genes for RT-qPCR data normalisation in aging studies. *Sci Rep* 9, 13970. <https://doi.org/10.1038/s41598-019-50035-0>.
- Gorrini, C., Harris, I.S., and Mak, T.W. (2013). Modulation of oxidative stress as an anticancer strategy. *Nat Rev Drug Discov* 12, 931–947. <https://doi.org/10.1038/nrd4002>.
- Grevelding, C.G., Langner, S., and Dissous, C. (2018). Kinases: Molecular stage directors for schistosome development and differentiation. *Trends Parasitol* 34, 246–260. <https://doi.org/10.1016/j.pt.2017.12.001>.
- Grünblatt, E., and Riederer, P. (2016). Aldehyde dehydrogenase (ALDH) in Alzheimer's and Parkinson's disease. *J Neural Transm (Vienna)* 123, 83–90. <https://doi.org/10.1007/s00702-014-1320-1>.
- Guidi, A., Mansour, N.R., Paveley, R.A., Carruthers, I.M., Besnard, J., Hopkins, A.L., Gilbert, I.H., and Bickle, Q.D. (2015). Application of RNAi to genomic drug target validation in schistosomes. *PLoS Negl Trop Dis* 9, e0003801. <https://doi.org/10.1371/journal.pntd.0003801>.
- Haerberlein, S., Angrisano, A., Quack, T., Lu, Z., Kellershohn, J., Blohm, A., Grevelding, C.G., and Hahnel, S.R. (2019). Identification of a new panel of reference genes to study pairing-dependent gene expression in *Schistosoma mansoni*. *Int J Parasitol* 49, 615–624. <https://doi.org/10.1016/j.ijpara.2019.01.006>.
- Hald, J., and Jacobsen, E. (1948). A drug sensitizing the organism to ethyl alcohol. *Lancet* 2, 1001–1004. [https://doi.org/10.1016/s0140-6736\(48\)91514-1](https://doi.org/10.1016/s0140-6736(48)91514-1).
- Han, D., Wu, G., Chang, C., Zhu, F., Xiao, Y., Li, Q., Zhang, T., and Zhang, L. (2015). Disulfiram inhibits TGF- β -induced epithelial-mesenchymal transition and stem-like features in breast cancer via ERK/NF- κ B/Snail pathway. *Oncotarget* 6, 40907–40919. <https://doi.org/10.18632/oncotarget.5723>.

- Hanks, S.K., and Hunter, T. (1995). Protein kinases 6. The eukaryotic protein kinase superfamily: kinase (catalytic) domain structure and classification. *FASEB J* 9, 576–596. <https://doi.org/10.1096/fasebj.9.8.7768349>.
- Happich, F.A., and Boray, J.C. (1969). Quantitative diagnosis of chronic fasciolosis. 2. The estimation of daily total egg production of *Fasciola hepatica* and the number of adult flukes in sheep by faecal egg counts. *Aust Vet J* 45, 329–331. <https://doi.org/10.1111/j.1751-0813.1969.tb05012.x>.
- Harnischfeger J, Beutler M, Salzig D, et al. (2021). Biochemical characterization of the recombinant schistosome tegumental protein SmALDH_312 produced in *E. coli* and baculovirus expression vector system. *Electron J Biotechnol* 54, 26–36. <https://doi.org/10.1016/j.ejbt.2021.08.002>.
- Hart, B.W., and Faiman, M.D. (1992). *In vitro* and *in vivo* inhibition of rat liver aldehyde dehydrogenase by S-methyl N,N-diethylthiolcarbamate sulfoxide, a new metabolite of disulfiram. *Biochem Pharmacol* 43, 403–406. [https://doi.org/10.1016/0006-2952\(92\)90555-w](https://doi.org/10.1016/0006-2952(92)90555-w).
- Hart, B.W., and Faiman, M.D. (1994). *In vivo* pharmacodynamic studies of the disulfiram metabolite S-methyl N,N-diethylthiolcarbamate sulfoxide: inhibition of liver aldehyde dehydrogenase. *Alcohol Clin Exp Res* 18, 340–345. <https://doi.org/10.1111/j.1530-0277.1994.tb00023.x>.
- Haselbeck, R.J., Hoffmann, I., and Duester, G. (1999). Distinct functions for *Aldh1* and *Raldh2* in the control of ligand production for embryonic retinoid signaling pathways. *Dev Genet* 25, 353–364. [https://doi.org/10.1002/\(SICI\)1520-6408\(1999\)25:4<353:AID-DVG9>3.0.CO;2-G](https://doi.org/10.1002/(SICI)1520-6408(1999)25:4<353:AID-DVG9>3.0.CO;2-G).
- Hassan, I., Khan, A.A., Aman, S., Qamar, W., Ebaid, H., Al-Tamimi, J., Alhazza, I.M., and Rady, A.M. (2018). Restrained management of copper level enhances the antineoplastic activity of imatinib *in vitro* and *in vivo*. *Sci Rep* 8, 1682. <https://doi.org/10.1038/s41598-018-19410-1>.
- Haydon, D.T., Cleaveland, S., Taylor, L.H., and Laurenson, M.K. (2002). Identifying reservoirs of infection: a conceptual and practical challenge. *Emerg Infect Dis* 8, 1468–1473. <https://doi.org/10.3201/eid0812.010317>.
- Hemer, S., and Brehm, K. (2012). *In vitro* efficacy of the anticancer drug imatinib on *Echinococcus multilocularis* larvae. *Int J Antimicrob Agents* 40, 458–462. <https://doi.org/10.1016/j.ijantimicag.2012.07.007>.
- Hida, K., Maishi, N., Akiyama, K., Ohmura-Kakutani, H., Torii, C., Ohga, N., Osawa, T., Kikuchi, H., Morimoto, H., Morimoto, M., et al. (2017). Tumor endothelial cells with high aldehyde dehydrogenase activity show drug resistance. *Cancer Sci* 108, 2195–2203. <https://doi.org/10.1111/cas.13388>.
- Hilton, J. Role of aldehyde dehydrogenase in cyclophosphamide-resistant L1210 leukemia. *Cancer Res.* 1984 Nov;44(11):5156-60. PMID: 6488175.
- Hodgkinson, J., Cwiklinski, K., Beesley, N.J., Paterson, S., and Williams, D.J.L. (2013). Identification of putative markers of triclabendazole resistance by a genome-wide analysis of genetically recombinant *Fasciola hepatica*. *Parasitology* 140, 1523–1533. <https://doi.org/10.1017/S0031182013000528>.

- Houhou, H., Puckelwaldt, O., Strube, C., and Haeblerlein, S. (2019). Reference gene analysis and its use for kinase expression profiling in *Fasciola hepatica*. *Sci Rep* 9, 15867. <https://doi.org/10.1038/s41598-019-52416-x>.
- Howe, K.L., Bolt, B.J., Shafie, M., Kersey, P., and Berriman, M. (2017). WormBase ParaSite - a comprehensive resource for helminth genomics. *Mol Biochem Parasitol* 215, 2–10. <https://doi.org/10.1016/j.molbiopara.2016.11.005>.
- Huang, H., Liao, Y., Liu, N., Hua, X., Cai, J., Yang, C., Long, H., Zhao, C., Chen, X., Lan, X., et al. (2016). Two clinical drugs deubiquitinase inhibitor auranofin and aldehyde dehydrogenase inhibitor disulfiram trigger synergistic anti-tumor effects *in vitro* and *in vivo*. *Oncotarget* 7, 2796–2808. <https://doi.org/10.18632/oncotarget.6425>.
- Jean, E., Laoudj-Chenivesse, D., Notarnicola, C., Rouger, K., Serratrice, N., Bonnieu, A., Gay, S., Bacou, F., Duret, C., and Carnac, G. (2011). Aldehyde dehydrogenase activity promotes survival of human muscle precursor cells. *J Cell Mol Med* 15, 119–133. <https://doi.org/10.1111/j.1582-4934.2009.00942.x>.
- de Jonge, H.J.M., Fehrmann, R.S.N., de Bont, E.S.J.M., Hofstra, R.M.W., Gerbens, F., Kamps, W.A., de Vries, E.G.E., van der Zee, A.G.J., te Meerman, G.J., and ter Elst, A. (2007). Evidence based selection of housekeeping genes. *PLoS One* 2, e898. <https://doi.org/10.1371/journal.pone.0000898>.
- Kandath, P.K., and Mitchum, M.G. (2013). War of the worms: how plants fight underground attacks. *Curr Opin Plant Biol* 16, 457–463. <https://doi.org/10.1016/j.pbi.2013.07.001>.
- Kasai, A., Jee, E., Tamura, Y., Kouzaki, K., Kotani, T., and Nakazato, K. (2022). Aldehyde dehydrogenase 2 deficiency promotes skeletal muscle atrophy in aged mice. *Am J Physiol Regul Integr Comp Physiol* 322, R511–R525. <https://doi.org/10.1152/ajpregu.00304.2021>.
- Kasimanickam, V.R. (2016). Expression of retinoic acid-metabolizing enzymes, ALDH1A1, ALDH1A2, ALDH1A3, CYP26A1, CYP26B1 and CYP26C1 in canine testis during post-natal development. *Reprod Domest Anim* 51, 901–909. <https://doi.org/10.1111/rda.12756>.
- Kasinathan, R.S., Morgan, W.M., and Greenberg, R.M. (2010). *Schistosoma mansoni* express higher levels of multidrug resistance-associated protein 1 (SmMRP1) in juvenile worms and in response to praziquantel. *Mol Biochem Parasitol* 173, 25–31. <https://doi.org/10.1016/j.molbiopara.2010.05.003>.
- Kastan, M.B., Schlaffer, E., Russo, J.E., Colvin, O.M., Civin, C.I., and Hilton, J. (1990). Direct demonstration of elevated aldehyde dehydrogenase in human hematopoietic progenitor cells. *Blood*. 1990 May 15;75(10):1947-50. PMID: 2337669.
- Katsyv, I., Wang, M., Song, W.M., Zhou, X., Zhao, Y., Park, S., Zhu, J., Zhang, B., and Irie, H.Y. (2016). EPRS is a critical regulator of cell proliferation and estrogen signaling in ER+ breast cancer. *Oncotarget* 7, 69592–69605. <https://doi.org/10.18632/oncotarget.11870>.
- Kaur, P., and Goyal, N. (2022). Pathogenic role of mitogen activated protein kinases in protozoan parasites. *Biochimie* 193, 78–89. <https://doi.org/10.1016/j.biochi.2021.10.012>.
- Kellershohn, J., Thomas, L., Hahnel, S.R., Grünweller, A., Hartmann, R.K., Hardt, M., Vilcinskis, A., Grevelding, C.G., and Haeblerlein, S. (2019). Insects in anthelmintics research:

- Lady beetle-derived harmonine affects survival, reproduction and stem cell proliferation of *Schistosoma mansoni*. *PLoS Negl Trop Dis* *13*, e0007240. <https://doi.org/10.1371/journal.pntd.0007240>.
- Kelley, J.M., Elliott, T.P., Beddoe, T., Anderson, G., Skuce, P., and Spithill, T.W. (2016). Current threat of triclabendazole resistance in *Fasciola hepatica*. *Trends Parasitol* *32*, 458–469. <https://doi.org/10.1016/j.pt.2016.03.002>.
- Khanehzad, M., Abbaszadeh, R., Holakuyee, M., Modarressi, M.H., and Nourashrafeddin, S.M. (2021). FSH regulates RA signaling to commit spermatogonia into differentiation pathway and meiosis. *Reprod Biol Endocrinol* *19*, 4. <https://doi.org/10.1186/s12958-020-00686-w>.
- Kibbe, W.A. (2007). OligoCalc: an online oligonucleotide properties calculator. *Nucleic Acids Res* *35*, W43–46. <https://doi.org/10.1093/nar/gkm234>.
- Kitson, T.M. (1983). Mechanism of inactivation of sheep liver cytoplasmic aldehyde dehydrogenase by disulfiram. *Biochem J* *213*, 551–554. <https://doi.org/10.1042/bj2130551>.
- Klonis, N., Xie, S.C., McCaw, J.M., Crespo-Ortiz, M.P., Zaloumis, S.G., Simpson, J.A., and Tilley, L. (2013). Altered temporal response of malaria parasites determines differential sensitivity to artemisinin. *Proc Natl Acad Sci U S A* *110*, 5157–5162. <https://doi.org/10.1073/pnas.1217452110>.
- Koop, D., Holland, N.D., Sémon, M., Alvarez, S., de Lera, A.R., Laudet, V., Holland, L.Z., and Schubert, M. (2010). Retinoic acid signaling targets *Hox* genes during the amphioxus gastrula stage: Insights into early anterior–posterior patterning of the chordate body plan. *Developmental Biology* *338*, 98–106. <https://doi.org/10.1016/j.ydbio.2009.11.016>.
- Koziol, U., Rauschendorfer, T., Zanon Rodríguez, L., Krohne, G., and Brehm, K. (2014). The unique stem cell system of the immortal larva of the human parasite *Echinococcus multilocularis*. *Evodevo* *5*, 10. <https://doi.org/10.1186/2041-9139-5-10>.
- La Rosa, P., Bielli, P., Compagnucci, C., Cesari, E., Volpe, E., Farioli Vecchioli, S., and Sette, C. (2016). Sam68 promotes self-renewal and glycolytic metabolism in mouse neural progenitor cells by modulating *Aldh1a3* pre-mRNA 3'-end processing. *Elife* *5*, e20750. <https://doi.org/10.7554/eLife.20750>.
- Lalor, R., Cwiklinski, K., Calvani, N.E.D., Dorey, A., Hamon, S., Corrales, J.L., Dalton, J.P., and De Marco Verissimo, C. (2021). Pathogenicity and virulence of the liver flukes *Fasciola hepatica* and *Fasciola gigantica* that cause the zoonosis fasciolosis. *Virulence* *12*, 2839–2867. <https://doi.org/10.1080/21505594.2021.1996520>.
- Lam, J.P., Mays, D.C., and Lipsky, J.J. (1997). Inhibition of recombinant human mitochondrial and cytosolic aldehyde dehydrogenases by two candidates for the active metabolites of disulfiram. *Biochemistry* *36*, 13748–13754. <https://doi.org/10.1021/bi970948e>.
- Laurence Després, and Sandrine Maurice (1995). The evolution of dimorphism and separate sexes in schistosomes. *The Royal Society* *262*, 175–180. <https://doi.org/10.1098/rspb.1995.0193>.

- Lei, H.-M., Zhang, K.-R., Wang, C.H., Wang, Y., Zhuang, G.-L., Lu, L.-M., Zhang, J., Shen, Y., Chen, H.-Z., and Zhu, L. (2019). Aldehyde dehydrogenase 1A1 confers erlotinib resistance via facilitating the reactive oxygen species-reactive carbonyl species metabolic pathway in lung adenocarcinomas. *Theranostics* 9, 7122–7139. <https://doi.org/10.7150/thno.35729>.
- Letunic, I., Doerks, T., and Bork, P. (2015). SMART: recent updates, new developments and status in 2015. *Nucleic Acids Res* 43, D257-260. <https://doi.org/10.1093/nar/gku949>.
- Li, H., Wang, J., Wu, C., Wang, L., Chen, Z.-S., and Cui, W. (2020). The combination of disulfiram and copper for cancer treatment. *Drug Discov Today* 25, 1099–1108. <https://doi.org/10.1016/j.drudis.2020.04.003>.
- Lindahl, R. (1992). Aldehyde dehydrogenases and their role in carcinogenesis. *Crit Rev Biochem Mol Biol* 27, 283–335. <https://doi.org/10.3109/10409239209082565>.
- Lipsky, J.J., Shen, M.L., and Naylor, S. (2001a). *In vivo* inhibition of aldehyde dehydrogenase by disulfiram. *Chem Biol Interact* 130–132, 93–102. [https://doi.org/10.1016/s0009-2797\(00\)00225-8](https://doi.org/10.1016/s0009-2797(00)00225-8).
- Lipsky, J.J., Shen, M.L., and Naylor, S. (2001b). Overview-*in vitro* inhibition of aldehyde dehydrogenase by disulfiram and metabolites. *Chem Biol Interact* 130–132, 81–91. [https://doi.org/10.1016/s0009-2797\(00\)00224-6](https://doi.org/10.1016/s0009-2797(00)00224-6).
- Liu, Z.J., Sun, Y.J., Rose, J., Chung, Y.J., Hsiao, C.D., Chang, W.R., Kuo, I., Perozich, J., Lindahl, R., Hempel, J., et al. (1997). The first structure of an aldehyde dehydrogenase reveals novel interactions between NAD and the Rossmann fold. *Nat Struct Biol* 4, 317–326. <https://doi.org/10.1038/nsb0497-317>.
- Livak, K.J., and Schmittgen, T.D. (2001). Analysis of relative gene expression data using real-time quantitative PCR and the 2(-Delta Delta C(T)) Method. *Methods* 25, 402–408. <https://doi.org/10.1006/meth.2001.1262>.
- Long, T., Cailliau, K., Beckmann, S., Browaeys, E., Trolet, J., Grevelding, C.G., and Dissous, C. (2010). *Schistosoma mansoni* Polo-like kinase 1: A mitotic kinase with key functions in parasite reproduction. *Int J Parasitol* 40, 1075–1086. <https://doi.org/10.1016/j.ijpara.2010.03.002>.
- Lu, Z., Sessler, F., Holroyd, N., Hahnel, S., Quack, T., Berriman, M., and Grevelding, C.G. (2017). A gene expression atlas of adult *Schistosoma mansoni* and their gonads. *Sci Data* 4, 170118. <https://doi.org/10.1038/sdata.2017.118>.
- Lu, Z., Zhang, Y., and Berriman, M. (2018). A web portal for gene expression across all life stages of *Schistosoma mansoni*. *BioRxiv* 308213. <https://doi.org/10.1101/308213>.
- Manikandan, P., and Nagini, S. (2018). Cytochrome P450 structure, function and clinical significance: A review. *Curr Drug Targets* 19, 38–54. <https://doi.org/10.2174/1389450118666170125144557>.
- Mansour, T.E., and Mansour, J.M. (1962). Effects of serotonin (5-hydroxytryptamine) and adenosine 3',5'-phosphate on phosphofructokinase from the liver fluke *Fasciola hepatica*. *J Biol Chem* 237, 629–634. [https://doi.org/10.1016/S0021-9258\(18\)60345-X](https://doi.org/10.1016/S0021-9258(18)60345-X).

- Mao, P., Joshi, K., Li, J., Kim, S.-H., Li, P., Santana-Santos, L., Luthra, S., Chandran, U.R., Benos, P.V., Smith, L., et al. (2013). Mesenchymal glioma stem cells are maintained by activated glycolytic metabolism involving aldehyde dehydrogenase 1A3. *Proc Natl Acad Sci U S A* *110*, 8644–8649. <https://doi.org/10.1073/pnas.1221478110>.
- Marchitti, S.A., Brocker, C., Stagos, D., and Vasiliou, V. (2008). Non-P450 aldehyde oxidizing enzymes: the aldehyde dehydrogenase superfamily. *Expert Opin Drug Metab Toxicol* *4*, 697–720. <https://doi.org/10.1517/17425255.4.6.697>.
- Martín, L., Fanarraga, M.L., Aloria, K., and Zabala, J.C. (2000). Tubulin folding cofactor D is a microtubule destabilizing protein. *FEBS Lett* *470*, 93–95. [https://doi.org/10.1016/s0014-5793\(00\)01293-x](https://doi.org/10.1016/s0014-5793(00)01293-x).
- Mas-Coma & M.D. Bargues (1997). Human liver flukes: A review. *Research and Reviews in Parasitology* *57*, 145–218.
- McCammick, E.M., McVeigh, P., McCusker, P., Timson, D.J., Morphey, R.M., Brophy, P.M., Marks, N.J., Mousley, A., and Maule, A.G. (2016). Calmodulin disruption impacts growth and motility in juvenile liver fluke. *Parasit Vectors* *9*, 46. <https://doi.org/10.1186/s13071-016-1324-9>.
- McCusker, P., McVeigh, P., Rathinasamy, V., Toet, H., McCammick, E., O'Connor, A., Marks, N.J., Mousley, A., Brennan, G.P., Halton, D.W., et al. (2016). Stimulating neoblast-like cell proliferation in juvenile *Fasciola hepatica* supports growth and progression towards the Adult Phenotype *in vitro*. *PLoS Negl Trop Dis* *10*, e0004994. <https://doi.org/10.1371/journal.pntd.0004994>.
- McVeigh, P., McCammick, E.M., McCusker, P., Morphey, R.M., Mousley, A., Abidi, A., Saifullah, K.M., Muthusamy, R., Gopalakrishnan, R., Spithill, T.W., et al. (2014). RNAi dynamics in Juvenile *Fasciola* spp. Liver flukes reveals the persistence of gene silencing *in vitro*. *PLoS Negl Trop Dis* *8*, e3185. <https://doi.org/10.1371/journal.pntd.0003185>.
- Mic, F.A., Molotkov, A., Fan, X., Cuenca, A.E., and Duester, G. (2000). RALDH3, a retinaldehyde dehydrogenase that generates retinoic acid, is expressed in the ventral retina, otic vesicle and olfactory pit during mouse development. *Mech Dev* *97*, 227–230. [https://doi.org/10.1016/s0925-4773\(00\)00434-2](https://doi.org/10.1016/s0925-4773(00)00434-2).
- Mills, P.B., Struys, E., Jakobs, C., Plecko, B., Baxter, P., Baumgartner, M., Willemsen, M.A.A.P., Omran, H., Tacke, U., Uhlenberg, B., et al. (2006). Mutations in antiquitin in individuals with pyridoxine-dependent seizures. *Nat Med* *12*, 307–309. <https://doi.org/10.1038/nm1366>.
- Mirkes, P.E., Ellison, A., and Little, S.A. (1991). Role of aldehyde dehydrogenase (ALDH) in the detoxication of cyclophosphamide (CP) in rat embryos. *Adv Exp Med Biol* *284*, 85–95. https://doi.org/10.1007/978-1-4684-5901-2_11.
- Moazeni, M., and Ahmadi, A. (2016). Controversial aspects of the life cycle of *Fasciola hepatica*. *Exp Parasitol* *169*, 81–89. <https://doi.org/10.1016/j.exppara.2016.07.010>.
- Modok, S., Mellor, H.R., and Callaghan, R. (2006). Modulation of multidrug resistance efflux pump activity to overcome chemoresistance in cancer. *Curr Opin Pharmacol* *6*, 350–354. <https://doi.org/10.1016/j.coph.2006.01.009>.

- Mok, S., Imwong, M., Mackinnon, M.J., Sim, J., Ramadoss, R., Yi, P., Mayxay, M., Chotivanich, K., Liong, K.-Y., Russell, B., et al. (2011). Artemisinin resistance in *Plasmodium falciparum* is associated with an altered temporal pattern of transcription. *BMC Genomics* 12, 391. <https://doi.org/10.1186/1471-2164-12-391>.
- Morawietz, C.M., Houhou, H., Puckelwaldt, O., Hehr, L., Dreisbach, D., Mokosch, A., Roeb, E., Roderfeld, M., Spengler, B., and Haerberlein, S. (2020). Targeting kinases in *Fasciola hepatica*: Anthelmintic effects and tissue distribution of selected kinase inhibitors. *Front Vet Sci* 7, 611270. <https://doi.org/10.3389/fvets.2020.611270>.
- Moreb, J.S. (2008). Aldehyde dehydrogenase as a marker for stem cells. *Curr Stem Cell Res Ther* 3, 237–246. <https://doi.org/10.2174/157488808786734006>.
- Moreb, J.S., Ucar, D., Han, S., Amory, J.K., Goldstein, A.S., Ostmark, B., and Chang, L.-J. (2012). The enzymatic activity of human aldehyde dehydrogenases 1A2 and 2 (ALDH1A2 and ALDH2) is detected by Aldefluor, inhibited by diethylaminobenzaldehyde and has significant effects on cell proliferation and drug resistance. *Chem Biol Interact* 195, 52–60. <https://doi.org/10.1016/j.cbi.2011.10.007>.
- Morel, M., Vanderstraete, M., Cailliau, K., Lescuyer, A., Lancelot, J., and Dissous, C. (2014). Compound library screening identified Akt/PKB kinase pathway inhibitors as potential key molecules for the development of new chemotherapeutics against schistosomiasis. *Int J Parasitol Drugs Drug Resist* 4, 256–266. <https://doi.org/10.1016/j.ijpddr.2014.09.004>.
- Muzio, G., Maggiora, M., Paiuzzi, E., Oraldi, M., and Canuto, R.A. (2012). Aldehyde dehydrogenases and cell proliferation. *Free Radic Biol Med* 52, 735–746. <https://doi.org/10.1016/j.freeradbiomed.2011.11.033>.
- Nelson, M.-A.M., Baba, S.P., and Anderson, E.J. (2017). Biogenic aldehydes as therapeutic targets for cardiovascular disease. *Curr Opin Pharmacol* 33, 56–63. <https://doi.org/10.1016/j.coph.2017.04.004>.
- Novobilský, A., and Höglund, J. (2015). First report of closantel treatment failure against *Fasciola hepatica* in cattle. *Int J Parasitol Drugs Drug Resist* 5, 172–177. <https://doi.org/10.1016/j.ijpddr.2015.07.003>.
- O'Brien, P.J., Siraki, A.G., and Shangari, N. (2005). Aldehyde sources, metabolism, molecular toxicity mechanisms, and possible effects on human health. *Crit Rev Toxicol* 35, 609–662. <https://doi.org/10.1080/10408440591002183>.
- O'Connell, E.M., Bennuru, S., Steel, C., Dolan, M.A., and Nutman, T.B. (2015). Targeting filarial Abl-like kinases: Orally available, food and drug administration-approved tyrosine kinase inhibitors are microfilaricidal and macrofilaricidal. *J Infect Dis* 212, 684–693. <https://doi.org/10.1093/infdis/jiv065>.
- Olson, P.D., and Tkach, V.V. (2005). Advances and trends in the molecular systematics of the parasitic Platyhelminthes. *Adv Parasitol* 60, 165–243. [https://doi.org/10.1016/S0065-308X\(05\)60003-6](https://doi.org/10.1016/S0065-308X(05)60003-6).
- Ortiz, P., Scarcella, S., Cerna, C., Rosales, C., Cabrera, M., Guzmán, M., Lamenza, P., and Solana, H. (2013). Resistance of *Fasciola hepatica* against triclabendazole in cattle in

- Cajamarca (Peru): a clinical trial and an *in vivo* efficacy test in sheep. *Vet Parasitol* 195, 118–121. <https://doi.org/10.1016/j.vetpar.2013.01.001>.
- Orywal, K., and Szmítkowski, M. (2017). Alcohol dehydrogenase and aldehyde dehydrogenase in malignant neoplasms. *Clin Exp Med* 17, 131–139. <https://doi.org/10.1007/s10238-016-0408-3>.
- Overend, D.J., and Bowen, F.L. (1995). Resistance of *Fasciola hepatica* to triclabendazole. *Aust Vet J* 72, 275–276. <https://doi.org/10.1111/j.1751-0813.1995.tb03546.x>.
- Oxberry, M.E., Reynoldson, J.A., and Thompson, R.C. (2000). The binding and distribution of albendazole and its principal metabolites in *Giardia duodenalis*. *J Vet Pharmacol Ther* 23, 113–120. <https://doi.org/10.1046/j.1365-2885.2000.00254.x>.
- Paranjpe, A., Zhang, R., Ali-Osman, F., Bobustuc, G.C., and Srivenugopal, K.S. (2014). Disulfiram is a direct and potent inhibitor of human O⁶-methylguanine-DNA methyltransferase (MGMT) in brain tumor cells and mouse brain and markedly increases the alkylating DNA damage. *Carcinogenesis* 35, 692–702. <https://doi.org/10.1093/carcin/bgt366>.
- Parés, X., Farrés, J., Kedishvili, N., and Duester, G. (2008). Medium- and short-chain dehydrogenase/reductase gene and protein families: Medium-chain and short-chain dehydrogenases/reductases in retinoid metabolism. *Cell Mol Life Sci* 65, 3936–3949. <https://doi.org/10.1007/s00018-008-8591-3>.
- Paul, M.K., and Mukhopadhyay, A.K. (2004). Tyrosine kinase – Role and significance in Cancer. *Int. J. Med. Sci.* 101–115. <https://doi.org/10.7150/ijms.1.101>.
- Penning, T.M. (2015). The aldo-keto reductases (AKRs): Overview. *Chem Biol Interact* 234, 236–246. <https://doi.org/10.1016/j.cbi.2014.09.024>.
- Pfaffl, M.W., Tichopad, A., Prgomet, C., and Neuvians, T.P. (2004). Determination of stable housekeeping genes, differentially regulated target genes and sample integrity: BestKeeper--Excel-based tool using pair-wise correlations. *Biotechnol Lett* 26, 509–515. <https://doi.org/10.1023/b:bile.0000019559.84305.47>.
- Pinto-Almeida, A., Mendes, T., Armada, A., Belo, S., Carrilho, E., Viveiros, M., and Afonso, A. (2015). The role of efflux pumps in *Schistosoma mansoni* praziquantel resistant phenotype. *PLoS One* 10, e0140147. <https://doi.org/10.1371/journal.pone.0140147>.
- Ploemen, J.P., van Iersel, M.L., Wormhoudt, L.W., Commandeur, J.N., Vermeulen, N.P., and van Bladeren, P.J. (1996). *In vitro* inhibition of rat and human glutathione S-transferase isoenzymes by disulfiram and diethyldithiocarbamate. *Biochem Pharmacol* 52, 197–204. [https://doi.org/10.1016/0006-2952\(96\)00142-6](https://doi.org/10.1016/0006-2952(96)00142-6).
- Pors, K., and Moreb, J.S. (2014). Aldehyde dehydrogenases in cancer: an opportunity for biomarker and drug development? *Drug Discov Today* 19, 1953–1963. <https://doi.org/10.1016/j.drudis.2014.09.009>.
- Puttini, S., Plaisance, I., Barile, L., Cervio, E., Milano, G., Marcato, P., Pedrazzini, T., and Vassalli, G. (2018). ALDH1A3 is the key isoform that contributes to aldehyde dehydrogenase activity and affects *in vitro* proliferation in cardiac atrial appendage progenitor cells. *Front Cardiovasc Med* 5, 90. <https://doi.org/10.3389/fcvm.2018.00090>.

- Radio, S., Fontenla, S., Solana, V., Matos Salim, A.C., Araújo, F.M.G., Ortiz, P., Hoban, C., Miranda, E., Gayo, V., Pais, F.S.-M., et al. (2018). Pleiotropic alterations in gene expression in Latin American *Fasciola hepatica* isolates with different susceptibility to drugs. *Parasit Vectors* 11, 56. <https://doi.org/10.1186/s13071-017-2553-2>.
- Ressurreição, M., De Saram, P., Kirk, R.S., Rollinson, D., Emery, A.M., Page, N.M., Davies, A.J., and Walker, A.J. (2014). Protein kinase C and extracellular signal-regulated kinase regulate movement, attachment, pairing and egg release in *Schistosoma mansoni*. *PLoS Negl Trop Dis* 8, e2924. <https://doi.org/10.1371/journal.pntd.0002924>.
- Rinaldi, G., Morales, M.E., Cancela, M., Castillo, E., Brindley, P.J., and Tort, J.F. (2008). Development of functional genomic tools in trematodes: RNA interference and luciferase reporter gene activity in *Fasciola hepatica*. *PLoS Negl Trop Dis* 2, e260. <https://doi.org/10.1371/journal.pntd.0000260>.
- Rivett, A.J., Mason, G.G., Murray, R.Z., and Reidlinger, J. (1997). Regulation of proteasome structure and function. *Mol Biol Rep* 24, 99–102. <https://doi.org/10.1023/a:1006814306401>.
- Rizzo, W.B. (2016). Genetics and prospective therapeutic targets for Sjögren-Larsson syndrome. *Expert Opin Orphan Drugs* 4, 395–406. <https://doi.org/10.1517/21678707.2016.1154453>.
- Robinson, M.W., Trudgett, A., Hoey, E.M., and Fairweather, I. (2002). Triclabendazole-resistant *Fasciola hepatica*: beta-tubulin and response to *in vitro* treatment with triclabendazole. *Parasitology* 124, 325–338. <https://doi.org/10.1017/s003118200100124x>.
- Robinson, M.W., Menon, R., Donnelly, S.M., Dalton, J.P., and Ranganathan, S. (2009). An integrated transcriptomics and proteomics analysis of the secretome of the helminth pathogen *Fasciola hepatica*: proteins associated with invasion and infection of the mammalian host. *Mol Cell Proteomics* 8, 1891–1907. <https://doi.org/10.1074/mcp.M900045-MCP200>.
- Rodríguez-Zavala, J.S., Calleja, L.F., Moreno-Sánchez, R., and Yoval-Sánchez, B. (2019). Role of aldehyde dehydrogenases in physiopathological processes. *Chem Res Toxicol* 32, 405–420. <https://doi.org/10.1021/acs.chemrestox.8b00256>.
- Roossinck, M.J. (2005). Symbiosis versus competition in plant virus evolution. *Nat Rev Microbiol* 3, 917–924. <https://doi.org/10.1038/nrmicro1285>.
- Rowan, W.B. (1956). The mode of hatching the egg of *Fasciola hepatica*. *Exp Parasitol* 5, 118–137. [https://doi.org/10.1016/0014-4894\(56\)90009-1](https://doi.org/10.1016/0014-4894(56)90009-1).
- Rowcliffe, S.A., and Ollerenshaw, C.B. (1960). Observations on the bionomics of the egg of *Fasciola hepatica*. *Ann Trop Med Parasitol* 54, 172–181. <https://doi.org/10.1080/00034983.1960.11685973>.
- Roy, M., Connor, J., Al-Niimi, A., Rose, S.L., and Mahajan, A. (2018). Aldehyde dehydrogenase 1A1 (ALDH1A1) expression by immunohistochemistry is associated with chemo-refractoriness in patients with high-grade ovarian serous carcinoma. *Hum Pathol* 73, 1–6. <https://doi.org/10.1016/j.humpath.2017.06.025>.

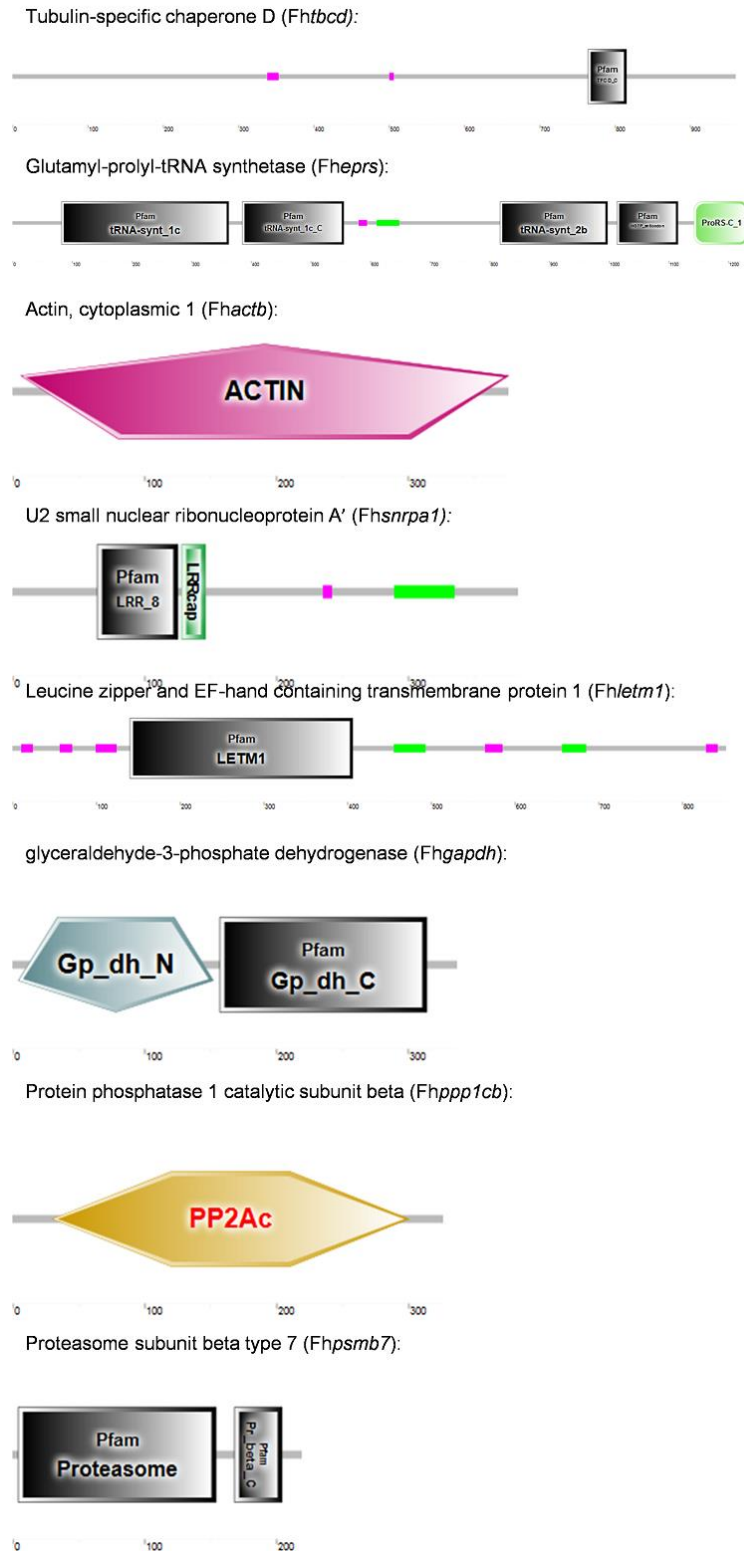
- Salahudeen, M.S., and Nishtala, P.S. (2017). An overview of pharmacodynamic modelling, ligand-binding approach and its application in clinical practice. *Saudi Pharm J* 25, 165–175. <https://doi.org/10.1016/j.jsps.2016.07.002>.
- Sangster, N.C. (1999). Anthelmintic resistance: past, present and future. *Int J Parasitol* 29, 115–124; discussion 137-138. [https://doi.org/10.1016/s0020-7519\(98\)00188-x](https://doi.org/10.1016/s0020-7519(98)00188-x).
- Santiago Mas-Coma, M. Adela Valero, M. Dolores Bargues (2015). Fasciola and Fasciolopsis. In *Biology of Foodborne Parasites*, pp. 371–404.
- Schneider, C.A., Rasband, W.S., and Eliceiri, K.W. (2012). NIH Image to ImageJ: 25 years of image analysis. *Nat Methods* 9, 671–675. <https://doi.org/10.1038/nmeth.2089>.
- Schubert, A., Koziol, U., Cailliau, K., Vanderstraete, M., Dissous, C., and Brehm, K. (2014). Targeting *Echinococcus multilocularis* stem cells by inhibition of the Polo-like kinase EmPlk1. *PLoS Negl Trop Dis* 8, e2870. <https://doi.org/10.1371/journal.pntd.0002870>.
- Schulman, M.D., Valentino, D., Cifelli, S., and Ostlind, D.A. (1982a). Dose-dependent pharmacokinetics and efficacy of MK-401 against old, and young-mature infections of *Fasciola hepatica* in the rat. *J Parasitol* 68, 603–608.
- Schulman, M.D., Ostlind, D.A., and Valentino, D. (1982b). Mechanism of action of MK-401 against *Fasciola hepatica*: inhibition of phosphoglycerate kinase. *Mol Biochem Parasitol* 5, 133–145. [https://doi.org/10.1016/0166-6851\(82\)90016-0](https://doi.org/10.1016/0166-6851(82)90016-0).
- Scimone, M.L., Kravarik, K.M., Lapan, S.W., and Reddien, P.W. (2014). Neoblast specialization in regeneration of the planarian *Schmidtea mediterranea*. *Stem Cell Reports* 3, 339–352. <https://doi.org/10.1016/j.stemcr.2014.06.001>.
- Seo, S., Oh, M., Park, Y., and Kim, S. (2018). DeepFam: deep learning based alignment-free method for protein family modeling and prediction. *Bioinformatics* 34, i254–i262. <https://doi.org/10.1093/bioinformatics/bty275>.
- Shaha, S., Patel, K., Saadat, S., Panahi, S., de Almeida, M.M., Voronova, A., and Riddell, M. (2022). Human placenta and trophoblasts simultaneously express three isoforms of atypical protein kinase-c. *Placenta* 119, 39–43. <https://doi.org/10.1016/j.placenta.2022.01.015>.
- Shoriki, T., Ichikawa-Seki, M., Suganuma, K., Naito, I., Hayashi, K., Nakao, M., Aita, J., Mohanta, U.K., Inoue, N., Murakami, K., et al. (2016). Novel methods for the molecular discrimination of *Fasciola* spp. on the basis of nuclear protein-coding genes. *Parasitol Int* 65, 180–183. <https://doi.org/10.1016/j.parint.2015.12.002>.
- Sievers, F., Wilm, A., Dineen, D., Gibson, T.J., Karplus, K., Li, W., Lopez, R., McWilliam, H., Remmert, M., Söding, J., et al. (2011). Fast, scalable generation of high-quality protein multiple sequence alignments using Clustal Omega. *Mol Syst Biol* 7, 539. <https://doi.org/10.1038/msb.2011.75>.
- Silver, N., Best, S., Jiang, J., and Thein, S.L. (2006). Selection of housekeeping genes for gene expression studies in human reticulocytes using real-time PCR. *BMC Mol Biol* 7, 33. <https://doi.org/10.1186/1471-2199-7-33>.

- Singh, S., Brocker, C., Koppaka, V., Chen, Y., Jackson, B.C., Matsumoto, A., Thompson, D.C., and Vasiliou, V. (2013). Aldehyde dehydrogenases in cellular responses to oxidative/electrophilic stress. *Free Radical Biology and Medicine* 56, 89–101. <https://doi.org/10.1016/j.freeradbiomed.2012.11.010>.
- Singh, S., Arcaroli, J., Chen, Y., Thompson, D.C., Messersmith, W., Jimeno, A., and Vasiliou, V. (2015). ALDH1B1 Is Crucial for Colon Tumorigenesis by Modulating Wnt/ β -Catenin, Notch and PI3K/Akt Signaling Pathways. *PLoS One* 10, e0121648. <https://doi.org/10.1371/journal.pone.0121648>.
- Skrott, Z., Mistrik, M., Andersen, K.K., Friis, S., Majera, D., Gursky, J., Ozdian, T., Bartkova, J., Turi, Z., Moudry, P., et al. (2017). Alcohol-abuse drug disulfiram targets cancer via p97 segregase adaptor NPL4. *Nature* 552, 194–199. <https://doi.org/10.1038/nature25016>.
- Skrott, Z., Majera, D., Gursky, J., Buchtova, T., Hajduch, M., Mistrik, M., and Bartek, J. (2019). Disulfiram's anti-cancer activity reflects targeting NPL4, not inhibition of aldehyde dehydrogenase. *Oncogene* 38, 6711–6722. <https://doi.org/10.1038/s41388-019-0915-2>.
- Sophos, N.A., and Vasiliou, V. (2003). Aldehyde dehydrogenase gene superfamily: the 2002 update. *Chem Biol Interact* 143–144, 5–22. [https://doi.org/10.1016/s0009-2797\(02\)00163-1](https://doi.org/10.1016/s0009-2797(02)00163-1).
- Srivastava, D., Singh, R.K., Moxley, M.A., Henzl, M.T., Becker, D.F., and Tanner, J.J. (2012). The three-dimensional structural basis of type II hyperprolinemia. *J Mol Biol* 420, 176–189. <https://doi.org/10.1016/j.jmb.2012.04.010>.
- Stagos, D., Chen, Y., Cantore, M., Jester, J.V., and Vasiliou, V. (2010). Corneal aldehyde dehydrogenases: multiple functions and novel nuclear localization. *Brain Res Bull* 81, 211–218. <https://doi.org/10.1016/j.brainresbull.2009.08.017>.
- Stergiou, I.E., Chatzis, L., Papanikolaou, A., Giannouli, S., Tzioufas, A.G., Voulgarelis, M., and Kapsogeorgou, E.K. (2021). Akt Signaling Pathway Is Activated in the Minor Salivary Glands of Patients with Primary Sjögren's syndrome. *Int J Mol Sci* 22. <https://doi.org/10.3390/ijms222413441>.
- Stroehlein, A.J., Young, N.D., Jex, A.R., Sternberg, P.W., Tan, P., Boag, P.R., Hofmann, A., and Gasser, R.B. (2015). Defining the *Schistosoma haematobium* kinome enables the prediction of essential kinases as anti-schistosome drug targets. *Sci Rep* 5, 17759. <https://doi.org/10.1038/srep17759>.
- Sukhdeo, M.V., and Mettrick, D.F. The behavior of juvenile *Fasciola hepatica*. *J Parasitol*. 1986 Aug;72(4):492-7. PMID: 3783343.
- Sukhdeo, M.V., Sangster, N.C., and Mettrick, D.F. (1988). Permanent feeding sites of adult *Fasciola hepatica* in rabbits? *Int J Parasitol* 18, 509–512. [https://doi.org/10.1016/0020-7519\(88\)90015-x](https://doi.org/10.1016/0020-7519(88)90015-x).
- Takimoto, K., Lindahl, R., and Pitot, H.C. (1992). Regulation of 2,3,7,8-tetrachlorodibenzo-p-dioxin-inducible expression of aldehyde dehydrogenase in hepatoma cells. *Arch Biochem Biophys* 298, 493–497. [https://doi.org/10.1016/0003-9861\(92\)90440-8](https://doi.org/10.1016/0003-9861(92)90440-8).
- Tamura, K., Stecher, G., and Kumar, S. (2021). MEGA11: Molecular Evolutionary Genetics Analysis Version 11. *Mol Biol Evol* 38, 3022–3027. <https://doi.org/10.1093/molbev/msab120>.

- Tian, G., Thomas, S., and Cowan, N.J. (2010). Effect of TBCD and its regulatory interactor Arl2 on tubulin and microtubule integrity. *Cytoskeleton (Hoboken)* 67, 706–714. <https://doi.org/10.1002/cm.20480>.
- Tonk, M., Vilcinskas, A., Grevelding, C.G., and Haeberlein, S. (2020). Anthelmintic activity of assassin bug venom against the blood fluke *Schistosoma mansoni*. *Antibiotics (Basel)* 9. <https://doi.org/10.3390/antibiotics9100664>.
- Untergasser, A., Cutcutache, I., Koressaar, T., Ye, J., Faircloth, B.C., Remm, M., and Rozen, S.G. (2012). Primer3--new capabilities and interfaces. *Nucleic Acids Res* 40, e115. <https://doi.org/10.1093/nar/gks596>.
- Vallari, R.C., and Pietruszko, R. (1982). Human aldehyde dehydrogenase: mechanism of inhibition of disulfiram. *Science* 216, 637–639. <https://doi.org/10.1126/science.7071604>.
- Vandesompele, J., De Preter, K., Pattyn, F., Poppe, B., Van Roy, N., De Paepe, A., and Speleman, F. (2002). Accurate normalization of real-time quantitative RT-PCR data by geometric averaging of multiple internal control genes. *Genome Biol* 3, RESEARCH0034. <https://doi.org/10.1186/gb-2002-3-7-research0034>.
- Vasiliou, V., and Nebert, D.W. (2005). Analysis and update of the human aldehyde dehydrogenase (ALDH) gene family. *Hum Genomics* 2, 138–143. <https://doi.org/10.1186/1479-7364-2-2-138>.
- Vasiliou, V., Pappa, A., and Estey, T. (2004). Role of human aldehyde dehydrogenases in endobiotic and xenobiotic metabolism. *Drug Metab Rev* 36, 279–299. <https://doi.org/10.1081/dmr-120034001>.
- Vasiliou, V., Thompson, D.C., Smith, C., Fujita, M., and Chen, Y. (2013). Aldehyde dehydrogenases: from eye crystallins to metabolic disease and cancer stem cells. *Chem Biol Interact* 202, 2–10. <https://doi.org/10.1016/j.cbi.2012.10.026>.
- Vassalli, G. (2019). Aldehyde dehydrogenases: Not just markers, but functional regulators of stem cells. *Stem Cells Int* 2019, 3904645. <https://doi.org/10.1155/2019/3904645>.
- Vauquelin, G., and Charlton, S.J. (2010). Long-lasting target binding and rebinding as mechanisms to prolong *in vivo* drug action. *Br J Pharmacol* 161, 488–508. <https://doi.org/10.1111/j.1476-5381.2010.00936.x>.
- Wang, L.-F., and Crameri, G. (2014). Emerging zoonotic viral diseases. *Rev Sci Tech* 33, 569–581. <https://doi.org/10.20506/rst.33.2.2311>.
- Wang, H., Li, Y., Zhou, D., Li, X., Jia, S., Qi, S., and Huang, J. (2021). Aldehyde dehydrogenase 1B1 is a potential marker of colorectal tumors. *Histol Histopathol* 36, 183–194. <https://doi.org/10.14670/HH-18-304>.
- Wang, K., Chen, X., Zhan, Y., Jiang, W., Liu, X., Wang, X., and Wu, B. (2013). Increased expression of ALDH1A1 protein is associated with poor prognosis in clear cell renal cell carcinoma. *Med Oncol* 30, 574. <https://doi.org/10.1007/s12032-013-0574-z>.
- Wendt, G.R., and Collins, J.J. 3rd (2016). Schistosomiasis as a disease of stem cells. *Curr Opin Genet Dev* 40, 95–102. <https://doi.org/10.1016/j.gde.2016.06.010>.

- Wesołowska, A., Zawistowska-Deniziak, A., Norbury, L.J., Wilkowski, P., Januszkiewicz, K., Pyziel, A.M., Zygnier, W., and Wędrychowicz, H. (2016). Immune responses in rats and sheep induced by a DNA vaccine containing the phosphoglycerate kinase gene of *Fasciola hepatica* and liver fluke infection. *Acta Parasitol* *61*, 212–220. <https://doi.org/10.1515/ap-2016-0030>.
- WHO, 2020 Neglected tropical diseases: Fascioliasis. <https://www.who.int/news-room/questions-and-answers/item/q-a-on-fascioliasis#:~:text=Fascioliasis%20is%20caused%20by%20two,may%20be%20transmitted%20to%20humans>.
- Winkelhagen, A.J.S., Mank, T., de Vries, P.J., and Soetekouw, R. (2012). Apparent triclabendazole-resistant human *Fasciola hepatica* infection, the Netherlands. *Emerg Infect Dis* *18*, 1028–1029. <https://doi.org/10.3201/eid1806.120302>.
- Wong, W.-R., Maher, S., Oh, J.Y., Brugman, K.I., Gharib, S., and Sternberg, P.W. (2021). Conserved missense variant in *ALDH1A3* ortholog impairs fecundity in *C. elegans*. *MicroPubl Biol* *2021*. <https://doi.org/10.17912/micropub.biology.000357>.
- Wu, K., Zhai, X., Huang, S., Jiang, L., Yu, Z., and Huang, J. (2021). Protein kinases: Potential drug targets against *Schistosoma japonicum*. *Front Cell Infect Microbiol* *11*, 691757. <https://doi.org/10.3389/fcimb.2021.691757>.
- Yin et al. (1993). Human high-Km aldehyde dehydrogenase (ALDH3): molecular, kinetic and structural features. *Adv Exp Med Biol*. 1993;328:87-98. doi: 10.1007/978-1-4615-2904-0_11. PMID: 8493944.
- Yokoyama, Y., Zhu, H., Lee, J.H., Kossenkov, A.V., Wu, S.Y., Wickramasinghe, J.M., Yin, X., Palozola, K.C., Gardini, A., Showe, L.C., et al. (2016). BET Inhibitors Suppress ALDH Activity by Targeting *ALDH1A1* Super-Enhancer in Ovarian Cancer. *Cancer Res* *76*, 6320–6330. <https://doi.org/10.1158/0008-5472.CAN-16-0854>.
- Yoo, W.G., Kim, T.I., Li, S., Kwon, O.S., Cho, P.Y., Kim, T.-S., Kim, K., and Hong, S.-J. (2009). Reference genes for quantitative analysis on *Clonorchis sinensis* gene expression by real-time PCR. *Parasitol Res* *104*, 321–328. <https://doi.org/10.1007/s00436-008-1195-x>.
- Yoshida, A., Hsu, L.C., and Davé, V. (1992). Retinal oxidation activity and biological role of human cytosolic aldehyde dehydrogenase. *Enzyme* *46*, 239–244. <https://doi.org/10.1159/000468794>.
- Zha, J., Chen, F., Dong, H., Shi, P., Yao, Y., Zhang, Y., Li, R., Wang, S., Li, P., Wang, W., et al. (2014). Disulfiram targeting lymphoid malignant cell lines via ROS-JNK activation as well as Nrf2 and NF-κB pathway inhibition. *J Transl Med* *12*, 163. <https://doi.org/10.1186/1479-5876-12-163>.

7. SUPPLEMENTARY FIGURES



Supplementary Figure 1. Results from SMART analysis of amino acid sequences from selected reference gene candidates and kinases of *F. hepatica*.

Supplementary Table 1. Expression stability of candidate reference genes based on three different life stages of *F. hepatica*: newly excysted juveniles (NEJs), immature worms, and adults. Ranking was based on an analysis using four different algorithms: NormFinder, BestKeeper, geNorm, and the ΔC_t method. Candidate reference genes selected for further analyses are written in bold.

Rank	NormFinder		BestKeeper		geNorm		ΔC_t method	
	Ref.gene	Stability value M	Ref.gene	Coeff. of correlation r	Ref.gene	Stability value M	Ref.gene	
1	Fheprs	0.118	Fhactb	0.972	Fhtbcd, Fheprs	0.298	Fheprs	0.562
2	Fhpsmb7	0.194	Fhtbcd	0.971			Fhtbcd	0.600
3	Fhtbcd	0.209	Fheprs	0.970	Fhpsmb7	0.360	Fhpsmb7	0.618
4	Fhsnrpa1	0.306	Fhpsmb7	0.936	Fhsnrpa1	0.415	Fhsnrpa1	0.661
5	Fhactb	0.361	Fhgapdh	0.922	Fhletm1	0.513	Fhactb	0.800
6	Fhletm1	0.366	Fhsnrpa1	0.810	Fhppp1cb	0.597	Fhletm1	0.819
7	Fhppp1cb	0.540	Fhletm1	0.610	Fhactb	0.672	Fhppp1cb	0.966
8	Fhgapdh	0.592	Fhppp1cb	0.305	Fhgapdh	0.751	Fhgapdh	0.989

Supplementary Table 2. Expression stability of candidate reference genes during *in vitro* growth of *F. hepatica* from newly excysted juveniles (NEJs) to 4-week-old juvenile worms.

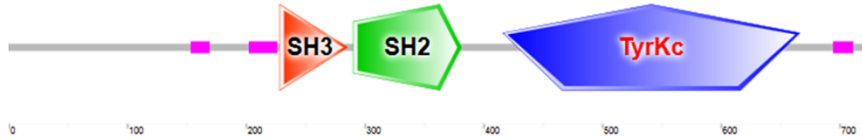
The ranking was based on an analysis using four different algorithms: NormFinder, BestKeeper, geNorm, and the ΔC_t method. Candidate reference genes selected for further analyses are written in bold.

Rank	NormFinder		BestKeeper		geNorm		ΔC_t method	
	Ref.gene	Stability value M	Ref.gene	Coeff. of correlation	Ref.gene	Stability value M	Ref.gene	
1	Fhpsmb7	0.177	Fhpsmb7	0.971	Fhtbcd, Fheprs	0.170	Fhtbcd	0.564
2	Fhtbcd	0.196	Fhtbcd	0.945			Fhpsmb7	0.577
3	Fheprs	0.242	Fhsnrpa1	0.935	Fhpsmb7	0.269	Fheprs	0.600
4	Fhsnrpa1	0.263	Fheprs	0.883	Fhactb	0.317	Fhsnrpa1	0.661
5	Fhactb	0.340	Fhppp1cb	0.817	Fhsnrpa1	0.424	Fhactb	0.686
6	Fhletm1	0.469	Fhactb	0.730	Fhgapdh	0.532	Fhletm1	0.902
7	Fhppp1cb	0.596	Fhletm1	0.670	Fhletm1	0.651	Fhgapdh	0.988
8	Fhgapdh	0.620	Fhgapdh	0.201	Fhppp1cb	0.756	Fhppp1cb	1.072

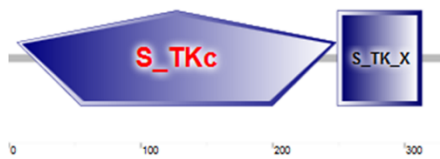
ABL proto-oncogene 1, non-receptor tyrosine kinase (*Fhabl1*):



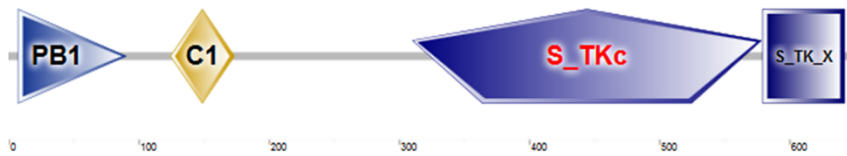
ABL proto-oncogene 2, non-receptor tyrosine kinase (*Fhabl2*):



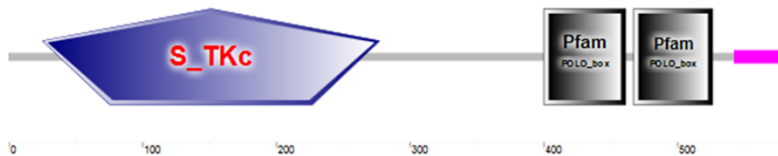
Rac-alpha serine/threonine-protein kinase (*Fhakt1*):



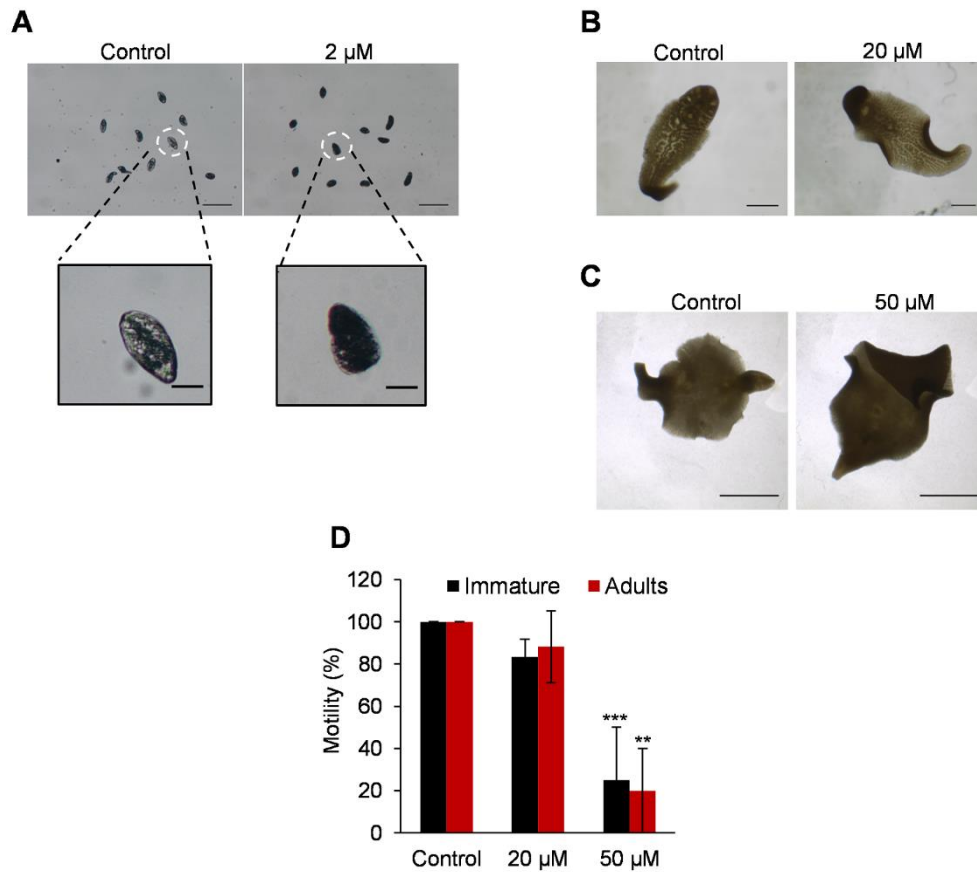
Protein kinase C (*Fhpkc*):



Polo-like kinase 1 (*Fhplk1*):



Supplementary Figure 2. Results from SMART analysis of amino acid sequences from selected kinases of *F. hepatica*.



Supplementary Figure 3. Effect of triclabendazole (TCBZ) on intra-mammalian stages of *F. hepatica*. (A) Morphological damage of NEJs shown by bright-field microscopy after treatment with 2 μ M of the anti-fascioloid drug TCBZ. A closer look at damaged and intact NEJs (highlighted in white circles) is shown in higher magnification. (B) Absence of any phenotypic changes in immature flukes after treatment with 20 μ M TCBZ, whereas a change in the morphology of adults was observed when these were treated with 50 μ M TCBZ (C). (D) The motility of immatures and adult's worms was significant decreased upon treatment with 50 μ M TCBZ. Average values of 8 immature flukes and 10-12 adults and biological replicates with SEM of two independent experiments (for NEJs and immature flukes) and three independent experiments (for adult flukes) are shown. Scale bars: for NEJs 500 μ m (whole) and 100 μ m (zoom). For immature fluke, scale bar = 1 mm, and for adults, scale bar = 5 mm. Significant differences are indicated with *** $p < 0.001$ (Mann-Whitney test).

ACKNOWLEDGMENTS

At this moment, and while writing the acknowledgments part, I ask myself a very disturbing question that no mortal can answer. *Is it fate that brought me here or fate has been challenged?*

Almost four years ago I came out from a very bad experience, and I was trying hard to find a new Ph.D. position. I kept struggling until the day when I received a call from Prof. Dr. Christoph Grevelding offering me a position in his lab. He took my hand and for that, I will be eternally grateful. I would like to thank him for all the fruitful scientific discussions that we've had during the working as well as the writing periods.

I would like to express my sincere gratitude to my supervisor PD. Dr. Simone Häberlein for her continuous support throughout my Ph.D. study and research, for her patience, motivation, enthusiasm, and immense knowledge. Thank you, a lot, for all your advice. You have been pushing me forward for the past four years to bring the best out of me, and here I am at the last step of my Ph.D. and the first step in a long and endless journey in science. Thank you for your guidance and support throughout the writing period. I could not have imagined having better than you as an advisor and mentor for my Ph.D. study.

I would like to thank Prof. Dr. Nikola-Michael Prpic-Schäper for accepting to be my first supervisor in faculty 8.

This work was funded by the LOEWE Centre for Novel Drug Targets against Poverty-Related and Neglected Tropical Infectious Diseases (DRUID), which is part of the excellence initiative of the Hessen State Ministry of Higher Education, Research, and the Arts (HMWK). Therefore, I would like to thank all the DRUID family for the summer schools as well as the meetings and conferences that we have had and all the scientific discussions.

I thank my fellow lab mates, new and former, in the lab of Prof. Grevelding as well as other labs of the parasitology institute, who for some of them have already become friends and are no longer simple colleagues. Thanks to all of you who have contributed in a way to the accomplishment of this work, to the stimulating discussions, and for all the fun we have had in the last four years. Also, I thank my friends in Lebanon and France, as well as the ones that I have made here in Germany.

Last but not the least, I would like to thank my family for the sacrifice that they have made, and the support that they have been giving me for the past few years.

CONTRIBUTIONS

Publications

Hicham Houhou, Tom Gallinger, Michael Weber, Noah-Julien Strasheim, Georg Rennar, Wiebke Obermann, Patrick Mäder, Christina Strube, Franco F. Falcone, Arnold Grünweller, Denise Salzig, Peter Czermak, Martin Schlitzer, Christoph G. Grevelding, Simone Haeberlein (2022). **Identification and evaluation of aldehyde dehydrogenase as drug target in the liver fluke *Fasciola hepatica***. (In preparation).

Morawietz, C.M., **Houhou, H.**, Puckelwaldt, O., Hehr, L., Dreisbach, D., Mokosch, A., Roeb, E., Roderfeld, M., Spengler, B., and Haeberlein, S. (2020). **Targeting kinases in *Fasciola hepatica*: Anthelmintic effects and tissue distribution of selected kinase inhibitors**. Front Vet Sci 7, 611270. <https://doi.org/10.3389/fvets.2020.611270>.

Houhou, H., Puckelwaldt, O., Strube, C., and Haeberlein, S. (2019). **Reference gene analysis and its use for kinase expression profiling in *Fasciola hepatica***. Sci Rep 9, 15867. <https://doi.org/10.1038/s41598-019-52416-x>.

Conferences

2021 - 29th Annual meeting of the German Society for Parasitology.

Talk: Identification of Aldehyde dehydrogenases as novel anti-helminthic target in *Fasciola hepatica*.

14th Annual GGL Conference 2021, 29-30 September 2021, Giessen, Germany.

Talk: Identification of aldehyde dehydrogenases as novel anthelmintic targets in *Fasciola hepatica*.

13th Annual GGL Conference 2020, 29-30 September 2020, Giessen, Germany.

Talk: Identification of aldehyde dehydrogenases as novel anthelmintic targets in *Fasciola hepatica*.

2019 - DRUID retreat

Talk: Attacking liver and blood flukes by targeting their Aldehyde dehydrogenases activity.

2019 - 20th Anniversary Drug Design & Development Seminar (DDDS) of the German Society for Parasitology.

Poster: ABL kinases as potential targets for candidate compounds in the liver fluke *Fasciola hepatica*.

2019 – DRUID meeting.

Poster: Aldehyde dehydrogenases as targets for effective compounds against blood and liver flukes.

12th Annual GGL Conference 2019, 04-05 September 2019, Giessen, Germany.

Poster: Aldehyde dehydrogenases as targets for effective compounds against the liver fluke *Fasciola hepatica*

11th Annual GGL Conference 2018, 19-20 September 2018, Giessen, Germany.

Poster: Identification of novel targets and candidate compounds against the liver fluke *Fasciola hepatica*.

2015 – 3rd Symposium "Chromatin changes in differentiation and malignancies".

DECLARATION

I declare that this thesis is my original work and other sources of information have been properly quoted. This work has not been previously presented to obtain any other degree from any other university.

Ich erkläre: Ich habe die vorgelegte Dissertation selbständig und ohne unerlaubte fremde Hilfe und nur mit den Hilfen angefertigt, die ich in der Dissertation angegeben habe. Alle Textstellen, die wörtlich oder sinngemäß aus veröffentlichten Schriften entnommen sind, und alle Angaben, die auf mündlichen Auskünften beruhen, sind als solche kenntlich gemacht. Bei den von mir durchgeführten und in der Dissertation erwähnten Untersuchungen habe ich die Grundsätze guter wissenschaftlicher Praxis, wie sie in der "Satzung der Justus-Liebig-Universität Gießen zur Sicherung guter wissenschaftlicher Praxis" niedergelegt sind, eingehalten.

Signed: _____

Date: _____